Structural and functional elucidation of the Type VIIb secretion system from *Staphylococcus aureus*

Strukturelle und funktionelle Analyse des Typ VIIb Sekretionssystems aus *Staphylococcus aureus*

Doctoral thesis for a doctoral degree at the Graduate School of Life Sciences,
Julius-Maximilians-Universität Würzburg,
Section: Infection and Immunity

submitted by
Nicole Aline Mietrach
from Steinitz

Würzburg, June 2020

Submitted on: .....

Members of the thesis committee:

Chair Person:

Primary Supervisor: Dr. Sebastian Geibel

Supervisor (Second): Prof. Thomas Müller

Supervisor (Third): Prof. Gilles Phan

Date of Public Defense:.....

Date of Receipt of Certificates: .....

Summary

The Type VII secretion system (T7SS) is linked to virulence and long-term pathogenesis in a broad range of Gram-positive bacteria, including the human commensal and pathogen *Staphylococcus aureus*. The Type VIIb secretion system (T7SSb) is responsible for the export of small toxic proteins, which induce antibacterial immune responses and mediate bacterial persistence in the host. In addition, it is also involved in bacterial competition. The T7SSb requires several proteins to build up the secretion machinery. This work focuses on the structural and functional investigation of the motor ATPase EssC and the putative pore forming, multi-pass membrane component EsaA. Both proteins are indispensable for substrate secretion.

EssC belongs to the FtsK/SpoIIIE ATPase family and is conserved among the T7SSs. It contains three C-terminal, cytosolic ATPase domains, designated as EssC-D1, -D2 and -D3, whereby EssC-D3 is the most distal one. In this thesis, I am presenting the crystal structure of the EssC-D3 at 1.7 Å resolution. As the deletion of EssC-D3 abrogates substrate export, I have demonstrated that this domain comprises a hydrophobic, surface-exposed pocket, which is required for substrate secretion. More specifically, I have identified two amino acids involved in the secretion process. In addition, my results indicate that not only EssC-D3 is important for substrate interaction but also EssC-D2 and/or EssC-D1. Unlike in the related Yuk T7SSb of *Bacillus subtilis*, the ATPase activity of D3 domain contributes to substrate secretion. Mutation of the modified Walker B motif in EssC-D3 diminishes substrate secretion completely.

The membrane protein EsaA encompasses an extracellular segment spanning through the cell wall of *S. aureus*. I was able to reveal that this part folds into a stable domain, which was crystallized and diffracted up to 4 Å. The first attempts to dissolve the structure failed due to a lack of homologues structures. Therefore, crystals for single-wavelength anomalous dispersion, containing selenomethionyl-substitutes, were produced and the structure solution is still in progress. Preliminary experiments addressing the function of the extracellular domain indicate an important role in substrate secretion and bacterial competition.

Zusammenfassung

Das Typ VII Sekretionssystem (T7SS) ist wichtig für Virulenz und Langzeit-Pathogenität von Gram-positiven Bakterien. Zu diesen gehört auch *Staphylococcus aureus*, bekannt als Kommensal und Pathogen im Menschen.
Das Typ VIIb Sekretionssystem (T7SSb) exportiert kleine, toxische Proteine, die antibakterielle Immunantworten auslösen und für bakterielle Persistenz verantwortlich sind. Außerdem ist es an dem Konkurrenzkampf zwischen Bakterien beteiligt.
Das System benötigt verschiedene Komponenten, um eine Sekretion zu ermöglichen. Diese Doktorarbeit konzentriert sich auf zwei dieser Proteine, die ATPase EssC und das Membranprotein EsaA. Beide Komponenten sind unentbehrlich für eine vollständige Funktionalität.
EssC gehört zu der Familie der FtsK/SpoIIIE ATPasen und ist evolutionär in allen T7SSs erhalten. EssC besitzt drei C-terminale, zytosolische ATPase Domänen, bezeichnet als EssC-D1, -D2 und D3, wobei EssC-D3 C-terminal gelegen ist.
In dieser Arbeit präsentiere ich die Kristallstruktur der ATPase Domäne EssC-D3, aufgelöst bis zu 1.7 Å. Die Domäne ist unabdingbar für die Sekretion. Durch die Strukturauflösung wurde eine hydrophobe, Oberflächen-exponierte Substrat-Bindetasche bestimmt, die eine essenzielle Rolle für den Export der toxischen Substrate einnimmt. Durch dieses Projekt konnten zwei Aminosäuren in dieser Tasche bestimmt werden, die für den Prozess der Substratsekretion wichtig sind. Weiterhin wurde bewiesen, dass nicht nur EssC-D3, sondern auch die ATPase Domäne EssC-D2 und/oder EssC-D1 mit den Substraten interagieren kann. Im Gegensatz zu dem verwandten T7SSb in *Bacillus subtilis*, verfügt EssC-D3 über ATPase Aktivität und ermöglicht dadurch den Substratexport.
Das Membranprotein EsaA besitzt einen extrazellulären Abschnitt, der sich durch die Zellwand von *S. aureus* erstreckt. Dieser extrazelluläre Part besteht aus einer stabilen Domäne, welche kristallisiert werden konnte und bis zu 4 Å diffraktiert. Aufgrund von fehlenden homologen Strukturen konnte die Struktur der Domäne noch nicht bestimmt werden. Für die Phasenbestimmung, die wichtig für die Strukturauflösung ist, wurden Kristalle mit Selenomethionyl-Substituten hergestellt. Die Strukturauflösung ist noch nicht beendet. Erste Experimente bezüglich der extrazellulären Domäne zeigen, dass diese ebenfalls wichtig für die

Substratsekretion und zusätzlich am Konkurrenzkampf zwischen Bakterien beteiligt ist.

Table of Contents

I. Introduction

I.1 Infections with multi-drug resistant bacteria

About 80 years ago, the discovery of penicillin and its antibiotic effect, led to a major breakthrough in clinical medicine. In the following years, different classes of antibiotics were found and their usage against bacterial infections saved millions of lives [1, 2]. However, bacterial resistance against antibiotics started to appear shortly afterwards and increased rapidly. Nowadays, the World Health Organization (WHO) considers a "post-antibiotic era", where common infections become a serious issue again, a possible scenario for the 21st century [3].

One of the biggest concerns is the methicillin-resistant *Staphylococcus aureus* (MRSA) [4]. MRSA strains have spread worldwide and show resistance against methicillin and its derivatives. The resistance is mediated by the alternative penicillin-binding protein (PBP2a), which is encoded by *mecA* on the staphylococcal cassette mec (SCCmec), a mobile genetic element. At least six different types of SCCmec are known and exclusively encode resistance genes for β-lactam antibiotics [5, 6]. MRSA causes one of the most frequently occurring infections and is difficult to treat because of its multi-drug resistance. In 2017 for example, 324 000 hospitalizations due to MRSA infections were estimated and the deaths due to these infections surmounted to 12 000 people. This number corresponds to 1/3 of deaths, which are related to multi-drug resistant bacteria [7]. Earlier on, *S. aureus* was described as a hospital-associated pathogen. Patients were often infected because of poor hygienic measures in hospitals. Health care-associated infections (HAIs) decreased by about 50 % between 2005 and 2011 as a result of more aggressive hygienic measures. In contrast, community-acquired MRSA infections started to increase and do not follow the trend of HAIs [8, 9]. Moreover, the spreading of MRSA in animals raises a major concern as well [10, 11].

Apart from penicillin-like β-lactam antibiotics, *S. aureus* is already resistant against, other drugs like glycopeptides, which is why linezolid or newly found β-lactams are being used to treat MRSA infections. Meanwhile there is evidence that MRSA has developed resistance against glycopeptides and linezolid, too [12, 13]. These facts should lead to the conclusion that *S. aureus* infections have to be elucidated in more detail to develop new drug therapies.

I.2 *Staphylococcus aureus*

I.2.1 Commensal and opportunistic pathogen

Staphylococci are Gram-positive bacteria, which can infect both humans and animals. One of the most pathogenic species is *S. aureus* [14]. It is round-in shape (coccal), forms grape-like clusters and when grown on a blood agar plate, presents golden colonies caused by the production of carotenoid staphyloxanthin [15, 16]. As a Gram-positive bacterium, *S. aureus* is shielded from the environment by a single lipid membrane and a 20-40 nm thick cell wall, which is composed of a peptidoglycan layer and a polysaccharide capsule [17].

Usually, *S. aureus* acts as a commensal and colonizes 30 % of the human population, preferably colonizing the nasal cavities [18]. This nasal colonization has a great influence on contracting a nosocomial or community acquired bacteremia [19], which can lead to severe diseases like endocarditis, septic arthritis, osteoarticular, skin, soft tissue and pleuropulmonary infections. Another grave risk factor in contracting a nosocomial bacteremia are implantated prosthetic devices [20, 21]. Why *S. aureus* shifts its behavior from the commensal to the pathogenic state remains still unclear [22]. It was reported that specific genes (*sdrC*, *fnbA*, *fhuD*, *sstD*, and *hla*) are upregulated when acting as a pathogen. These genes encode pore-forming toxins and proteins, which are involved in biofilm formation and iron-uptake [23]. During an acute infection, *S. aureus* secretes several pore-forming exotoxins (α-toxin, γ-toxin, PVL, LukAB, LukED and LukMF), which lyse different cell types, like leukocytes, erythrocytes, endothelial cells of blood vessels and epithelial tissue, as well as the β-toxin, which makes cells vulnerable to other components [24]. Additionally, the bacterium needs several defense mechanisms to survive and successfully disseminate in the bloodstream. *S. aureus* possesses various tools to defend and evade the innate and adaptive immune system.

I.2.2 Defense mechanism to evade the host immune system

S. aureus circulates in the bloodstream and thereby reaches peripheral organs. This is an important step to start several infection sites. In order to survive in the host, *S. aureus* had to evolve various mechanisms to overcome the innate and acquired immune system (Fig. 1). For example, it can tackle neutrophil attacks by: 1) releasing phenol-soluble modulins (PSMs), which disrupt the neutrophilic plasma membrane

[25], 2) producing staphyloxanthin to neutralize neutrophils [26], 3) secreting the chemotaxis inhibiting protein (CHIP), to keep neutrophils away from the infection site [27] and 4) evading the extracellular DNA (eDNA), which is produced by neutrophils to bind pathogens through expression of a nuclease [28]. *S. aureus* is able to survive when phagocytized by polymorphonuclear leukocytes and uses them as vehicles to enter tissues [29]. Additionally, *S. aureus* can avoid phagocytosis by releasing a protein called clumping factor A (ClfA). ClfA, a cell-wall anchored sortase, binds to fibrinogen and induces staphylococcal agglutination. Thereby *S. aureus* circumvents phagocytosis [30]. CflA is also involved in the adhesion to the vascular epithelium [31].

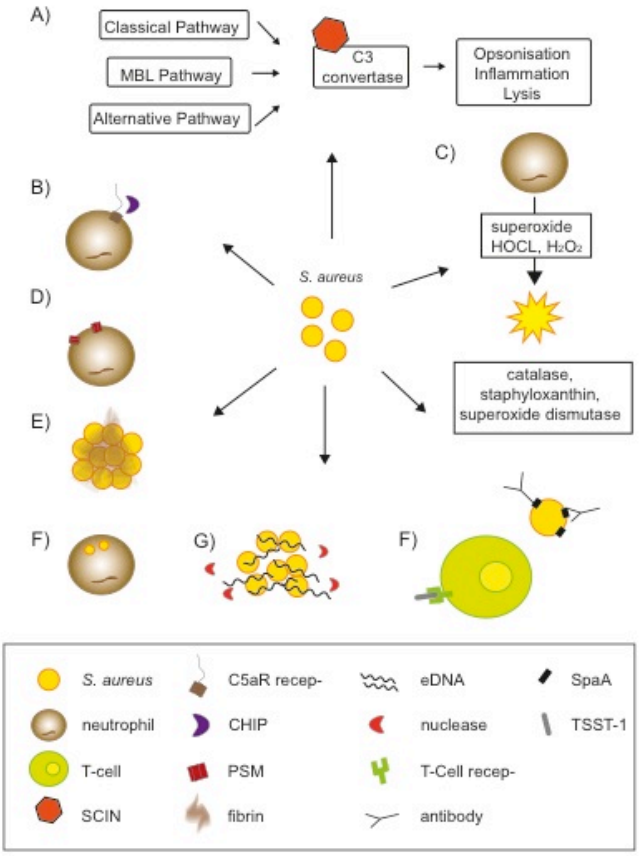

Fig. 1: Defense mechanism of *S. aureus* to evade the human immune system.
A) Inhibition of the complement system by using the staphylococcal complement inhibitor (SCIN). B) Interference with neutrophil chemotaxis by secretion of the chemotaxis inhibiting protein (CHIP). C) Neutralization of ROS using specific pigments and enzymes. D) Destruction of the neutrophil membrane using phenol-soluble modulins (PSMs). E) Agglutination using clumping factor A to bind fibrin and thereby avoid phagocytation. F) Bacteria survive in neutrophils and use them as carriers. G) Evasion from the extracellular DNA (eDNA) by secreting a nuclease, which can cleave eDNA. F) Inactivation of the acquired immune system by releasing toxins: The toxic shock syndrome toxin-1 (TSST-1)) binds to the T-cell receptor. Staphylococcal protein A (SpA)) is expressed on the bacterial surface and binds to antibodies.

Another major component of the innate immune system is the complement system, which can be deactivated by *S. aureus*. A key role in all three complement pathways plays the convertase C3. *S. aureus* secretes the staphylococcal complement inhibitor (SCIN), which binds and inhibits the C3 convertase. Consequently, phagocytosis, opsonization and all downstream processes are impaired [32]. Another mechanism to circumvent the innate and acquired immune system, is to signal the end of an inflammation. When excessive tissue damage is caused, a high adenosine concentration is a key signal for the innate and acquired immune system in order to stop the inflammation response. *S. aureus* encodes a gene for an adenosine synthase, which catalyzes ADP and AMP producing adenosine and thereby mimics the end of an infection [33]. *S. aureus* also contains other components that interfere with the acquired immune system. For example, it secretes the toxic shock syndrome toxin-1 (TSST-1) and staphylococcal protein A (SpA), which in turn impair B- and T-cell responses [34, 35]. SpA is also able to bind to the Fc part of antibodies and thereby prevents opsonophagocytation of *S. aureus* [35]. The pathways of defense mechanisms presented here, demonstrate that *S. aureus* has a broad spectrum to counteract the host immune system.

I.2.3 Staphylococcal abscess formation and replication

When *S. aureus* enters a peripheral organ, it starts to form abscesses and thereby destroys healthy tissue. Staphylococcal abscess formation can be described in four stages, starting from the bacteremia until rupture of the abscess to release *S. aureus* progeny (Fig. 2) [36, 37]. In stage I, *S. aureus* spreads through the body using the blood system and evades the host immune system with its several defense mechanisms, which are described in I.2.2. While dissemination to peripheral organs occurs within 3 h, histopathological abscess formation cannot be noticed until 48 h after contraction. In the second stage, *S. aureus* begins an infection by entering the tissue of a peripheral organ and starts its abscess formation. Immune cells are being sent to the inflammation site, actively recruited by *S. aureus* and thereby contributing to tissue damage. At the third stage after four to five days, the bacteria build a central staphylococcal abscess community (SAC), which is surrounded by an eosinophilic pseudocapsule containing fibrinogen deposits, followed by a ring of healthy and necrotic immune cells and defined by a rim of fibrin and extracellular matrix. Shielded from the immune cells, *S. aureus* is then able to replicate. The abscess matures over

weeks and destroys healthy tissue. In the last stage, the abscess bursts and *S. aureus* can spread through the body to infect new organs [38]. In stage IV, two components were described to assume a key role: the extracellular adhesion protein (Eap) and the Type VIIb secretion system (T7SSb). Eap was reported to act in several ways. On the one hand, it can interact as a super-antigen, inducing pro-inflammatory cytokine production, on the other hand, it interferes with neutrophil attacks and T-cell activation [39, 40]. The Type VII secretion system (T7SS) was first observed in *Mycobacterium tuberculosis* and linked to virulence and pathogenicity [41, 42]. Since then, several studies were published, describing various functions of the T7SS. In *S. aureus*, the T7SSb is involved in abscess maturation and long-term persistence of an infection [43]. Therefore, a detailed investigation of this system will be helpful to develop new strategies to tackle *S. aureus* infections.

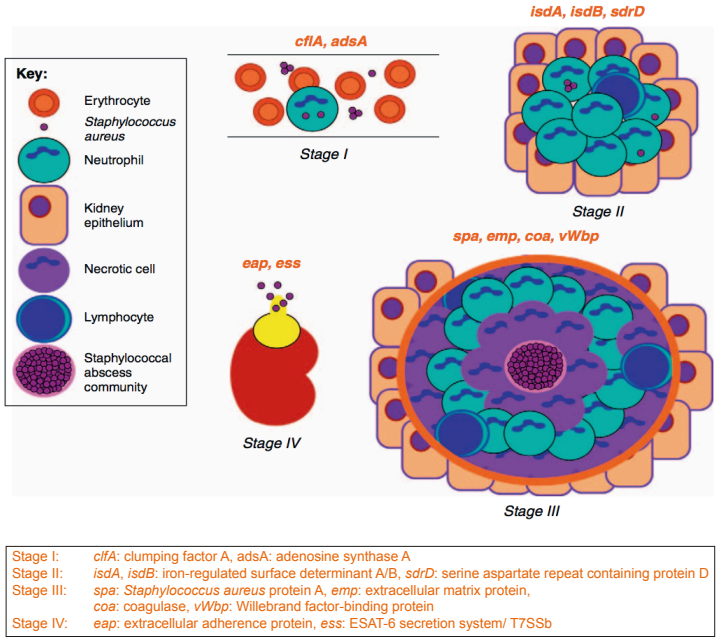

Fig. 2: Working model for staphylococcal abscess formation in four stages.
Up-regulated genes are indicated for every stage (*cursive*, orange)[a]. Stage I: *S. aureus* survives in the bloodstream and evades the immune system. Stage II: *S. aureus* enters peripheral tissue and attracts immune cell. Staphylococcal abscess formation starts. Stage III: Staphylococcal abscess community (SAC) is formed in the center of the abscess. The SAC is surrounded by fibrin deposits (pink rim), necrotic and healthy immune cells and shielded from the surrounding area by eosinophilic material (orange rim). Stage IV: The abscess ruptures and *S. aureus* is released. The T7SSb secretion system designated is as *ess*. Figure adopted from [36] with permission of the publisher.

[a] *clfA*: clumping factor A, *adsA*: adenosine synthase A, *isdA*, *isdB*: iron-regulated surface determinant A/B, *sdrD*: serine aspartate repeat containing protein D, *spa*: *Staphylococcus aureus* protein A, *emp*: extracellular matrix protein, *coa*: coagulase, *vWbp*: Willebrand factor-binding protein, *eap*: extracellular adherence protein, *ess*: ESAT-6 secretion system/ T7SSb

I.3 The Type VII secretion system

Bacteria use several secretion machineries to interact with their environment. Secretion systems have various tasks, such as lateral gene transfer, export of various proteins involved in signaling pathways, host interaction, virulence or nutrient scavenging, [44] and therefore work in different ways. The type III secretion system for example, is present in Gram-negative bacteria and injects bacterial effector proteins directly into the eukaryotic host cell using a long needle filament [45]. On the other hand, the type IV secretion is widely spread in Gram-positive and Gram-negative bacteria and is known to mediate conjugation of plasmid DNA as well as protein export. Accordingly, it differs in its architecture among bacteria [46].

The T7SS is restricted to Gram-positive bacteria. About 17 years ago the system was found in the Actinobacterium *Mycobacterium tuberculosis* and was linked to its pathogenicity and virulence [41]. Two small toxins, designated as ESAT-6 (early secreted antigenic target-6) and CFP-10 (culture filtrate protein-10kDa), were determined to produce a strong T-cell immune response [47, 48]. Since then architecture and function of the T7SS has been under investigation.

It was shown that not only Actinobacteria like *Mycobacterium tuberculosis*, *Mycobacterium bovis, Mycobacterium smegmatis* and *Thermomonospora curvata* comprise a T7SS [49, 50], but also bacteria belonging to the phylum Firmicutes such as *S. aureus, Streptococcus intermedius*, *Streptomyces coelicolor*, *Geobacillus thermodenitrificans*, *Bacillus subtilis* and *Bacillus anthracis* [43, 51-55]. To differentiate between the T7SS of Actinobacteria and Firmicutes, the two systems are now being called T7SSa and T7SSb, respectively. Both machineries share three conserved proteins: the virulence factors ESAT-6 and CFP-10, now called EsxA and EsxB, and an ATPase protein, which belongs to the FtsK/SpoIIIE family [51]. Both T7SSs require a set of different genes to mediate substrate translocation (Fig. 3, Fig. 6).

I.4 The T7SSa in Actinobacteria

I.4.1 The different T7SSa/Esx machineries in mycobacteria

Mycobacteria can contain up to five gene loci for the T7SSa. They are designated as Esx-1 to Esx-5 and differ in their function, as well as in their protein composition (Fig. 3) [50, 56]. Esx-1 is responsible for virulence of the bacteria by secreting the small

toxins EsxA and EsxB, which are missing in the attenuated vaccine strain *M. bovis* bacilli Calmette-Guérin [42]. *M. tuberculosis* is phagocytized by macrophages. Bacteria, which express the Esx-1, lyse the membrane of the phagolysosome and translocate into the cytosol [48]. In addition, Esx-3 and Esx-5 contribute to full virulence of the bacteria. Esx-3 is encoded in pathogenic and non-pathogenic mycobacteria and maintains cell survival [57] as well as iron/zinc acquisition and homeostasis [58]. Secreted proteins called EsxG and EsxH, which are required for iron uptake, have another role in pathogenic strains and contribute to virulence [59]. It is proven that EsxH inhibits the activation of T-helper cells ($CD4^+$) and the ability of effector $CD4^+$ T-cells to recognize infected macrophages [60]. Esx-5 is only present in slow-growing strains [61], which most of the pathogenic ones are. It is linked to nutrient uptake and secretes effector proteins, that are involved in immune evasion and virulence [62, 63]. These effector proteins, called PE/PPE, interact with the host immune receptors, for example the toll-like receptor 2, and the inflammasome [64]. The importance of Esx-5 concerning the nutrient uptake, involves the ability to permeabilize the outer membrane. Thereby, nutrients and fatty acids can be acquired, while bacterial resistance is still being maintained [63]. The function of Esx-2 is not yet known and protein secretion could not be observed [65, 66]. Esx-4 is described as the most ancestral T7SS and comprises fewer genes compared to the other Esx systems [61]. It was proposed that the Esx loci have evolved from the Esx-4 but so far, no function for Esx-4 in *M. tuberculosis* could be assigned. However, *Mycobacterium abscessus*, which is lacking the Esx-1 locus, needs Esx-4 for survival/replication. It is speculated that Esx-4 adopts the function of Esx-1 in *M. abscessus* [67].

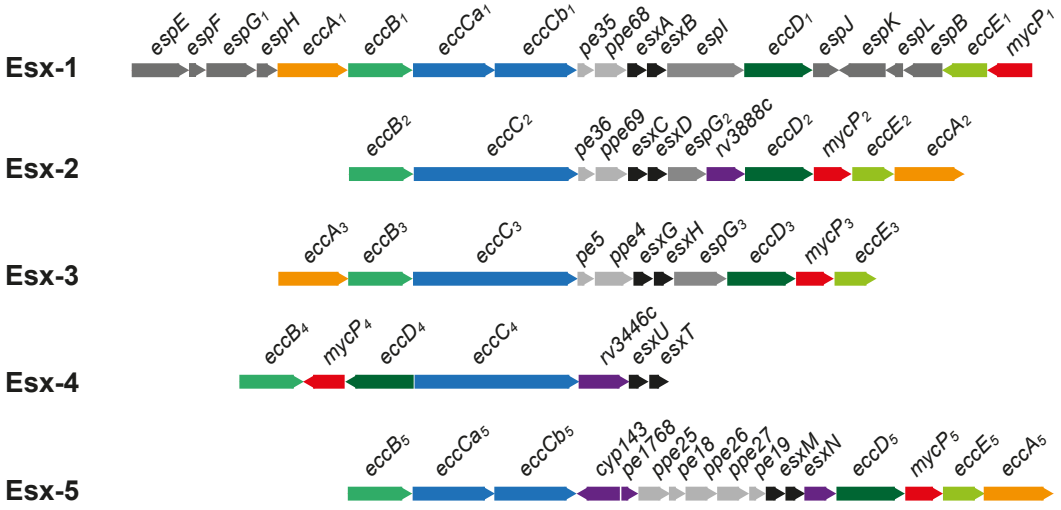

Fig. 3: Genomic organization of the five Esx loci in *M. tuberculosis*.
Conserved genes for ATPase are shown in blue, genes of core membrane proteins in green, mycosin in red, secreted proteins of WXG100 family in black, Esp and PPE/PE proteins in grey, soluble proteins in orange, region specific genes in purple. Figure adapted from [50], published under CC BY 4.0.

I.4.2 The core components of the T7SSa

Although T7SSa have different functions, they contain a set of five conserved membrane components, called EccB, EccC, EccD, EccE and MycP, which are essential for substrate translocation (Fig. 3) [68-70]. Esx-4, as the most archaic Esx-system, lacks the EccE. It therefore could be speculated, that EccE was dispensable for a mechanistically active T7SS. EccE has a molecular weight (MW) of 44 kDa and contains two transmembrane helices and an extracellular domain. EccB has a MW of 51 kDa, comprising a periplasmic N- and cytosolic C-terminal domain, which are connected by one transmembrane domain [70, 71]. The N-terminal domain was proposed to have ATPase activity and therefore should facilitate translocation of the substrates through the mycomembrane. Nevertheless, the question whether ATP is present in the periplasma, remains unclear and contradicts with this hypothesis [72, 73]. The hydrophobic EccD forms a dimer and possesses a N-terminal ubiquitin-like domain, followed by 11 transmembrane helices. Therefore, the protein was suggested to build a channel for the substrate export [71]. The EccD dimer forms a channel, which is hydrophobic and occupied by lipids, however, this pore is too small to transport hydrophilic, folded heterodimers and there is no evidence for a mechanism to open and close the pore. EccD is in consequence not considered to

contribute to the channel formation for substrate secretion [71, 74, 75]. The ATPase EccC belongs to the FtsK/SpoIIIE family and consists of two transmembrane helices and four ATPase domains. EccC has three functions: 1) hydrolyze ATP for substrate translocation, 2) interact with Esx substrates and 3) form the translocation channel [76, 77]. EccC will be described in more detail in I.7.4. The fifth core component, MycP, is a membrane-anchored protease belonging to the subtilisin family. Although the protease is not tightly associated with the secretion complex, MycP is essential for substrate secretion and stabilization of the core machinery from Esx-1 and Esx-5 [78, 79]. So far only one substrate was identified for MycP in Esx-1. It cleaves the C-terminal part of the substrate EspB. Nonetheless, proteolytic activity does not influence substrate secretion [69].

I.4.3 Assembly of the T7SSa core machinery

Information of complex assembly for the mycobacterial Esx-1, Esx-3 and Esx-5 are published. First studies addressing the stoichiometry of Esx-1 and Esx-5, calculate the normalized spectral abundance factor (NSAF). A ratio of 4:9:7:4:1 for EccB, EccCa, EccCb, EccE and EccD of Esx-1 from *M. tuberculosis* was hereby determined. NSAF analysis for Esx-5 from *M. tuberculosis* proposed a 1:2:1:1 ratio for EccB, EccC, EccE and EccD [79]. This result differs from the study of Houben et al.. In this study an antibody pull down was performed and revealed a ratio of 2:2:1:2 for the Esx-5 machinery, built up by EccB, EccC, EccE and EccD, respectively [70]. Beckham et al. provided structural insights, up to 13 Å, of the Esx-5 from *M. xenopi* by using electron microscopy (EM). The dimensions of the Esx-5 core complex suggested that the machinery is located in the inner membrane and has a six-fold symmetry. Further experiments, using labeling of the core components, were applied to define the localization of the T7SSa components in the EM map. EccC forms the central pore. EccB and EccD span around the ATPase, followed by EccE at the periphery [80]. A recently published study, using the technique of EM as well, discovered the assembly of a 900 kDa complex of the Esx-3 in *M. smegmatis*. Two identical protomers, consisting of EccB, EccC, EccD and EccE (ratio 1:1:2:1), formed a dimer. The structure of a single protomer was solved up to 3.7 Å. The EccC is present at the center of the pore and therefore suggested as pore forming protein, followed by EccB, which builds a fork at the periplasmatic site. This fork is important for complex stability. The two copies of EccD face each other in an antiparallel

fashion and build the scaffold for the Esx-3. The two EccDs interact with either EccB or EccE. As shown for the Esx-5, EccE is located at the periphery of the complex [74]. Both studies, Famelis et al. and Beckham et al., reported flexible domains in the cytosol, which were designated to the ATPase domains of EccC and a central pore with sufficient width (up to 5 nm diameter) to be able to transfer folded Esx dimers (Fig. 4) [74, 80]. Moreover Famelis et al. provided a mechanistic model for the pore opening. EccC contains a fourth ATPase domain, the DUF domain, which is linked to a stalk domain. The stalk domain connects the ATPase domains to the membrane and has extensive contact to two N-terminal helices of EccB. Substrate binding and subsequent ATPase hydrolysis of the ATPase domains, including the DUF domain, could directly trigger a conformational change, resulting in pore opening and closing [74].

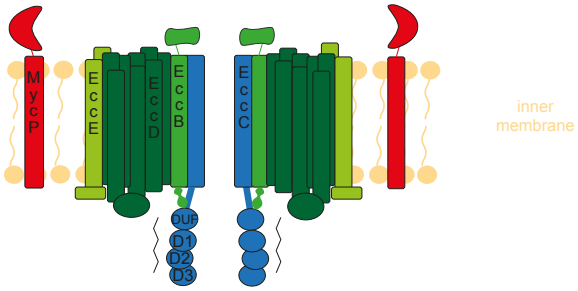

Fig. 4: Model of the core machinery from the T7SSa secretion system.
EccC (blue) is the pore forming protein surrounded by the membrane components EccB, EccD and EccE. EccB is in contact with the EccC and could mediate pore opening/closing. DUF, D1, D2, D3 indicate ATPase domains of EccC (blue). Black lines around the ATPase domains illustrate their flexibility.

I.4.4 Substrates of the T7SSa

Every Esx locus contains homologous genes to *esxA* and *esxB*, which belong to the WXG100 superfamily (Fig. 3) and build heterodimers, consisting of antiparallel α-helices (Fig. 5). EsxA/B are secreted by the Esx-1. The C-terminus of EsxB comprises a signal sequence Yxxx[D/E] (x= any amino acid (aa)), which is required for substrate translocation [81, 82]. It is known that Esx-1, Esx-3 and Esx-5 encode two other kinds of small proteins, which are secreted by the systems, called Esp and PE/PPE proteins (Fig. 3) [66]. These proteins show structural characteristics to EsxA/B. PE and PPE form a heterodimer, built up by a helix-bundle oriented in an antiparallel fashion. PPE contains the WXG motif and PE comprises the signal

sequence at the C-terminus (Fig. 5) [83, 84]. For the Esp proteins (Esx secretion-associated protein), it could be confirmed that EspC and EspF contain the secretion signal at the C-terminus and EspA and EspE comprise the WXG motif. Thus, EspC and EspA, as well as EspF and EspE form a complex and might be secreted as heterodimers [85]. An exception is EspB, which is secreted as a monomer, comprising the characteristically antiparallel helix-bundle, the WXG motif and the Yxxx[D/E] secretion signal [83]. Apart from the secretion signal, the C-terminal part of the substrates is important for interaction with the T7SS. This interaction will be addressed further in chapter I.7.2. Taken together, apart from EspB, all substrates will be secreted as heterodimers, comprising a side-by-side anti-parallel helix fold, the WXG motif and the C-terminal secretion signal Yxxx[D/E].

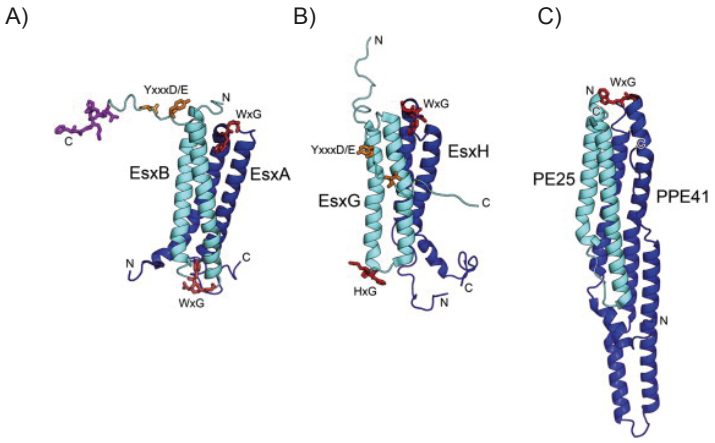

Fig. 5: Ribbon presentation of T7SSa substrates.
A) EsxA/EsxB, B) EsxG/EsxH and C) PE25/PPE41. The WXG motif is highlighted in red and Yxxx[D/E] secretion signal is shown in orange. Figure adopted from [66] with permission of the publisher.

I.5 The Type VIIb secretion system in Gram-positive bacteria

Bioinformatical studies showed that the T7SS is encoded in a broad range of Gram-positive bacteria [51]. Homologues of the two small WXG proteins EsxA and EsxB and the ATPase protein were found. Apart from these homologues, the protein composition of the T7SSb varies from the T7SSa and seems less complex (Fig. 6). Gram-positive bacteria encode only one T7SSb locus [51]. The T7SSb is not as well understood as the T7SSa. Most studies concern the translocation machinery of *S. aureus* and *B. subtilis* also known as Ess and Yuk pathways, respectively.

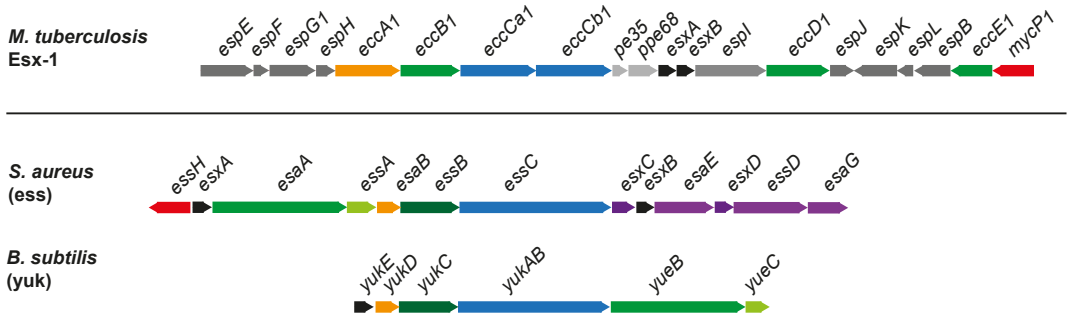

Fig. 6: Genomic organization of the T7SSb of *S. aureus* and *B. subtilis* compared to T7SSa. Conserved ATPase is shown in blue, membrane proteins in green, protease in red, secreted proteins of WXG100 family in black, Esp and PPE/PE proteins in grey, soluble proteins in orange, region specific genes/others in purple. Figure adapted from [86] with permission of the publisher.

The Yuk locus encloses six genes, designated as *yukAB*, *yukC*, *yukD*, *yukE*, *yueB* and *yueC*. YukE comprises the WXG motif and is secreted as homodimer when the other five components are expressed [87]. *YukAB* encodes the ATPase, belonging to the FtsK/SpoIIIE family. It contains three ATPase domains, whereby only ATPase activity of the N-terminal ATPase domain is required for substrate secretion [88]. The structure of YukD was solved and showed a strong resemblance to ubiquitin, although the typical double glycine motif at the C-terminal tail is missing. This motif is essential for ubiquitin to conjugate with other proteins [89]. The YueB comprises six transmembrane domains and an extracellular segment, extending through the cell wall and acting as phage receptor [90]. The protein composition of the Yuk system shows similarities to the translocation machinery of *S. aureus* [87].

Streptococcus intermedius contains a T7SSb as well. Recent studies address the secretion of effector proteins belonging to the LXG protein family via the T7SSb. The T7SSb is not well characterized, but deletion of the conserved ATPase EssC abrogates translocation of the substrates [91]. The proteins of the LXG protein family, called TelA, TelB and TelC, exert bacterial toxicity and therefore can only be expressed with their antitoxins, designated as TipA, TipB and TipC. These antitoxins are encoded in close proximity to their effector toxins (Fig. 7) [91, 92].

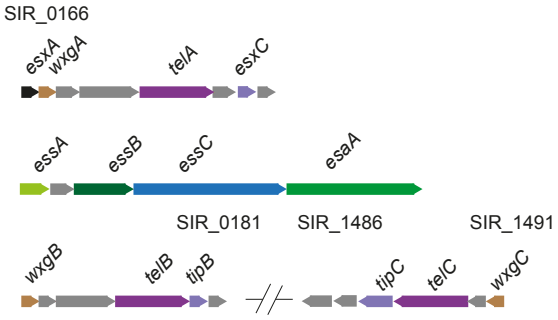

Fig. 7: Genomic presentation of the T7SSb and LXG proteins of *Streptococcus intermedius* strain B196.
T7SS components are shown in green and blue, secreted Esx substrate in black, secreted LXG toxins in dark purple, immunity proteins in light purple, WXG100-like proteins in brown, other proteins in grey. Figure adapted from [91], published under CC0 1.0.

I.6 The T7SSb in the pathogenic *S. aureus*

Initially, the T7SSb in *S. aureus* was called the Ess pathway. Therefore, genes were designated as *ess* (ESAT-6 like secretion system), *esa* (ESAT-6 like secretion accessory) or *esx* (ESAT-6 like secretion extracellular).

Firstly, this nomenclature pointed out which proteins are indispensable for substrate secretion (Ess), secreted proteins (Esx) and proteins belonging to the T7SSb locus but are not required for substrate translocation [93]. During the last 15 years, more information about the T7SSb became available, revealing that proteins, which were thought to be dispensable for the substrate secretion, are actually necessary for the translocation process. Hence, the nomenclature does not reflect protein function anymore.

The T7SSb has been found in strains with the multi-locus sequence type clonal complex (CC) 8, CC5 and CC1. The strains Newman, USA300, RN6390, COL and SA113 for example, belong to the CC8 [77]. It has been reported that the T7SSb locus has an operonic organization enclosing 12 genes starting with the small substrate *esxA*. However, an investigation of five *S. aureus* strains from the CC8 showed, that *esxA* is a monocistronic gene in RN6390 and Newman, but not in COL, USA300 and SA113 [93]. Moreover, another component, *essH*, was detected and is located upstream of *esxA*. *EssH* does not belong to the T7SSb operon but is required for substrate secretion (Fig. 8) [94].

I.6.1 The T7SSb core machinery in *S. aureus*

EsxA and *esxC* frame four membrane proteins of the T7SSb, called EsaA, EssA, EssB and EssC (Fig. 8). First studies using nucleotide insertions revealed, that EssA, EssB and EssC are responsible for substrate secretion. EssA has a MW of 17 kDa, a transmembrane and an extracellular domain but its function is not known yet [43]. EssB has a MW of 52 kDa and forms a dimer. It has a transmembrane, an internal and external domain, whereby the N-terminal part has similarities to a serine/threonine kinase. It therefore is considered to be involved in protein-protein interaction [95]. The EssC (171 kDa) belongs to the FtsK/SpoIIIE family. It compromises two N-terminal forkhead-associated domains (FHA), a DUF and three ATPase domains, which are interconnected by two transmembrane helices [43, 51]. The ATPase will be described in more detail in I.7.5. Burts et al. showed that EsaA is not required for substrate secretion. They inserted transposons into *esaA*, *essA*, *essB* and *essC* and tested for substrate secretion. Secretion was abolished in *essA*, *essB* and *essC* mutants, but not in *esaA* mutants [43]. On the contrary, a deletion mutant of *esaA* was not able to export EsxA and EsxC anymore. Consequently, EsaA belongs to the core machinery of the T7SSb [93]. EsaA has a MW of 118 kDa and contains six membrane helices and an extracellular segment, spanning through the cell wall [96]. Taken together, all four membrane proteins are required for an active system. These observations led to the hypothesis that the membrane proteins interact with each other and build the T7SSb machinery.

A small cytosolic component of the T7SSb is EsaB. It has a MW of 10 kDa and is located between *essA* and *essB* in the operon (Fig. 8A). EsaB is structurally related to the YukD of *B. subtilis*. It shares a similar fold to ubiquitin but lacks the C-terminal double glycine motif required for conjugation with other proteins [97]. Studies with transposon insertion, using the strains Newman and USA300, showed that substrate secretion was not affected but an increase in the EsxC mRNA level was detected [43, 98]. Thereupon, EsaB was believed to be important for regulation of EsxC expression but not for substrate secretion. In contrast, Casabona et al. showed, that EsaB is a core component for the T7SSb in the *S. aureus* strain RN6390. The deletion of *esaB* abrogated EsxA and EsxC secretion and had no effect on the expression level of Esx substrates. Hydrophilic amino acids, which were conserved among EsaB homologues in Firmicutes, were found in EsaB. These amino acids all

face the same side of the small protein. An alanine scan of the amino acids confirmed, that the mutation of threonine at position 8 to alanine, abolishes secretion. However, the study could not determine whether the function of EsaB is altered because of the T8A mutation or if it interferes with protein folding. Finally, Casabona et al. suggested that EsaB interacts with T7SSb components and is responsible for post-translational modification [97].

Recently, another component of the T7SSb was explored. A hydrolase, designated as EssH and located upstream of *esxA*, is required for Esx substrate secretion as well. EssH is exported outside of the bacteria using the Sec pathway. The hydrolase is able to cleave wall peptides and pentaglycine bridges in order to open the way for the substrates through the 20 to 40 nm thick bacterial cell wall. A deletion mutant of EssH was unable to secrete Esx substrates [94].

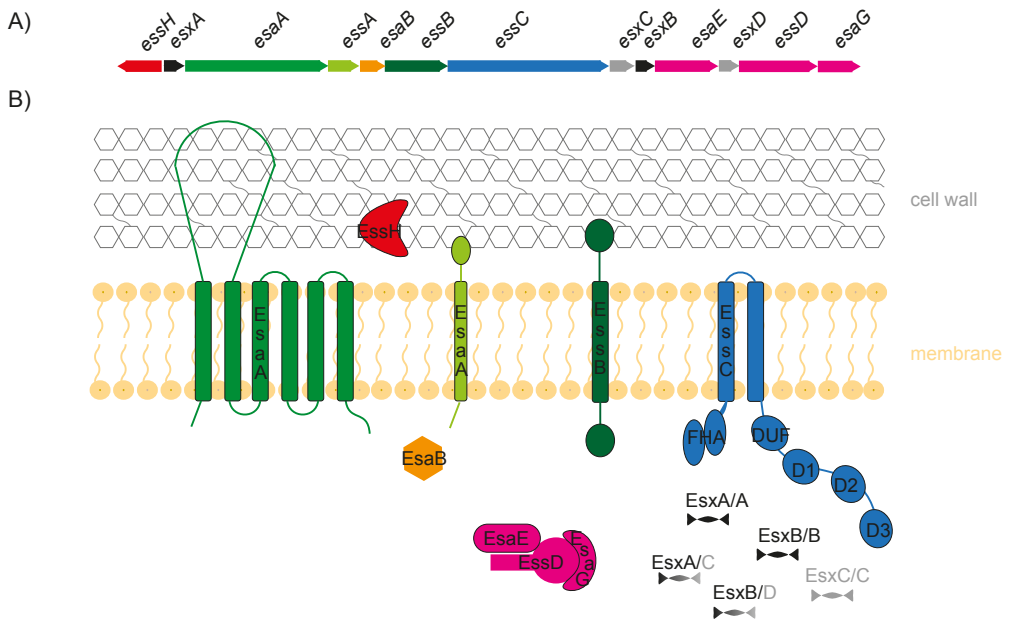

Fig. 8: Schematic representation of the T7SSb from *S. aureus*.
A) Genomic organization of the T7SSb operon, B) Topology of proteins in corresponding colors to A). Membrane proteins are shown in green and blue, secreted proteins in grey and black, toxin-antitoxin complex in pink, cytoplasmic protein in orange and extracellular protease in red. *EssH* does not belong to the T7SSb operon.

I.6.2 Interaction of the T7SSb core components in *S. aureus*

All four membrane proteins, as well as the cytosolic protein EsaB, are indispensable for substrate secretion and therefore considered to build the core machinery of the

T7SSb. Studies concerning the T7SSa, showed interaction of the core components and determined 1 MDa to 1.5 MDa complexes [74, 80]. So far, no similar study for the T7SSb has been published. First attempts by Jäger et al. reported no interaction between the four membrane proteins using *in vivo* and *in vitro* crosslinking techniques. Nevertheless, they could show homo-oligomerization of EsaA, EssB and EssC [99]. In contrast, Ahmed et al. demonstrated binding of EsaA to the transmembrane domain of EssB using *in vitro* crosslinking experiments and bacterial two-hybrid assays [100]. Another protein, Flotillin A, was indentified to contribute to the assembly of the secretion machinery. Flotillin A is a scaffold protein, mediating interaction of proteins in bacterial membranes [101]. However, the general T7SSb architecture, the stoichiometry of proteins or specific protein interaction of all membrane proteins are still not known.

I.6.3 Substrates of the T7SSb in *S. aureus*

The T7SSb encodes four genes of small virulence factors, called *esxA*, *esxB*, *esxC* and *esxD*. They are ~100 amino acids long and form homo- and heterodimers: EsxA•EsxA, EsxA•EsxC, EsxB•EsxB, EsxB•EsxD, EsxC•EsxC (Fig. 8B) [102, 103]. In contrast to the mycobacterial substrates, EsxA and EsxB do not form heterodimers. EsxA and EsxB contain the WXG motif and therefore belong to the WXG100 protein superfamily [51]. The EsxA structure exhibits two side-by-side antiparallel helices, whereby the hairpin bend comprises the WXG motif (Fig. 9) [103]. Both proteins play an important role in long-term persistence [43]. It was shown that EsxA delays apoptosis of infected epithelial cells [104] and that EsxB interferes with regulatory and anti-inflammatory cytokine production [105].

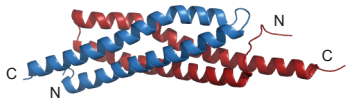

Fig. 9: Ribbon presentation of the EsxA homodimer of *S. aureus*.
Monomers are highlighted in blue and red. Figure adopted from [103] with the permission of the publisher.

EsxC and EsxD do not have a WXG motif but are substrates of the T7SSb. While EsxC was shown to be required for *S. aureus* persistence [98], EsxD contains the Yxxx[D/E] secretion signal [102], important for substrate translocation of mycobacterial proteins. Poulsen et al. showed that also a broader conserved pattern,

Hxxx[D/E]xxhxxxH (h=less conserved hydrophobic aa, H=highly conserved hydrophobic aa, x=any aa) at the C-terminus of T7SS substrates, functions as a secretion signal. This pattern was found in EsxA and EsxD of *S. aureus* [106]. Anderson et al. reported that deletion of one of the four Esx substrates, diminished secretion of all of them in *S. aureus* USA300 [102]. Consequently, every Esx protein might have a distinct role during the translocation process in the strain USA300.

Another component of the T7SSb, which was thought to be a membrane protein for a long time, is EssD, also called EsaD. It has been demonstrated that EssD is not required for secretion of the small Esx substrates, but increases *S. aureus* long-term persistence [107]. In 2017, it was discovered that EssD, which has a MW of 58 kDa, is another substrate of the T7SSb. It contains a domain for nuclease activity and therefore is important for bacterial competition. It can only be expressed with EsaG, which inhibits the nuclease activity in the cytoplasm. This toxin-antitoxin complex is known as polymorphic toxin system. Apart from EsaG, EssD expression depends on another protein, called EsaE. EsaE stabilizes EssD and mediates interaction with the ATPase EssC. Therefore it is important for the secretion process. Taken together, EsaG and EsaE are responsible to maintain EssD in a secretion-competent and catalytic inactive conformation until EssD secretion (Fig. 8) [108].

I.7 The conserved ATPase of the T7SS

I.7.1 The FtsK/SpoIIIE protein family

The ATPase of the T7SS is conserved among the phyla Actinobacteria and Firmicutes. The EccC/EssC belongs to the protein family FtsK/SpoIIIE and plays a key role in the secretion machinery.

Members of the FtsK/SpoIIIE family can be found in a broad range of species and facilitate a variety of processes. For example, they are involved in conjugation and DNA packing of eukaryotes, bacteria and viruses [109]. FtsK and SpoIIIE transport double stranded (ds) DNA and contain four N-terminal transmembrane helices, followed by three cytosolic ATPase domains designated as α, β and γ domain [110]. SpoIIIE is required for chromosomal DNA translocation in *B. subtilis* from the mother cell to the prespore [111]. SpoIIIE builds active hexamers, which bind to specific recognition patterns on the dsDNA. Cycles of ATP binding and hydrolysis create the conformational motion to transport the dsDNA across bacterial membranes. Whether

hexamerization of SpoIIIE is induced by DNA binding or if SpoIIIE assembles into a hexamer prior to DNA binding, is still under discussion [112].

FtsK acts in the late stage of chromosomal segregation in *E. coli* and most eubacteria. Initially it was identified as member of the RecA-family. Proteins of this family build hexameric ring structures, including nucleotide-binding pockets between the subunits [113]. Hexameric ring formation of FtsK was confirmed by EM and depends on DNA binding. Massey et al. proposed a "rotary inchworm model" for DNA translocation (Fig. 10). In this model, DNA is passed from subunit to subunit of the hexamer, whereby the α- and β-domains undergo a conformational change and push the DNA downwards. This process is energized by ATP hydrolysis [114].

Taken together, FtsK/SpoIIIE ATPases build active hexamers, bind and transport substrates and deliver energy for the translocation process by ATP hydrolysis.

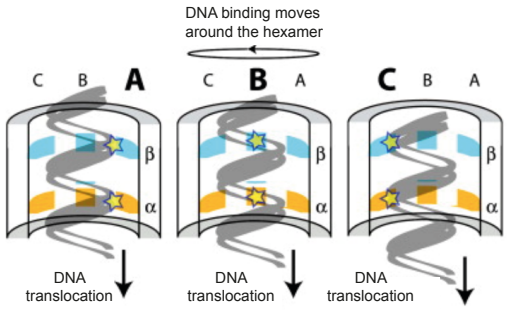

Fig. 10: Rotary inchworm model of DNA translocation by hexameric FtsK.
Within a hexameric ring, DNA is passed around the subunits (A, B, C, active subunit indicated by stars), and continuously translocated downward. Figure adopted from [114] with the permission of the publisher.

I.7.2 The VirB/D4 of T4SS-an ATPase with coupling function

The T4SS is widely spread among bacteria (Gram-positive, Gram-negative and *archae*) [115] and translocates DNA and proteins in a cell-to-cell contact dependent manner. One of the best-characterized T4SS is the VirB/D4 machinery of the Gram-negative bacterium *Agrobacterium tumefaciens*. The VirB/D4 has four major components, among them the type IV coupling protein (T4CP) VirD4 [116]. The T4CP has the ability to interact with T4SS substrates, which contain one or two translocation signals [116]. In *A. tumefaciens* VirD4 binds the substrates independently of the VirB subunits of the T4SS.

VirD4 and VirD4-like T4CPs contain the nucleotide-binding motifs Walker A and Walker B (I.7.3). Substrate translocation was stalled, when mutations were inserted into the nucleotide-binding motifs of VirD4. Substrate transfer from VirD4 to the VirB subunits was still possible [117]. It was shown that the VirD4 homologue, TrwB, assembles into a hexamer, forming a ring-like structure with a 20 Å wide channel [118]. Consequently, the VirD4 and VirD4-like proteins resemble the FtsK/SpoIIIE family. They build active hexamers, which facilitate substrate interaction and hydrolyze ATP to translocate substrates through the bacterial membrane.

I.7.3 The nucleotide-binding motifs Walker A and Walker B and the arginine finger

ATP binding and hydrolysis requires two nucleotide-binding motifs, named Walker A and Walker B. The Walker A motif, GxxxxGK[T/S] (x=any aa), coordinates the β- and γ-phosphates of the ATP with its lysine. The hydroxyl group of the threonine/serine is required to coordinate the Mg^{2+}, which stabilizes the phosphate groups of the ATP. Therefore, the Walker A motif is also known as the phosphate binding loop. The Walker B motif, hhhhDE (h=hydrophobic aa), contributes to the coordination of the Mg^{2+}-ATP and provides an active water molecule with the “catalytic” glutamate carboxylate group for ATP hydrolysis. The activated water molecule attacks the γ-phosphate and cleaves it from the ATP molecule. This nucleophilic attack releases energy, which results in a mechanical motion [119].

Another component, which is important for ATPase activity, is the arginine finger. The arginine finger is a particular arginine residue located in close proximity to the γ-phosphate of the ATP molecule. The arginine interacts with the γ-phosphate and mediates a proper positioning of the ATP molecule within the nucleotide-binding site. It is speculated that the arginine finger also plays an important role in stabilizing the transition state of the nucleotide during ATP hydrolysis. Therefore it is considered to be a part of the Walker A and Walker B motif [120]. In addition, the arginine finger contributes to oligomerization of ATPases [121]. The arginine residues stabilize the dimerization of two subunits in ATPases, which form ring-shaped hexamers [122].

FtsK and TrwB also contain an arginine finger. The arginine residue of the neighboring subunit completes the active site for ATP hydrolysis [114, 123].

I.7.4 The multi-functional protein EccC of T7SSa

I.7.4.1 Topology of the mycobacterial EccC

All Esx loci contain a gene for the ATPase, designated as *eccC*. EccC contains one membrane domain consisting of two α-helices and a cytosolic domain of unknown function (DUF), followed by three ATPase domains, called D1 to D3 [50]. A recently published study indicates that the DUF domain is a fourth ATPase domain in the mycobacterial EccC (I.7.4.3) [74]. Taking a closer look, the Esx-1 and Esx-5 loci have two *eccC* genes, called *eccCa* and *eccCb*. While *eccCa* encodes the transmembane domain, DUF and D1 domain, *eccCb* encompasses the D2 and D3 domain (Fig. 3). The secretion machinery is only active when EccCa and EccCb interact with each other [41].

I.7.4.2 EccC-the coupling protein

First structural insights of all three ATPase domains were provided from EccC of *T. curvata*. The crystal structure exhibited a central β-sheet surrounded by α-helices. This structure is known as Rossmann fold. In addition, EccC-D3 co-crystallized with a C-terminal peptide of the small toxin EsxB. Two hydrophobic amino acids of EsxB, valine 98 and leucine 102, interacted with a hydrophobic pocket in EccC-D3. This interaction was mediated by two isoleucines, 1163 and 1179, and the leucine 1208 [76]. Another recently published study demonstrated the structure of EccC-D3 domains from *M. tuberculosis* Esx-1, -2, -3 and -5. The structures of the D3 domains showed a Rossmann fold and therefore were structurally similar to EccC-D3 of *T. curvata*. Moreover, interaction of EsxB with the D3 domain could be confirmed for Esx-1 from *M. tuberculosis*. Several amino acids of EccC-D3 (L423, A425, Q437, A441, N445, L442, L446, R449, F469 and V471) were determined to form a substrate-binding site [124]. Both studies showed interaction between the ATPase D3 and the C-terminus of the substrate EsxB. However, interaction was not observed by the C-terminal secretion motif (Yxxx[D/E]). In consequence this secretion signal is involved in a different stage during secretion and not responsible for ATPase-substrate interaction.

I.7.4.3 Activity of the ATPase domains

Rosenberg et al. investigated the ATPase activity of the domains D1 to D3. They demonstrated that EccC-D1 alone supplies energy for substrate translocation in *T.*

curvata. The crystal structure of EccC-D1 showed a low-nucleotide-affinity state, which was induced by an interaction of the linker between the ATPase domain D1 and D2 and a conserved arginine in EccC-D1. Mutation of the arginine increased the ATPase activity. Consequently, the linker-pocket interaction allosterically regulated the ATPase activity of EccC-D1. Mutations of the equivalent residues in EccC-D2 and EccC-D3 did not affect ATPase activity. The domains D2 and D3 showed only basal ATPase activity *in vitro* and therefore might have auxiliary or regulatory functions. Moreover, EccC was only active when it formed hexamers. Hexamerization of EccC was induced by addition of EsxB-peptide. Moreover, EccC-D1 has a conserved arginine finger, which is required for ATPase activity. This finding implies that multimerization is necessary to form an active catalytic site for ATP hydrolysis [76].

As mentioned in chapter I.4.3, the EccC of the Esx-3 has a fourth ATPase domain. The structure of the DUF domain resembles the ATPase domains D1-D3. The DUF domain includes a Walker B (hhhhDD) and a degenerated Walker A motif (GxxxxHRT). Mutation of the Walker B motif abolished substrate secretion, whereby a mutation in the Walker A motif from arginine to a threonine had no effect [74].

I.7.4.4 EccC-the pore forming protein

As described in I.4.3, EccC is considered as pore forming protein and is located at the center of the T7SSa secretion machinery. The DUF domain is connected to the stalk domain, which consists of two α-helices and a short β-sheet. The stalk domain links the ATPase domains with the transmembrane domain. Substrate binding and subsequent ATP hydrolysis of all ATPase domains could trigger a conformational change. EssB notices this conformational change because of its interaction with the stalk domain. Subsequently, this signal stimulates EccB to open/close the channel [74].

In summary, three functions can be designated to the mycobacterial EccC: 1) ATPase hydrolysis, 2) pore formation and 3) substrate interaction.

I.7.5 The ATPase EssC of the T7SSb

EssC exhibits a similar topology compared to EccC. It contains two N-terminal FHA domains, two transmembrane helices, a cytosolic DUF domain and the three C-

terminal ATPase domains (Fig. 8B). Deletion of the most C-terminal D3 domain abrogates secretion of T7SSb substrates in *S. aureus* [55].

The FHA domains show a β-sandwich fold and are structurally similar to each other. More than 200 proteins contain a FHA module, enclosing common motifs to mediate various functions. These common motifs were not observed in *S. aureus* [125]. Zoltner et al. revealed structural information about the EssC of the T7SSb in non-pathogenic *G. thermodenitrificans*. They solved the structure of the FHA domains and the ATPase domain D2 and D3 of EssC. The FHA domains share structural similarities with the FHA domains of *S. aureus*. Different attempts to identify interaction partners were unsuccessful, too. Nevertheless, Zoltner et al. reported that the FHA domains contribute to the production of a stable, active EssC protein. Structures of the EssC-D2 and EssC-D3 from *G. thermodenitrificans* share similarities with the ATPase domains of T7SSa. The EssC-D2 was crystallized with ATP, whereby no nucleotide could be detected in EssC-D3. Instead, the possible nucleotide-binding site in EssC-D3 is occupied by an α-helix. Nevertheless, a conformational change could provide enough space to accommodate the nucleotide [55].

FtsK/SpoIIIE ATPases form active hexameric oligomers [114]. Zoltner et al. proposed a model for a hexameric organization of EssC in *G. thermodenitrificans*, whereby neither EssC-D2 nor EssC-D3 sterically interfere with each other or adjacent domains. Based on this model, EssC builds a channel in a tube-like structure, which is broad enough to translocate Esx dimers (Fig. 11) [55].

Apart from one bioinformatical study, predicting the structures of the ATPase domains D1-D3 from *S. aureus*, no information about folding or function of the ATPase domains is available. The structure prediction showed a Rossmann fold, which is typical for the ATPase domains [126].

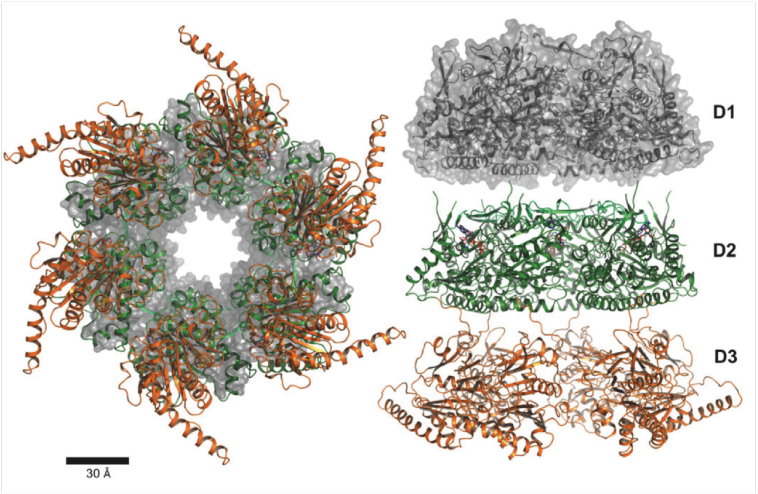

Fig. 11: Hexameric model of EssC from *G. thermodenitrificans*.
D3 depicted in orange, D2 in green and D1 in grey. ATPase domains are arranged in a hexameric ring, resulting in a tube-like structure. The central pore is broad enough to transport Esx dimers. Figure adopted from [55], published under CC 4.0.

I.8 The T7SSb is involved in bacterial competition

S. aureus preferably colonizes the nasal cavities. Besides *S. aureus*, the human nose also hosts other bacteria, like *Corynebacterium* and *Propionibacterium*, and contains a complex bacterial community [127, 128]. Bacteria, which share the same niche, rarely coexist next to each other passively. In fact, they rather engage in cooperative interactions or compete against each other for nutrients and space [129]. Therefore, bacteria have evolved various strategies to increase their competitiveness. Important factors to survive in a niche are efficient nutrient acquisition and surface attachment.

In addition, bacteria contain a large set of antibacterial weapons to kill or inhibit proliferation of the competing species or strains [128, 130, 131]. Bioinformatical analyses observed a system called polymorphic toxin (PT) system, which is used for competition in related bacterial strains. This system is based on a secreted multi-domain toxin and a protective immunity protein. Both proteins are encoded in close proximity to each other. The immunity protein or antitoxin has two functions: It protects the cell from autointoxication and inhibits toxic activity of toxins, produced from clonemates [129, 132]. In fact, the T7SSb secretes PTs for bacterial competition. Secreted toxins are also called effector proteins in literature. *Streptococcus intermedius* encodes three effector proteins, which are secreted by

the T7SSb, as well as their antitoxins (I.5; Fig. 7). TelA and TelB belong to these PTs and are toxic in the bacterial cytoplasm. Production of the antitoxins, TipA and TipB, protects the bacterium from autointoxication. However, TipA and TipB are not substrates of the T7SSb and remain in the cytoplasm [91, 92]. Until now, one PT for the T7SSb in *S. aureus* was detected. As described in chapter I.6.3, EssD contains a nuclease domain and is co-expressed with EsaG. While EsaG inhibits the nuclease activity in the bacteria and is not secreted with EssD. Interestingly, *S. aureus* strains lacking EssD produce EsaG-like proteins, probably for protection [108]. In addition, Anderson et al. reported a homologue of EssD in the non-pathogenic *B. subtilis* [107]. The function of bacterial competition could be a conserved role of the T7SSb [108]. Nonetheless, it is not known how effector proteins, like TelA, TelB or EssD, reach their compartment of activity such as the cytoplasm of the competitor (Fig. 12D).

Other secretion systems like the Type I secretion system (T1SS), Type IV secretion system (T4SS) and Type VI secretion system (T6SS) are known to secrete PT's as well (Fig. 12) [133]. T4SS and T6SS secrete effector proteins across the membranes directly into the target cell in a cell-to-cell contact-depended manner [117, 134]. The main function of the T6SS is in fact the delivery of toxins into competitors. The secretion system functions like a "nano-crossbow". It forms a tubular structure, containing an inner tube tipped by a spike complex and is surrounded by a sheath-like structure. Contraction of the sheath drives the inner tube through the membrane(s) of the target cell (Fig. 12C) [135]. The T4SS contacts the recipient cell using a pilus-like structure. This pilus might be responsible for stable and specific contact with the target cell as well as for effector secretion (Fig. 12B) [136].

The T1SS is known to export proteins via the inner and outer membrane into the extracellular space [137]. In contrast, recent findings described the killing of the neighboring bacterium via cell-to-cell contact mediated by the Cdz (contact-dependent inhibition by glycine zipper) T1SS in *Caulobacter cresentus*. Two surface-exposed proteins, called CdzC and CdzD, kill the neighboring cell through direct physical contact. CdzC and CdzD contain a glycine-zipper repeat causing aggregation. CdzC forms large aggregates that are heat and SDS stable. CdzC/D associate with surface proteins of the outer membrane from the producer cell, forming fibril-like aggregates ranging from 50-250 nm. However, these fibrils do not

only consist of CdzC but also surface-exposed proteins of the producer cell [138]. Killing of CdzC/D is caused by pore formation in the inner membrane of the recipient cell (Fig. 12A)[139]. The killing mechanism is restricted to other *C. crescentus* strains, which do not express the immunity protein CdzI, and a limited number of other α-Proteobacteria [138].

Taken together, models for cell contact dependent effector delivery into the target cell for T1SS, T4SS and T6SS are present. In contrast, a model for T7SS has not yet been proposed.

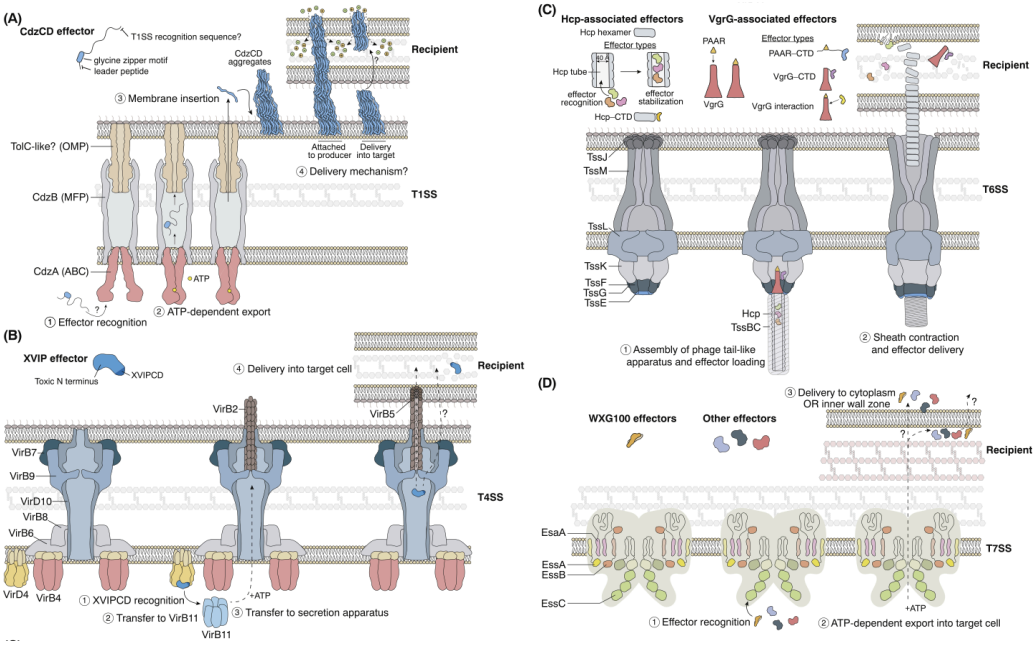

Fig. 12: Schematic presentation of contact dependent effector protein secretion of T1SS, T4SS, T6SS and T7SS for bacterial competition

A) Secretion of CdzC/D via CdzABC T1SS and an unknown OMP. CdzC/D associates with surface proteins of the producer cell and forms fibril-like aggregates. Aggregates contact recipient cell. CdzC/D enters the competitor cell via PerA and introduces pores into the inner membrane. B) Assembly of the VirB/D4 T4SS. The T7SS4 mediates contact to the recipient cell via a pilus, which is build up by VirB2 and VirB5. Effector proteins might be transported via the pilus or by a yet unknown mechanism. C) The T6SS functions like a "nano-crossbow" and delivers effector proteins directly into the target cell. The needle-like structure is assembled and loaded with effector proteins upon detection of the recipient cell. D) Secretion of effector proteins via the T7SSb. Transport mechanism into the target cell is yet not known. Figure adopted from [133] with permission of the publisher.

Abbreviations: ABC: ATP-binding cassette, Hcp: hemolysin coregulated protein, MFP: membrane fusion protein, OMP: outer membrane protein, VgrG: valine–glycine-rich repeat protein G

I.9 Objectives of the work

The T7SSb plays an important role in virulence, abscess formation and long-term persistence of *S. aureus* [43, 47]. A molecular and functional understanding of the T7SSb is pivotal to the development of new antibacterial strategies, but this has been hampered due to the lack of structural and functional information on the membrane embedded secretion machine. The following study focuses on two important membrane components, the motor ATPase EssC and the putative pore forming protein EsaA, which are indispensable for the T7SSb secretion activity and therefore relevant targets for antimicrobial therapy.

In the mycobacterial T7SSa, the ATPase interacts with secreted substrates and energizes their transport. However, how substrates interact with the T7SSb secretion apparatus and its ATPase has remained unknown. The goal of this work was therefore to gain structural and mechanistic insight into the substrate-binding mode of the T7SSb.

Furthermore, no specific function has been assigned to EsaA yet. This protein contains a large extracellular segment, which encompasses 75 % of the entire protein and six membrane helices and was therefore hypothesized to be the pore-forming component of the T7SSb. The goal of this work was to gain first insights into the structure and function of EsaA.

II. Results

II.1 Structural elucidation of EssC and its ATPase domains

The EssC is conserved among the T7SS and belongs to the core components of the machinery. Several studies address the ATPase of the T7SSa and its interaction with substrates [76, 82, 124]. Only little is known about the ATPase of the T7SSb. This section focuses on the protein EssC of *S. aureus* USA300, its ATPase domains and the interaction with small Esx substrates.

II.1.1 EssC and EssCΔD3 expression shows oligomerization of the protein

Deletion of the most C-terminal ATPase domain EssC-D3 already abolishes substrate secretion [55]. To investigate the function of EssC and its most C-terminal domain, the full-length EssC and EssC lacking the D3 domain (EssCΔD3) were designed and proteins were expressed in *E. coli*. Proteins were isolated from the membrane using 0.5 % n-Dodecyl β-maltoside (DDM) and purified by affinity chromatography (AC) followed by size-exclusion chromatography (SEC). The SEC profile of full-length EssC and EssCΔD3 showed several peaks, which indicate different oligomeric states of the protein. EssC formed an oligomer of a high MW (> 1 MDa), that could also be an aggregate since it migrates in the void volume of the column. Additionally a hexamer (~ 1 MDa), a trimer (~500 kDa) and a monomer (~170 kDa) were detected. Oligomerization of the proteins was confirmed by Blue-Native gel electrophoresis (BN-PAGE, Fig. 13). However, sodium dodecyl sulfate polyacrylamide gel electrophoresis (SDS-PAGE) revealed that the peak indicating a trimer (peak at 15 ml) not only results from oligomerization but also from degradation of the protein (Fig. 13A). The elution profile of EssCΔD3 is similar to that of full-length EssC. The peak at a retention volume of 15 ml is absent. The SDS-PAGE showed no degradation of the protein (Fig. 13B). Consequently, the prominent band at ~40 kDa of full-length EssC could indicate degradation of the C-terminal ATPase domains. The product at 40 kDa could correspond to EssC-D3 and the faint band at ~60 kDa to EssC-D2D3.

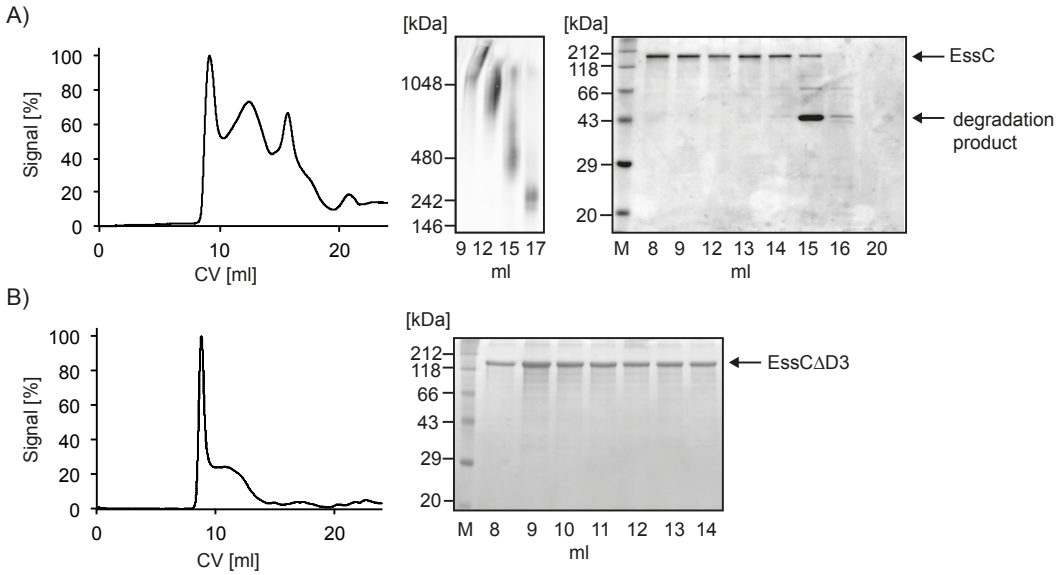

Fig. 13: Protein purification of EssC and EssCΔD3.
A) Full-length EssC: SEC profile of superose6 Increase (left), western blot analysis of BN-PAGE against Strep-Tactin II (EssC) confirming different oligomeric states of SEC (middle). 10 % SDS-PAGE shows a degradation product of EssC at ~40 kDa (right). B) EssCΔD3: SEC profile of superose6 Increase (left) and 10 % SDS-PAGE (right).

II.1.2 EssC-D2D3 forms high molecular weight oligomers

Different studies about the T7SSa determine the ATPase domain D3 as the interaction partner for substrates [76, 124]. To gain more structural information about the EssC ATPase domains, different constructs of the C-terminal cytosolic part were designed.

Expression of all three ATPase domains, including the DUF domain (aa 533-1479), was attempted. The fragment was cloned into different pET and IBA vectors. These vector systems contain different promotors (tet and T7 promotors) as well as tags and tag positions. Nevertheless, protein expression failed (data not shown).

The ATPase domains D2 and D3, starting at aa 977 until 1479, were cloned into the pET vector system and the construct was called EssC-D2D3. The protein was expressed and purified. The profile of the SEC showed different oligomeric states. The peak at the retention volume at 12 ml, indicating a decamer according to the manufacturer protocol [140], was used for crystallization. Crystallization with several different conditions failed probably due to impurities of the sample (Fig. 14). Different attempts (salt wash, heparin AC, ion-exchange chromatography) did not result in more pure EssC-D2D3. Recombinant EssC-D2D3 was used for fluorescence quenching experiments.

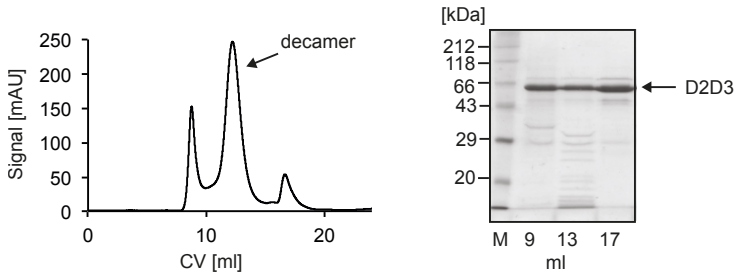

Fig. 14: Protein purification of EssC-D2D3.
SEC profile superose6 Increase showing different oligomeric states of EssC-D2D3 (left). 12 % SDS-PAGE shows EssC-D2D3 at ~60 kDa (right)

II.1.3 Structural elucidation of EssC-D3 reveals a Rossman fold including a hydrophobic patch

The ATPase domain D3, beginning at aa 1248 until 1479, was expressed, purified and crystallized (Fig. 15A, B). The SEC showed more than one oligomeric state of EssC-D3 (Fig. 15C). The crystals of the monomeric protein grew within 24 h at 18 °C and revealed an octahedral shape. Protein crystals were obtained in 1.2-1.8 M ammonium citrate tribasic, pH 7.0 using the hanging drop method and had a maximum size of 0.05-0.1 mm^2. For X-ray crystallography, crystals were transferred into mother liquor supplemented with 25 % (v/v) glycerol and stored in liquid nitrogen. Diffraction data was obtained from proteins, which crystallized in 1.6 M ammonium citrate tribasic, pH 7.0 with a dimension of ~0.1 mm^2.

The crystals diffracted to a resolution of 1.7 Å. Phases were obtained using single-wavelength anomalous dispersion of sulfur atoms (Table 1). The structure exhibited a central β-sheet, consisting of nine β-sheets, which are surrounded by 10 α-helices (Fig. 16A). Superimpositions of EssC-D3 of *S. aureus* (*Sa*) with the structure of EccC-D3 from *T. curvata* (*Tc*) showed a similar fold (Fig. 16C). EccC-D3 of *T. curvata* contains a hydrophobic binding pocket for the *Tc*EsxB containing three hydrophobic amino acids, which are responsible for substrate interaction and secretion (I1163, I1179 and L1208).

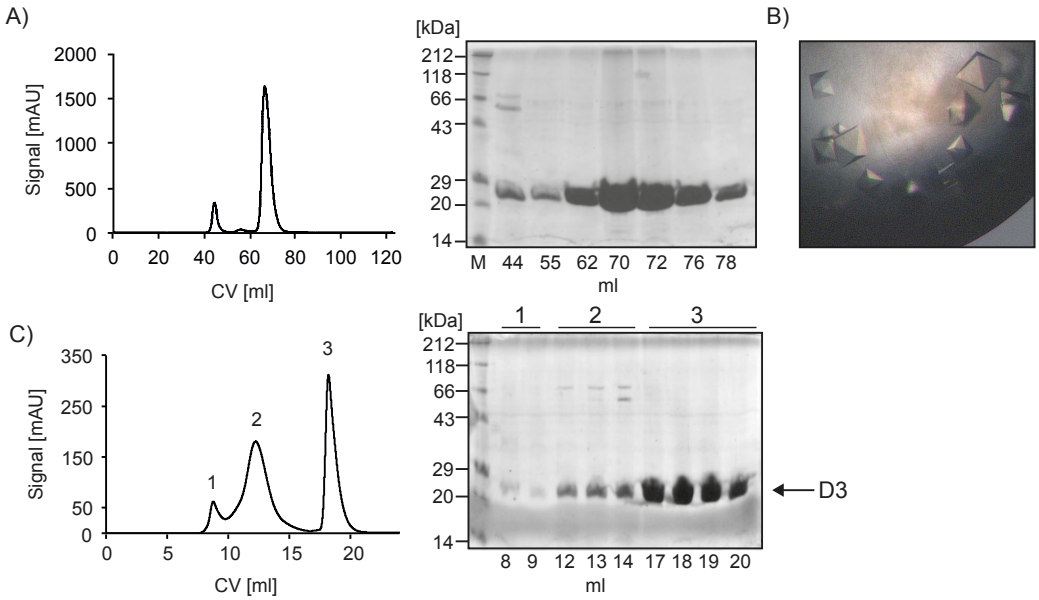

Fig. 15: Protein purification and crystallization of EssC-D3.
A) SEC profile of superdex75 pg (left) indicating EssC-D3 monomer and 12 % SDS-PAGE (middle) showing purified EssC-D3. B) Picture of EssC-D3 crystals showing an octahedral shape. C) SEC profile of superose6 Increase (left) and 12 % SDS-PAGE of EssC-D3 (right) indicating different oligomerization levels.

A structurally similar pocket is observed in *Sa*EssC-D3 as well, but its amino acid composition is different. I identified six solvent exposed amino acids in this cleft. L1358 and F1370 build a small hydrophobic patch, which is surrounded by the polar amino acids C1325, N1342 and Q1363 as well as Y1376, whereby only its hydroxyl group is exposed. Structural comparison of the *Sa*EssC-D3 and *Tc*EccD-D3 showed that N1342, L1358 and S1374 of *S. aureus* correspond to the amino acids I1163, I1179 and L1208 of *T. curvata* (Fig. 16E).

Besides the elucidation of the potential substrate-binding site, EssC-D3 was examined regarding its capability of ATP binding. *Tc*EccC-D3 comprises a Walker A (GxxxxGK[S/T]) and B (hhhhDD) motif, while *Sa*EssC-D3 contains a degenerated Walker B motif (hhhhND), N1379 and D1380 (Fig. 16B, Fig. S 2). ATP was not detected in *Sa*EssC-D3 crystals. The structure of *Tc*EccC-D3 was crystallized with ATP, revealing an α-helix close to the ATP molecule. Superimposition of *Sa*EssC-D3 and *Tc*EccC-D3 showed that the α-helix 3 would clash with the ATP molecule in *S. aureus* (Fig. 16C). Presumably, *Sa*EssC-D3 has to undergo a conformational change before ATP binding is possible.

Meanwhile another study showed the structure of EccC-D3 for Esx-1, Esx-2, Esx-3 and Esx-5 of *M. tuberculosis* (*Mt*) [124]. All structures exhibit the Rossman fold (Fig. 16D). Moreover, *Mt*EccC-D3 of Esx-1 was co-crystallized with the *Mt*EsxB peptide (PDB: 6J19). The aa L94, M98 and F100 of EsxB play an important role for interaction with *Mt*EccC-D3. In *Mt*EccC-D3 several aa (L423, A425, Q437, A441, N445, L442, L446, R449, F469 and Val471) were mentioned as substrate-recognition site [124]. Among these are the aa A425, L442 and V471, which are the corresponding aa for the substrate-binding site in *T. curvata* (I1163, I1179 and L1208) and *S. aureus* (N1342, L1358 and S1374, Fig. 16E,F).

Table 1: Data collection and refinement statistics of EssC-D3 crystal structure

Data Set	EssC-D3 native (PDB: 6TV1)	EssC-D3 (S-SAD)
Wavelength (Å)	1.0332	1.7712
Resolution Range (Å)	19.75-1.7	124.53-1.9
Space group	$P4_32_12$	$P4_32_12$
Cell dimension a, b, c (Å);	91.03, 91.03, 124.51;	90.750, 90.750, 124.530;
α=β=γ (°)	90	90
Molecules/asymmetric unit	1	1
R_{meas} (%)[a]	0.04807 (1.652)[b]	6.9 (207.0)
I/σI	25.71 (1.20)	21.85 (0.76)
Completeness (%)	99.66 (98.72)	99.2 (90.1)
Multiplicity	8.7 (8.8)	12.3 (7.3)
CC1/2	1 (0.542)	1 (0.3)
R_{work} (%)[c]	0.1528 (0.3037)	
R_{free} (%)[d]	0.1724 (0.3392)	
Average B factors (Å^2), protein	38.57	
Average B factors (Å^2), solvent	48.76	
Number of atoms (nonhydrogen)	2104	
Solvent	97	
Ligand (1 x glycerol)	6	
Rmsd bond lengths (Å)	0.007	
Rmsd bond angles (°)	0.77	
Ramachandran favored (%)	96.88	
Ramachandran allowed (%)	3.12	
Ramachandran outliers (%)	0	
Clashscore	6.22	
Number of unique reflections	57937 (5635)	81565 (5506)

[a] R_{meas} as defined by Diederichs and Karplus [141]
[b] values in parenthesis refer to the highest resolution shell
[c] $R_{work} = \Sigma||F_o| - |F_c||/\Sigma|F_o|$, F_o= observed structure factor, F_c =calculated structure factor
[d] R_{free} as defined by Brünger [142]

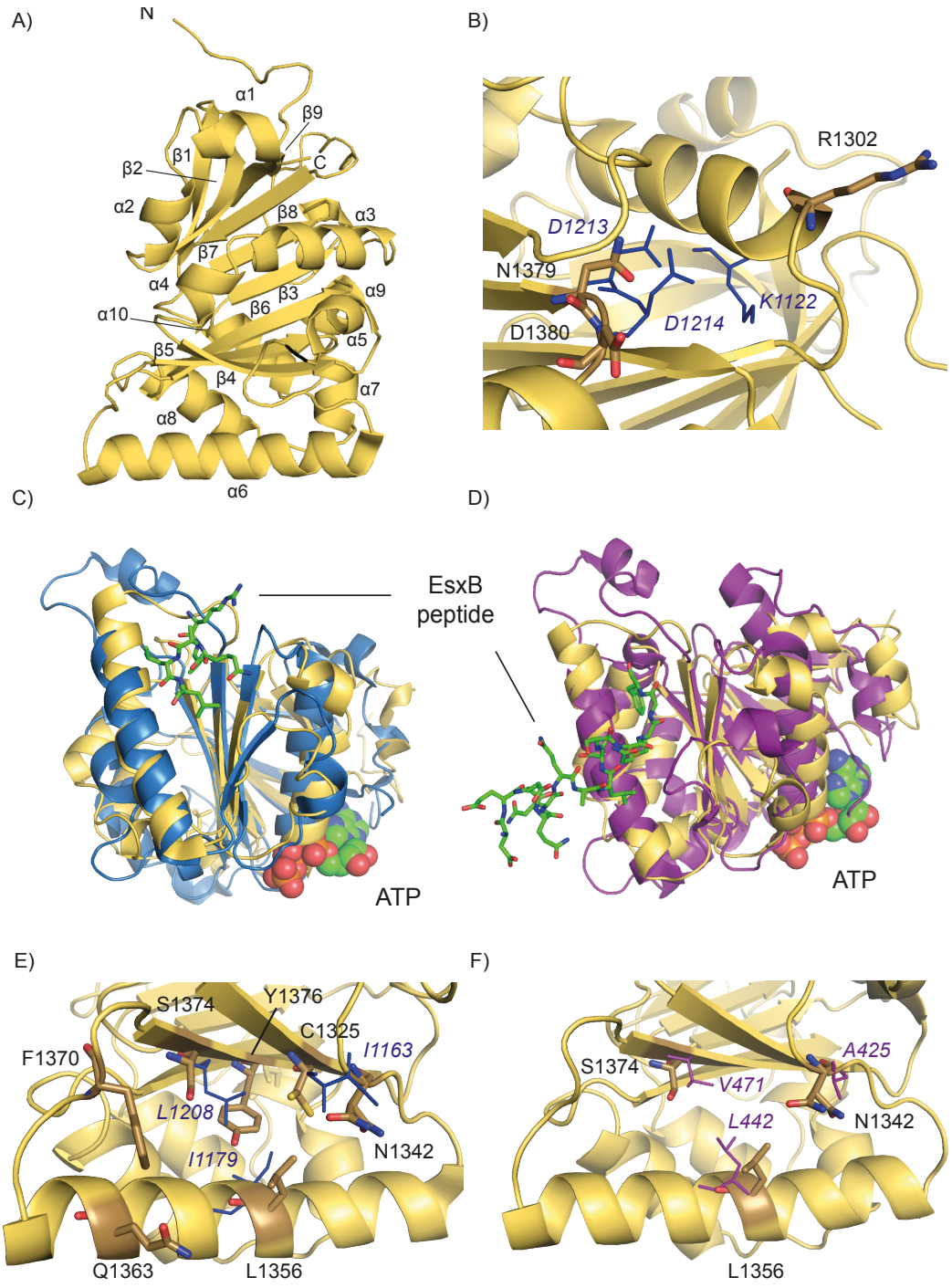

Fig. 16: Structural comparison of EssC-D3 of T7SSb with EccC-D3 of T7SSa.
A) Crystal structure of *Sa*EssC-D3 USA300_FPR3757. B) ATP binding site of *Sa*EssC-D3, Walker B motif of *S. aureus* (yellow) and corresponding amino acids of *T. curvata* (sticks, blue). K1122 belongs to the Walker A motif, no Walker A motif was found in *Sa*EssC-D3, an arginine (yellow) in close proximity could mediate interaction with nucleotides. C, D) Superimposition of *Sa*EssC-D3 (yellow) and EccC-D3 T7SSa from *T. curvata* (blue) and Esx-1 from *M. tuberculosis* (magenta), which shows the bound EsxB-peptide (green) and ATP molecule (green spheres). E, F) Amino acid composition of the substrate-binding pocket of *T. curvata* (blue) and *M. tuberculosis* (magenta) and corresponding amino acids of *S. aureus* (yellow).

II.2 EssC and its function as a coupling protein

II.2.1 The hydrophobic patch has an impact on EsxC secretion

To investigate the importance of the hydrophobic cleft in EssC-D3 for T7SSb functionality, I tested secretion of EsxC in *S. aureus* USA300 mutants. For this purpose, an in-frame deletion of EssC was generated. EssC-*wild type* (*wt*) was re-introduced into *S. aureus* USA300 *ΔessC* using the pLac vector, containing a T7 promotor. EssC was not integrated into the genome (*pessC*). Secretion was restored but remained approximately 30 % lower compared to the *wt* (Fig. 17). *EssCΔd3* and nine point mutations for the potential substrate-binding site were generated using the pLac vector. It is known that *essCΔd3* is not able to secrete EsxC and therefore was used as negative control [55]. The membrane fraction was isolated to demonstrate EssC membrane localization (Fig. 17A) and the supernatant were precipitated to analyze EsxC secretion (Fig. 17B). The presented western blots are representative of three individual experiments. I observed weak signals for EsxC in *ΔessC* and *essCΔD3*, which can be attributed to autolysis of *S. aureus* (Fig. 17B).

The point mutations of *L1356A* and *S1374A*, which correspond to the hydrophobic amino acids of *T. curvata* L1163 and I1179, showed a strong reduction of secretion compared to the complementation of EssC. The double mutant *L1356A/S1374A* did reduce EsxC secretion. Mutations of the other amino acids did not show a strong effect on EsxC secretion (Fig. 17B). In summary this result showed that EssC-D3 contains a hydrophobic cleft, which is important for substrate secretion.

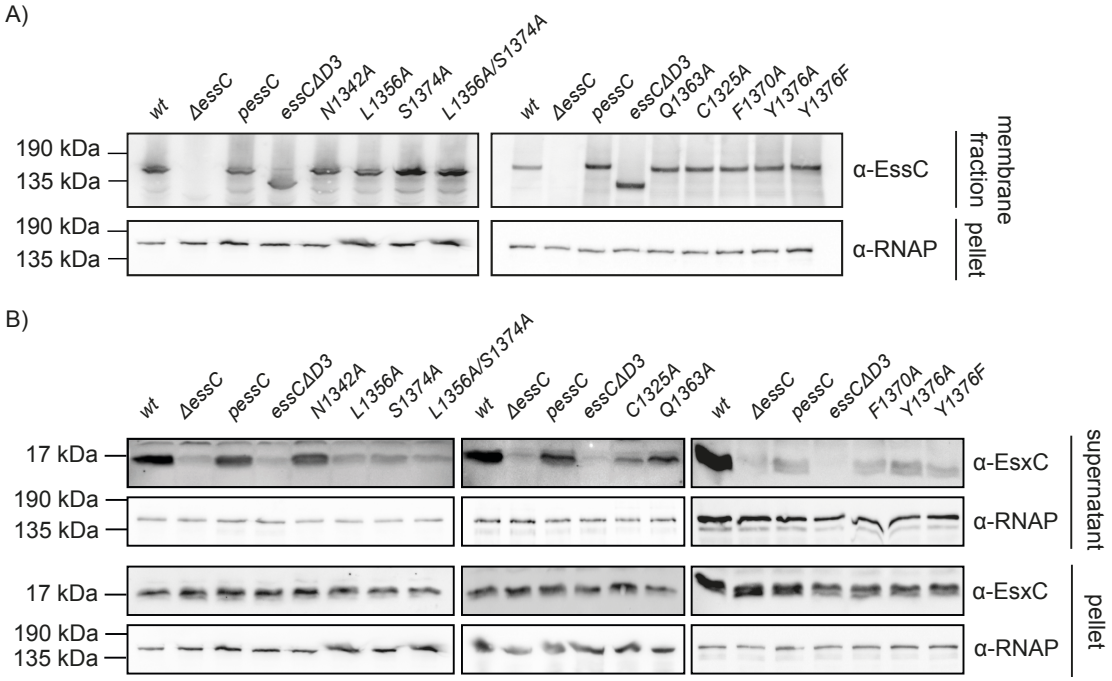

Fig. 17: Impact of the hydrophobic patch in EssC-D3 on EsxC secretion.
A) Western blot using specific antibody against EssC confirming localization of EssC variants in the membrane. Detection of RNA polymerase subunit β (RNAP, 150 kDa) in the cell pellet was used as loading control. B) Supernatant of *S. aureus* cultures was tested for substrate secretion using a specific antibody against EsxC. Cell lysis was detected using the specific antibody against RNAP in the supernatant. Cell pellets were analyzed for EsxC expression (specific antibody against EsxC) and used as loading control (specific antibody against RNAP).

II.2.2 Interaction studies of EssC and Esx substrates

I demonstrated that two hydrophobic amino acids of EssC-D3 affect substrate secretion of T7SSb. This result indicates that EssC might act as a coupling protein in *S. aureus* as has been reported for EccC of the T7SSa [76, 124]. Thus, different interaction studies between EssC and the substrates EsxB and EsxC were performed to investigate the role of EssC as coupling protein.

II.2.2.1 *In vitro* crosslinking experiments do not detect EssC-D3 and Esx substrate interaction

It was shown that the aa of the hydrophobic pocket of EccC-D3 from *T. curvata* and *M. tuberculosis* directly interact with the C-terminal part of EsxB [76, 124]. EssC-D3 of *S. aureus* contains a surface-exposed hydrophobic pocket as well, which has an impact on EsxC secretion. *In vitro* crosslinking experiments were conducted to investigate if recombinant EsxB or EsxC directly interact with EssC-D3 of *S. aureus*

USA300. Disuccinimidyl suberate (DSS), with a length of 11.4 Å, was used for crosslinking recombinant EssC-D3 with the substrates EsxB and EsxC. EsxB and EsxC were expressed using the pET vector system. Both substrates eluted as dimers as described in the literature [103].

DSS is able to react with NHS esters and forms stable amide bonds between lysines. Ess-D3 contains 20 lysines, EsxB and EsxC comprise 12 and 21 lysines, respectively. After incubation with the crosslinker the samples were analyzed using SDS-PAGE. EssC-D3 was crosslinked with itself. The SDS-PAGE showed dimers, trimers, tetramers, pentamers and hexamers (Fig. 18B). This result underlines the hypothesis that EssC is prone to oligomerization. No crosslinking could be observed between EssC-D3 and the substrate. However, EsxC and EsxB, which have a MW of 15 kDa and 11 kDa, were crosslinked with themselves, whereby EsxB only oligomerized as dimer and EsxC showed dimers, trimers, tetramers and high MW oligomeric states (Fig. 18D-E).

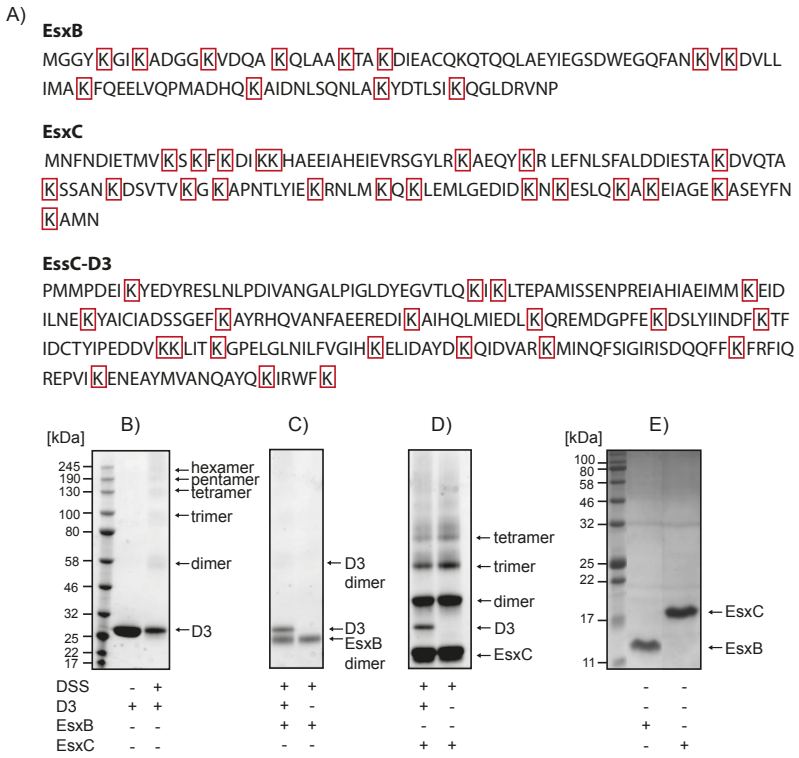

Fig. 18: Investigation of substrate binding to EssC-D3 using *in vitro* crosslinking.
A) Sequences of EsxB, EsxC and EssC-D3 of *S. aureus*. Lysines are highlighted in red boxes. B-D) 12 % SDS-PAGES of crosslinking experiments, B) D3 ± DSS C) D3 + EsxB + DSS and EsxB + DSS, D) D3 + EsxC + DSS and EsxC + DSS, E) 15 % SDS-PAGE of EsxB and EsxC. No crosslinking between ATPase and substrates was observed. ATPase and substrates crosslink with themselves.

II.2.2.2 EssC and EssCΔD3 interact with substrates EsxB and EsxC

Direct interaction of EssC-D3 with the substrate was not detected. Consequently, I investigated the interaction of full-length EssC with the substrates. Co-migration assays were performed to elucidate if EssC interacts with EsxB and/or EsxC. For this, two different approaches were conducted (Fig. 19). In the double pull-down experiment both proteins contain different N- or C-terminal tags. The sample is applied to the first AC and the peak fraction of the elution step is subsequently applied to a second AC-column. Peak fractions of the elution step from both AC's were analyzed via SDS-PAGE and western blot. If proteins interact with each other, both proteins should be detected after the second AC in the elution step (Fig. 19A). The second approach couples AC with subsequent SEC. Peak fractions of the SEC were analyzed by BN-PAGE to detect co-migration of proteins. For this assay, only the ATPase contained a C-terminal tag (Fig. 19B).

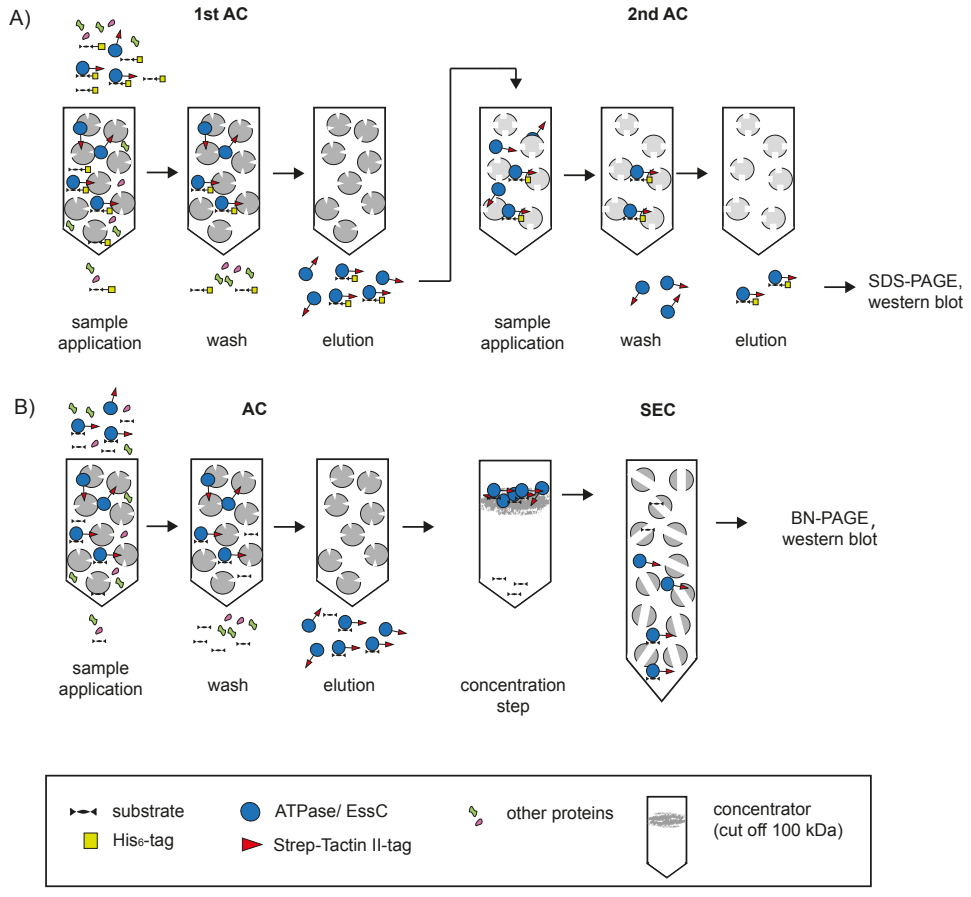

Fig. 19: Schematic representation of the assays.
A) Double pull-down assay using HiTrap-Strep and HiTrap-His AC. B) Co-migration assay using HiTrap-Strep AC combined with SEC.

II.2.2.2.1 Double pull-down assay

The full-length ATPase EssC was co-expressed with the substrate EsxB or EsxC in *E. coli* and a double pull-down assay was performed. EssC contained a C-terminal TwinStrep-Tactin II-tag and the substrates EsxB/C contained a N-terminal Histidin$_6$-tag (His) (Fig. 19A). The membrane fraction was isolated and applied to a HiTrap-Strep column. The SDS-PAGE showed EssC in the elution fraction (Fig. 20A). Afterwards, these fractions were loaded on a HiTrap-His column to analyze whether substrate was left in the peak fraction of the elution step from the first AC. The SDS-PAGE and western blots determined EssC and substrate after the second pull-down in the elution fraction (Fig. 20B, C). Thus, EssC interacts with EsxB and EsxC. The result could be distorted by interaction of the tags. A second pull-down assay, which requires only one protein with a tag was performed.

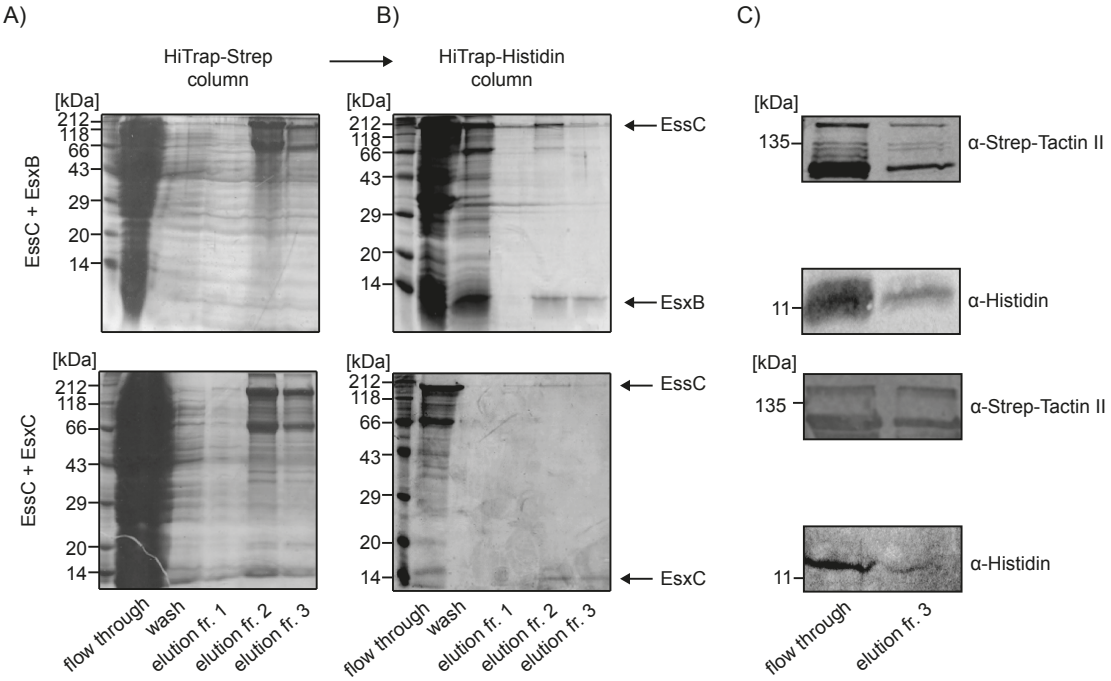

Fig. 20: Double pull-down assay of EssC with the substrates EsxB and EsxC.
ATPase + substrate were co-expressed and purified by a two-step AC. A) SDS-PAGE after first AC for EssC + EsxB (top) and EssC + EsxC (bottom) detecting EssC in elution fraction. B) SDS-PAGE after second AC for EssC + EsxB (top) and EssC + EsxC (bottom) detecting EssC and substrate in the elution fraction. C) Western blot using specific antibodies against His$_6$-tag (α-substrate) and Strep-Tactin II (α-EssC) to detected EssC and substrates in the elution fraction.

II.2.2.2.2 Affinity chromatography coupled with subsequent size-exclusion chromatography

Results of the double pull-down assay showed EssC-EsxB and EssC-EsxC interaction. To confirm this result, the experiment was slightly modified and co-migration of EssC and substrates was tested. Therefore, EssC, carrying a TwinStrep-Tactin II-tag was co-expressed with the substrate, having no tag. After AC, the peak fraction of the elution step was subjected to SEC (Fig. 19 B). The peak fractions were analyzed on a BN-PAGE and visualized by western blot using specific antibodies against the substrates and the Strep-Tactin II fused to EssC. The SEC profile showed several oligomeric states, which were confirmed by the BN-PAGE. The ATPase was present as a high MW oligomer (> 1 MDa), a hexamer (~1 MDa) and a trimer (~ 500 kDa). Co-migration of substrate and ATPase was observed in the high oligomeric state and the hexamer (Fig. 21A, C). According to the literature, the D3 domain is responsible for substrate binding [76, 124]. *In vitro* crosslinking experiments showed no interaction between EssC-D3 and EsxB or EsxC. I consequentially raised the question whether the EssΔD3 is able to co-migrate with EsxB or EsxC. EssΔD3 was co-expressed with the substrates and the same assay as described above was performed. EssCΔD3 was observed in different oligomeric states. Western blot analysis detected co-migration of EsxB and EsxC with EssCΔD3 at the retention volume corresponding to a hexamer and high MW oligomer (Fig. 21B, D). Thus, EssC did not require EssC-D3 to interact with EsxB and EsxC. Recapitulated, both assays confirmed interaction between EssC and the substrates EsxB and EsxC. The results revealed that substrate binding is not exclusively mediated by EssC-D3.

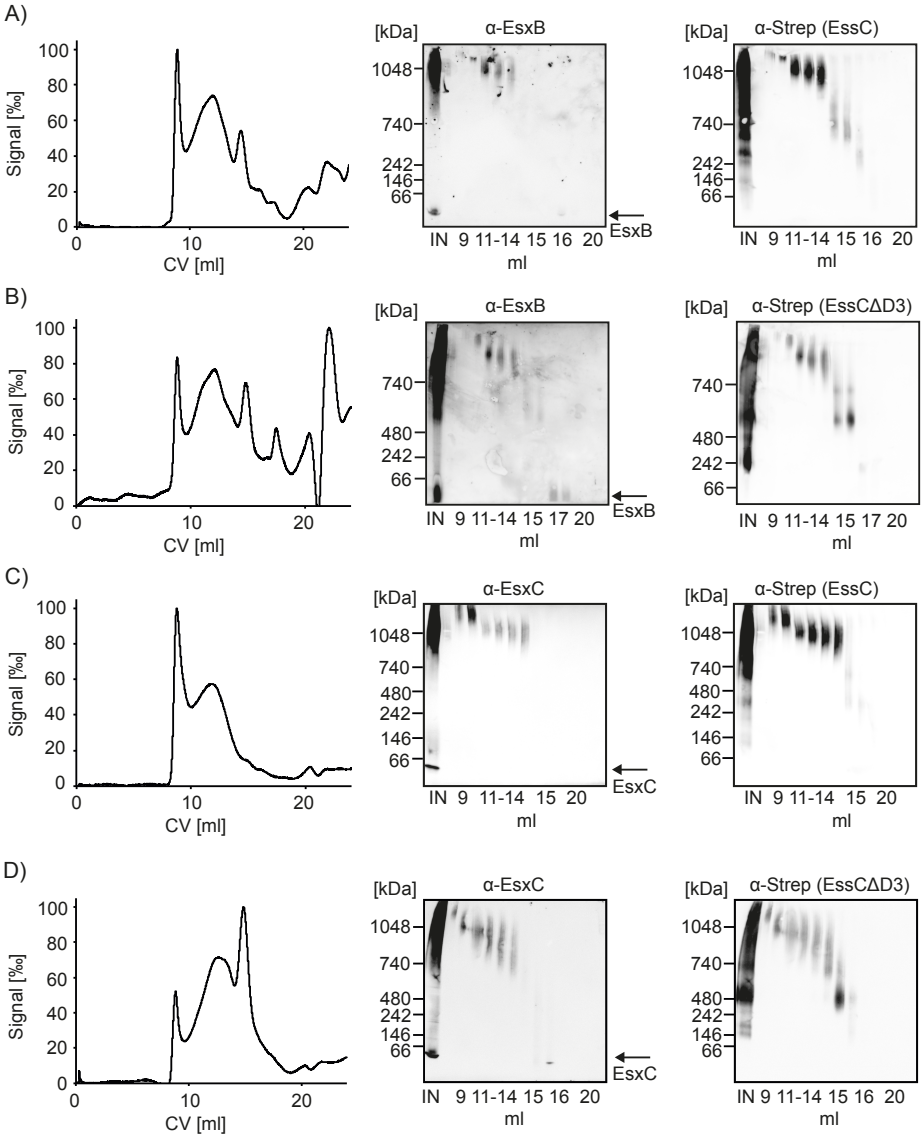

Fig. 21: Co-migration assay of EssC and EssCΔD3 with the substrates EsxB and EsxC.
ATPase + substrate were co-expressed, purified by AC and SEC (left). SEC fractions were separated by BN-PAGE and analyzed via western blot using specific antibodies against EsxB, EsxC (middle) and the Strep-Tactin II-tag detecting EssC and EssCΔD3 (right), A) EssC + EsxB, B) EssCΔD3 + EsxB, C) EssC + EsxC, D) EssCΔD3 + EsxC.

II.2.2.3 Affinity measurements between EsxB and EssC variants confirm protein-protein interaction

Fluorescence quenching experiments can be used to determine the affinity between two molecules by measuring the variation of the fluorescence signal, which can be caused by various processes like complex formation, molecular arrangements or energy transfer.

To confirm the results of the co-migration assays and to quantify binding between ATPase and substrates, measurements were performed with recombinant EssC and EssCΔD3 together with the EsxB homodimer. The ATPase hexamer (~1 MDa) was labeled with the fluorophore NT-647. Affinities between 1 to 10 µM were obtained for full-length EssC (K_d=8.5 ± 1.3 µM) and EssCΔD3 (K_d=1.6 µM ± 0.1 µM) (Fig. 22A, B). These results demonstrated that EssC is able to bind substrate in the absence of EssC-D3. To ensure that specific binding of EsxB to the EssC variants was detected the same experiments were conducted using BSA as the ligand. No interaction with BSA was detected (Fig. S 1).

This leads to two possibilities of substrate-EssC interaction: 1) EssC-D3 is dispensable for substrate binding or 2) the deletion of EssC-D3 exposes a binding site for substrates at the EssC-D2.

To determine if EssC-D3 alone can bind substrates the same measurements using recombinant EssC-D3 monomer and also EssC-D2D3 oligomer were performed. EsxB homodimer binds to EssC-D2D3 with an affinity of K_d=1.3 ± 0.4 µM, which is in a similar range as full-length EssC and EssCΔD3. No binding for EssC-D3 could be detected (Fig. 22C, D). This assay confirmed binding of EssC to the substrate but opened three possibilities of EssC-EsxB interaction: 1) EsxB interacts only with EssC-D2, 2) binding of EsxB to EssC-D3 is only possible when EssC-D2 is present or 3) EsxB can only bind to EssC-D3 as an oligomer. The third possibility would indicate that a single domain cannot bind substrates by itself but needs oligomerization of the EssC. This observation would be in line with the literature proposing six copies of the ATPase in the secretion system.

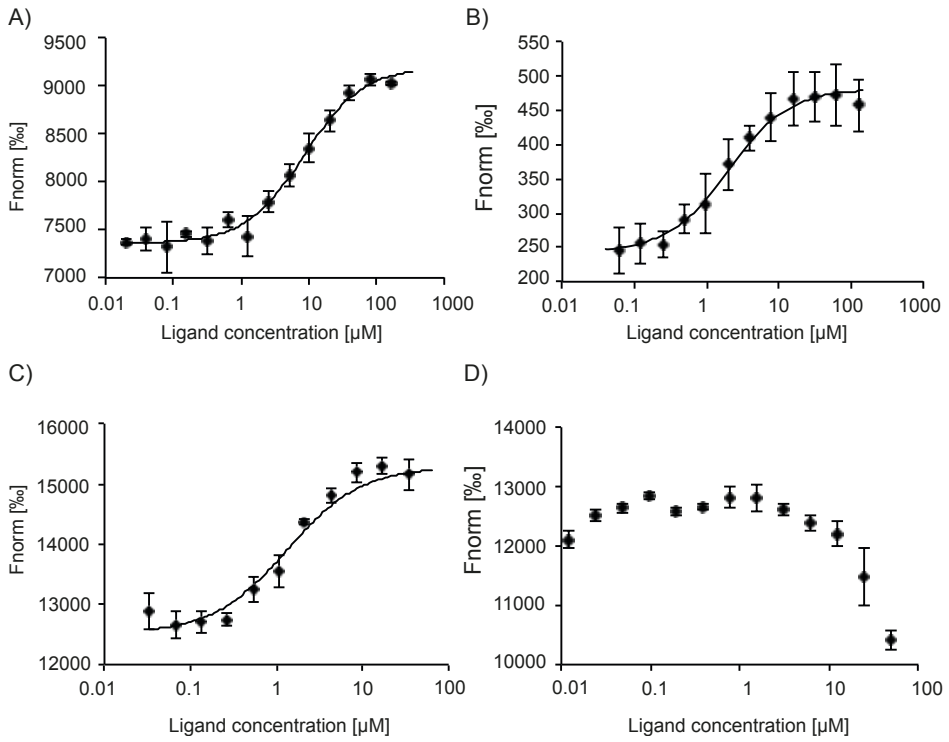

Fig. 22: Affinity measurements using fluorescence quenching of EsxB and different EssC variants.
EssC variants were labeled with fluorophore NT-647 and EsxB was titrated to the variant. A) EssC + EsxB B) EssCΔD3 + EsxB C) EssC-D2D3 + EsxB D) EssC-D3 + EsxB, experiments were carried out as technical triplicates, error bars present the standard deviation. Interaction was detected for full-length EssC, EssCΔD3 and EssC-D2D3 with the substrate EsxB.

II.2.3 *In vivo* experiments to do not detect EssC and Esx substrate interaction

II.2.3.1 Bacterial two-hybrid assay

So far, I showed interaction between ATPase and substrates with different *in vitro* assays. A bacterial two-hybrid assay was set up to investigate interactions between EssC and the substrates EsxB and EsxC *in vivo*. In addition, interaction of substrates with the membrane components, EsaA and EssB, of the T7SSb was investigated as well. The method is based on the dimerization of two functional complementary domains, T25 and T18, of the adenylate cyclase from *Bordetella pertussis*, which are fused to the proteins of interest. The adenylate cyclase is only active when its domains are in close proximity to each other due to the interaction of the fused proteins [143]. The active adenylate cyclase produces cAMP, which activates transcription of the *lacZ* gene, encoding the β-galactosidase. Consequently, bacteria

growing on a lysogenic broth (LB) medium supplemented with 5-bromo-4-chloro-3-indolyl-β-D-galactopyranoside (X-gal) can hydrolyze it and turn blue. Substrates were N-terminally fused to the T25 domain because several studies demonstrated that the C-terminal part of the substrates is important for interaction with the ATPase [81, 82]. EsaA, EssB and EssC were fused at the C- or N-terminal part to the T18 domain. Both variants were tested in the bacterial two-hybrid assay. Blue colonies were not observed in any combination of the assay, indicating no interaction between the membrane components and the substrates (Fig. 23). In contrast, *in vitro* experiments regarding the substrates, EsxB and EsxC, and the membrane component EssC already confirmed interaction. This raised the question if the bacterial two-hybrid assay provides a suitable system to determine protein interaction in *S. aureus*. The assay is performed in a heterologous expression system using different promotors for the proteins than in *S. aureus*. Abundance and localization of proteins could be impaired resulting in no interaction between the substrates and membrane components of T7SSb. Consequently, an alternative assay should be considered.

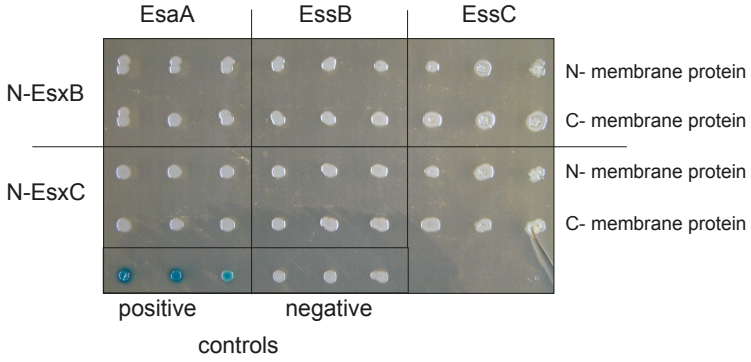

Fig. 23: Bacterial two-hybrid assay of substrates and membrane components.
EsaA, EssB and EssC were fused C- and N-terminally to the T18 domain, EsxB and EsxC were fused N-terminally to the T25 domain. Negative control was performed with vectors expressing only T25 and T18. Plasmids for the positive control expressed the leucine zipper of the transcription factor GCN4, as provided by the supplier.

II.2.3.2 *In vivo* crosslinking

An alternative technique to investigate protein-protein interactions is *in vivo* crosslinking. Some crosslinkers, for example para-formaldehyde (PFA), are able to diffuse through the cell membrane. PFA reacts with cysteine, histidine, lysine, tryptophan and arginine, but the molecules must be in close proximity (2 Å) [144]. *S. aureus* USA300 *wt* and *ΔessC* as well as the *ΔessC* strain complemented with the

essCΔd3 and *D1380A* were used for crosslinking. *D1380A* abolished substrate secretion by inhibition of ATP hydrolysis (II.3.1) and thereby might stall binding of EssC-EsxC. *S. aureus* cultures were grown until OD_{600}=2 and treated with PFA. Membrane fractions were isolated and samples were analyzed using SDS-PAGE, followed by western blot with specific antibodies against EsxC and EssC. Detection of interaction between EsxC and EssC was performed because the antibody against EsxC was more sensitive compared to the antibody against EsxB. Apart from the high background, results showed distinct bands for the *wt* and *D1380A* at ~190 kDa and for *essCΔd3* at ~160 kDa irrespectively of PFA treatment. This band was not visible in *ΔessC* showing that EssC alone migrated at ~190 kDa. (Fig. 24A). Samples treated with PFA showed no shift in MW of 15 kDa for EsxC monomer or ~25-30 kDa for EsxC homodimer or EsxA/EsxC dimer when compared to the non-treated PFA samples. Moreover, a signal at exactly the same MW for -/+ PFA samples was detected. Consequently, monomeric EssC does not interact with EsxC. In addition, a western blot using specific antibody against EsxC was performed. A signal at ~245 kDa was detected for all samples which were treated with PFA, also for *ΔessC*. Thus, this signal cannot indicate interaction between EssC and EsxC and could be explained by crosslinking of EsxC with another protein or itself (Fig. 24B). Crosslinking of EsxC with itself was observed in *in vitro* crosslinking experiments with DSS and revealed several oligomeric states, as well as a band at ~245 kDa (Fig. 18D). *S. aureus wt* showed two more bands at a higher MW. This signal indicates crosslinking of EssC, probably with itself, which would confirm that EssC forms high MW oligomers. The western blot against EsxC also showed signals for a MW higher than 245 kDa. These signals can be observed in the *ΔessC* mutant and therefore might not show crosslinking of EssC to EsxC.

Thus, initial crosslinking experiments with PFA as crosslinker did not identify interaction of EssC monomer with EsxC. Nonetheless, crosslinking of EsxC to a high MW oligomer of EssC cannot be excluded. All results considered, in order to elucidate if EssC binds to EsxC when present in a high MW oligomeric state, a deletion mutant of EsxC would be required. With this mutant it could be shown if the signals at a high MW are related to crosslinking of EssC with EsxC.

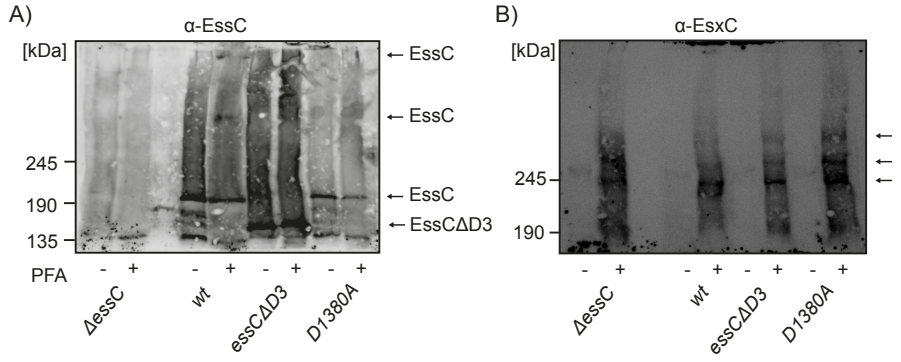

Fig. 24: *In vivo* crosslinking of EssC and EsxC.
Samples were separated on a 5 % SDS-PAGE and subsequently analyzed by western blot. A) Western blot using a specific antibody against EssC. B) Western blot using a specific antibody against EsxC. Western blots indicate no interaction between EssC and EsxC.

II.3 ATPase activity of the EssC-D3 domain

II.3.1 The degenerated Walker B motif influences EsxC secretion

The structure of EssC-D3 contains a degenerated Walker B motif (hhhhND instead of hhhhDE, Fig. 16B), where an asparagine is present between the hydrophobic aa and the aspartic acid. A Walker A motif (GxxxxGK[T/S]) was not detected. An arginine at position 1208 was observed, which could mimic the function of a lysine, but is not in close proximity to the nucleotide in the crystal structure. However, conformational changes could relocate the arginine to bring it in close proximity to the ATP molecule. The superimposition of the *Sa*EssC-D3 structure with *Tc*EccC-D3 revealed the α-helix 3 colliding with the ATP molecule indicating that *Sa*EssC-D3 is not able to bind ATP in this conformation (Fig. 16C). I mutated N1379 and D1380, which were determined as degenerated Walker B motif by structure alignment with TcEccC-D3, to an alanine and tested for EsxC secretion. Therefore, the pLac vector containing the mutation *N1379A* or *D1380A* was introduced into the *S. aureus* USA300 *ΔessC*. Both EssC mutants located in the membrane fraction (Fig. 25A) and showed a drastic impact on EsxC secretion. *N1379A* enhanced secretion compared to EssC *wt*, which was reintroduced into *S. aureus* USA300 *ΔessC* on the pLac vector (*pessC*). *D1380A* almost abrogates secretion (Fig. 25B). Consequently, the modified Walker B motif influenced secretion strongly and supported ATP binding/hydrolysis, affecting substrate secretion.

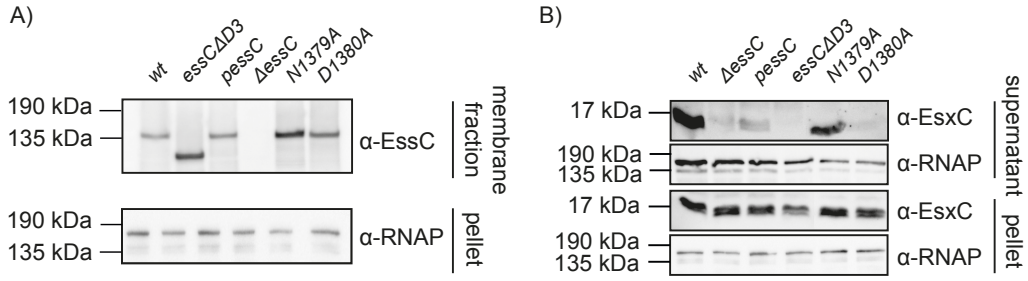

Fig. 25: Impact of the degenerated Walker B motif of EsxC secretion.
A) Western blot analysis using a specific antibody against EssC confirm the localization of EssC variants in the membrane. Detection of RNAP in the cell pellet was used as loading control. B) Supernatant of *S. aureus* USA300 cultures were tested for substrate secretion using specific antibody against EsxC. Cell lysis was detected using specific antibody against RNAP. Cell pellets were analyzed for EsxC expression (specific antibody against EsxC) and used as loading control (specific antibody against RNAP).

II.3.2 Ability of EssC and EssC-D3 to bind and hydrolyze ATP

The secretion assay of the degenerated Walker B motif mutants (*N1379A* and *D1380A*) revealed that EsxC secretion is influenced by the D3 domain. This result raised the question whether EssC-D3 is involved in ATP binding or hydrolysis. Thus, ATP affinity measurements and ATPase activity assays were performed. ATP affinity was tested using fluorescence quenching experiments with recombinant EssC hexamer and EssC-D3 monomer. The results of fluorescence quenching experiments showed that EssC hexamer does not interact with ATP, while EssC-D3 is able to bind ATP with low affinity (K_D= 2.6 ± 0.3 mM, Fig. 26A, B). Consequently, the D3 domain is involved in ATP binding. Full-length EssC might be unable to bind ATP molecule because it has to undergo a conformational change to make the ATP binding site accessible. For example, substrate binding could be responsible for the conformational change and therefore leads to ATP binding.

Since EssC-D3 showed ATP binding, this raised the question if EssC-D3 is able to hydrolyze ATP, when the C-terminal peptide of a substrate is present. Knowing that EsxC is also able to interact with EssC *in vitro*, EssC-D3 monomer, ATP and EsxC-peptide was incubated and tested for ATPase activity. The assay demonstrated that EssC-D3 alone is not able to hydrolyze ATP (Fig. 26C). The graph shows NADH oxidation to NAD^+, which is equivalent to ATP hydrolysis. After 100 seconds ATP was added to the experiment. The positive control showed a decrease of NADH, indicating ATPase activity whereby EssC-D3 with and without peptide did not oxidize NADH. Although, the negative result of EssC-D3 monomer does not rule out that

EssC-D3 is not important for ATP hydrolysis. But it showed that the D3 domain is not able to hydrolyze ATP on its own.

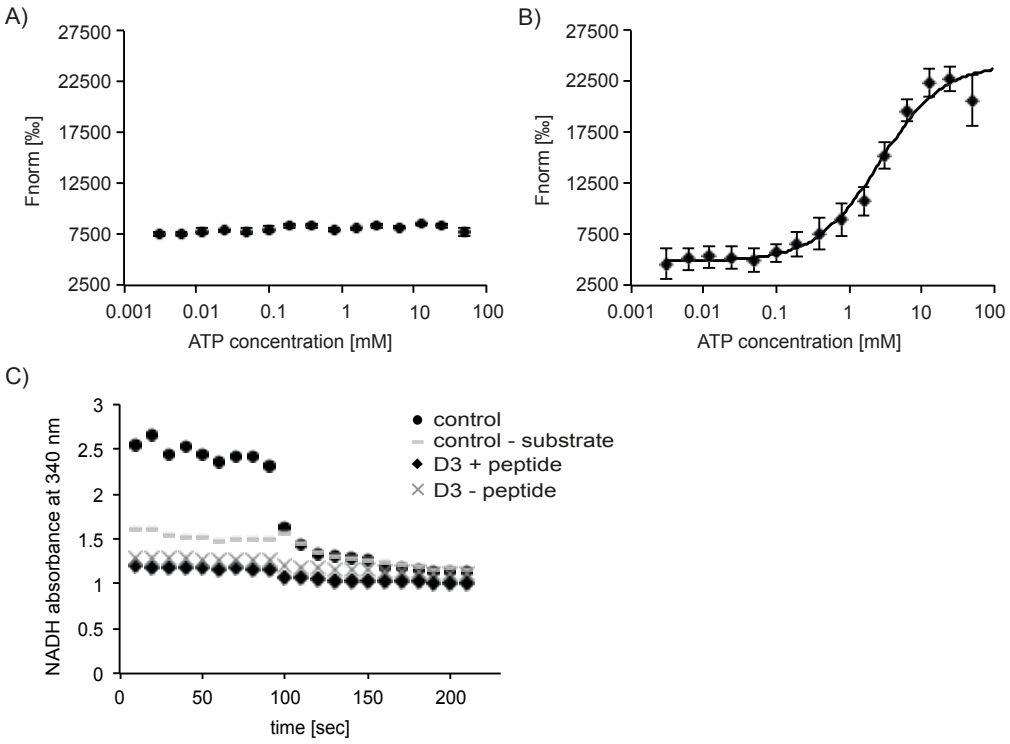

Fig. 26: ATP binding and hydrolysis of EssC and EssC-D3.
A/B) Affinity measurements using fluorescence quenching assay with A) EssC+ATP, B) EssC-D3+ATP. EssC hexamer and EssC-D3 monomer were labeled with fluorophore NT-647 and ATP was titrated to them. C) ATPase activity test using EssC-D3 monomer. ATP was added after 100 seconds and progression of NADH oxidation was measured at 340 nm. ■) control + substrate, -) control - substrate, ◆) EssC-D3 + peptide, ×) EssC - peptide. As positive controle the ATPase p97 provided by Petra Hänzelmann, Schindelin lab, Rudolf Virchow Zenter (RVZ), Würzburg, was used.

II.4 EsaA and its role for the T7SSb

EsaA is indispensable for substrate secretion of the T7SSb but its specific function is not known yet. Secondary structure prediction, using the online tool PSIPRED [76], suggested six transmembrane helices and an extracellular segment, which comprises 75 % of the whole protein. First hypotheses mention EsaA as pore forming protein, because it contains six membrane helices [93]. Although this function has not been proven so far. Therefore, the following part of the study investigates EsaA.

II.4.1 Structural characterization of the extracellular domain of EsaA

II.4.1.1 Expression, purification of full-length EsaA and EsaA_ex1 results in an unstable product

Expression and purification of full-length EsaA resulted in low yields. The profile of the SEC indicated a tetramer. The SDS-PAGE showed two bands, possibly caused by degradation of the protein (Fig. 27A). Analyzing both bands by fingerprint mass spectrometry showed missing amino acids especially of the membrane domain (Fig. S 3). Consequently, I decided to focus on the extracellular part of EsaA.

The aa 47 to 804 are located to the extracellular segment of EsaA. This part, designated as EsaAex_1, was expressed in *E. coli* under control of the tet promoter and purified using a HiTrap-Strep column followed by SEC. The SEC profile showed three prominent peaks indicating a high MW oligomer or aggregate, a tetramer and a dimer. SDS-PAGE of the peak fractions resulted in two bands at the same MW as for the full-length EsaA, which could not be separated from each other by AC or SEC (Fig. 27B). Thus, I raised the question, whether the extracellular segment exhibits domains that cannot be degraded by proteases.

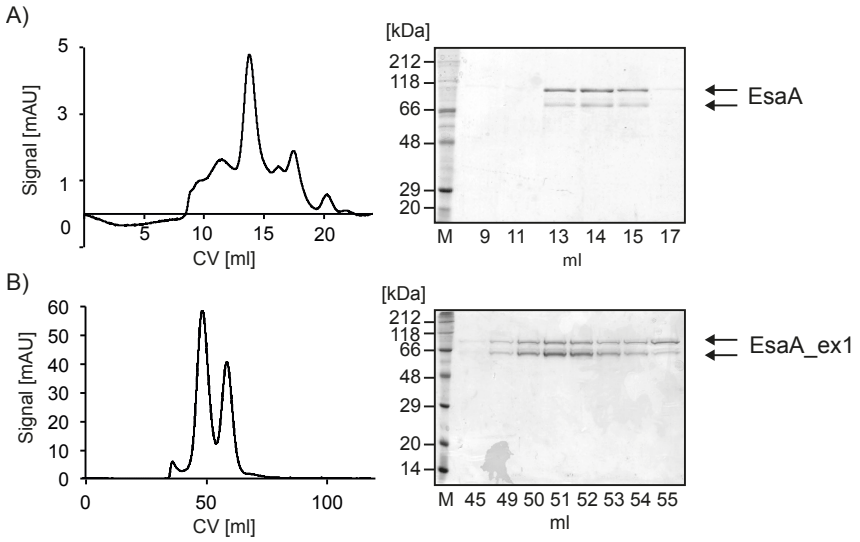

Fig. 27: Protein purification of full-length EsaA and EsaA_ex1.
A) EsaA full length protein: SEC profile of superose6 Increase (left) and 10 % SDS-PAGE (right). B) EsaA_ex1 SEC profile of sephacryl 300 pg (left) and 12 % SDS-PAGE (right). SDS-PAGES showed two bands for expressed protein.

II.4.1.2 Limited proteolysis of EsaA_ex1 indicates folding of its extracellular segment

To address the question whether the extracellular segment of EsaA folds into a domain, limited proteolysis with the proteases papain and trypsin was performed. In both experiments a protease resistant band at ~50 kDa was detected. This indicates that the extracellular segment is indeed structured and not disordered as previously assumed [93, 99] (Fig. 28A). The boundaries of the band at 50 kDa were determined, using fingerprint mass spectrometry. The product encompassed the aa from 275 until 669 (Fig. 28B).

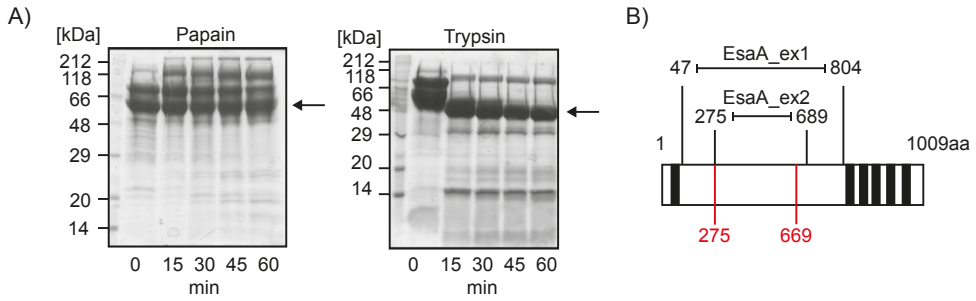

Fig. 28: Determination of the boundaries of the structural domain from EsaA_ex1.
A) Limited proteolysis of EsaA_ex1 with papain (left) and trypsin (right). Samples were analyzed on a 12 % SDS-PAGE. Arrows indicate product used for fingerprint mass spectrometry. B) Schematic presentation of full-length EsaA, EsaA_ex1, EsaA_ex2 (black) and result of the fingerprint mass spectrometry (red).

II.4.1.3 EsaA_ex2 purification and crystallization

Secondary structure prediction of the extracellular segment suggested that EsaA_ex1 contains several α-helices (PSIPRED, [145]). One α-helix encompasses residues 597 to 683, where the end of the limited proteolysis product was located. Consequently, the corresponding DNA fragment of the fingerprint mass spectrometry, including 60 bp downstream, was cloned into the pET16b vector (Fig. 28B) and designated EsaA_ex2. EsaA_ex2 was expressed, purified and crystallized (Fig. 29). An extensive screen using different pH values, PEG's, PEG concentrations and salt concentrations resulted in the octahedral shape but also in pyramidal and tetragonal protein crystals and needles (Fig. 29B).

Best diffraction data was collected from octahedral crystals grown in 0.2 M ammonium citrate tribasic pH 7.0, 16 % PEG 3350, using the hanging drop method. The diffraction of these crystals was limited to 5 Å, but cooling crystals to 4 °C 24 h before harvesting improved the diffraction up to 4 Å resolution (Table 2).

Attempts to solve the phase problem by molecular replacement failed due to the lack of homologous structures (< 20 % sequence identity). Consequently, different constructs of the extracellular domain varying in length were designed, in order to produce crystals, which might diffract better. These potential protein crystals could be used for sulfur single-wavelength anomalous dispersion to solve the phase problem.

Table 2: Diffraction data set of EsaA_ex2

Data	**EsaA_ex2**
Wavelength	0.9677
Temperature	100
Detector	EIGNER 4M
Crystal-to-detector distance [mm]	308.7
Rotation range per image [°]	0.05
Total rotation range [°]	180
Exposure time per image [s]	0.02
Space group	$P4_12_12$ or $P4_32_12$
a, b, c [Å]	197.544, 197.544, 368.334
α, β, γ [°]	90, 90, 90
Mosaicity [°]	0.09
Resolution range [Å]	20.0-4.0
Total number of reflections	1003682
Completeness [%]	98.6 (97.0)
Multiplicity	13.84
$I/\sigma(I)$	9.74 (0.98)[b]
R_{meas} [%][a]	23.9 (276.4)
Overall B factor from Wilson plot [Å]	153.1

[a] R_{meas} as defined by Diederichs and Karplus [141]
[b] $CC_{1/2}$ is 41.6 % in the outer shell, indicating that the data contain signal $I/\sigma(I)$ falls below 2.0 at 4.2 Å resolution

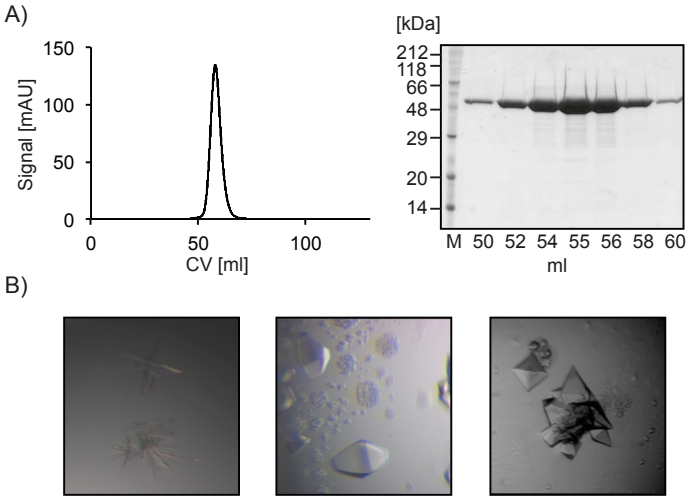

Fig. 29: Protein purification and crystallization of EsaA_ex2.
A) SEC profile of Sepharose200 pg (left) and 12 % SDS-PAGE (right). B) Crystal pictures of EsaA_ex2 showing different shapes.

To improve crystallization we re-assessed secondary structure prediction of EsaA with additional programs (PSIPRED [145], MoBiDB [146], Quick 2D [147]). All predictions showed several α-helices and only few β-sheets (Fig. S 4). Based on these predictions, five additional constructs were designed, cloned into the pET16b vector and then expressed and purified. EsaA_ex3, EsaA_ex6 and EsaA_ex7 crystallized in small rods and needles, but these crystals did not diffract. EsaA_ex4 and EsaA_ex5 did not crystallize (Table 3). The construct EsaA_ex2 was therefore used for further investigation of its structure and function. To solve the structure of EsaA_ex2, further information about the phases was needed. A selenomethionine (SeMet) derivative of EsaA_ex2 was produced, in order to solve the phase problem by the Single Anomalous Dispersion (SAD) method. Octahedral crystals of SeMet-EsaA_ex2 grew within 5 days in the same crystallization conditions as for the native protein. Structure resolution is still in progress.

Table 3: Construct boundaries of EsaA extracellular domain

Construct	Boundaries [aa]	Crystallization	Diffraction
EsaA_ex1	47-804	x	x
EsaA_ex2	275-689	✓	✓
EsaA_ex3	204-689	✓	x
EsaA_ex4	247-689	x	x
EsaA_ex5	275-689	x	x
EsaA_ex6	275-602	✓	x
EsaA_ex7	313-645	✓	x

II.4.1.4 EsaA_ex2 folds into a single domain consisting mainly of α-helices

Results of size-exclusion chromatography combined with multi-angle light scattering (SEC-MALS) showed that Esa_ex2 forms a dimer (Fig. 30A). Circular dichroism (CD) spectroscopy confirmed the result of the secondary structure prediction. EsaA_ex2 contained 70 % α-helices and 4 % β-sheets (Fig. 30B) [148]. Thermal unfolding of EsaA_ex2 demonstrated a single transition indicating a single domain. The melting temperature is at 34,5 °C (Fig. 30C).

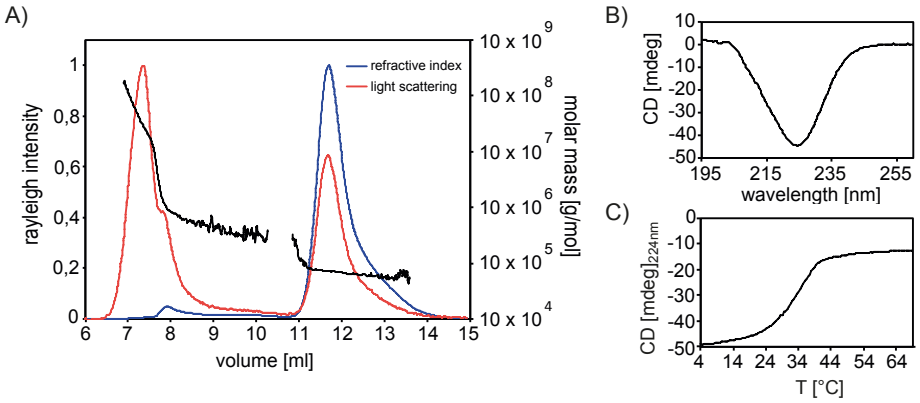

Fig. 30: Biochemical characterization of EsaA_ex2.
A) SEC-MALS with an Sephacryl200 12/300 GL detecting an EsaA_ex2 dimer B) CD spectroscopy indicating an α-helical structure. C) Thermal unfolding at 224 nm showing a single transition.

II.4.1.5 EM negative staining of EsaA_ex2 shows fibril-like structures

The EM became a powerful tool to investigate protein structures even of small proteins. In fact, the structure of proteins with a MW of less than 100 kDa was solved

through EM [149, 150]. However, structure elucidation of small proteins still remains very challenging via EM.

The SEC-MALS data showed that EsaA_ex2 forms dimers of ~100 kDa. The elution profile also detected a small peak at a retention volume of 8 ml. Both samples were used for negative staining. EM of EsaA_ex2 dimer did not detect any particles (data not shown). The sample of the peak fraction at a retention volume of 8 ml indicated a fibril-like shape of more than 100 nm in length (Fig. 31).

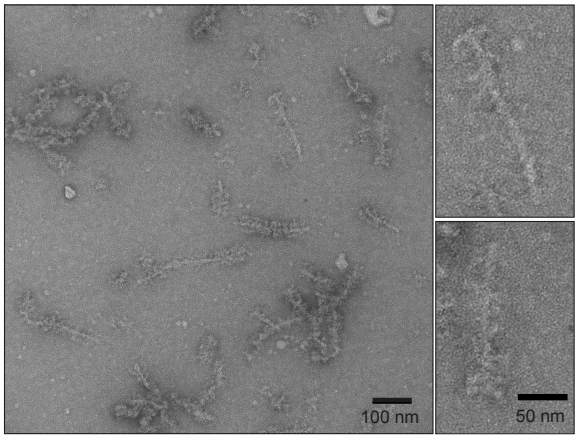

Fig. 31: EM negative stain of the extracellular domain from EsaA.
EM negative stain picture of the void fraction from EsaA_ex2 showing a fibril-like structure. Samples were stained with 3 % uranyl acetate and image was acquired at 4200-fold magnification.

II.4.2 Functional elucidation of the extracellular domain from EsaA

II.4.2.1 The extracellular domain affects substrate secretion

To gain a better understanding of the role of the extracellular domain, a deletion mutant missing the aa 275 until 689, was designed in *S. aureus* USA300. Three consecutive flag-tags were inserted instead of the extracellular domain, to verify EsaA expression and cellular localization (Fig. 32A). Western blot analysis showed expression and insertion of EsaAΔex2 into the membrane. Testing protein abundance of *essB*, which is located downstream of *esaA*, assured transcription, translation and localization into the membrane of proteins downstream of the T7SSb locus. The amount of EssB integrated into the membrane is slightly reduced compared to the *wt* (Fig. 32B), whereby the loading control showed same amount of loaded sample (Fig. 32C, bottom right). Consequently, T7SSb expression levels are lower in the *S. aureus esaAΔex2* mutant compared to the *wt*.

Nevertheless, the *esaAΔex2* was used to test for substrate secretion. *S. aureus* USA300 cultures were grown at 30 °C until OD_{600}=1 and the supernatant was analyzed for EsxC secretion (Fig. 32C). Expression of substrate EsxC in *S. aureus* USA300 *esaAΔex2* was slightly reduced when compared to *S. aureus wt,* but no EsxC could be detected in the supernatant (Fig. 32C). Therefore, it can be concluded that the extracellular domain of EsaA is required for secretion.

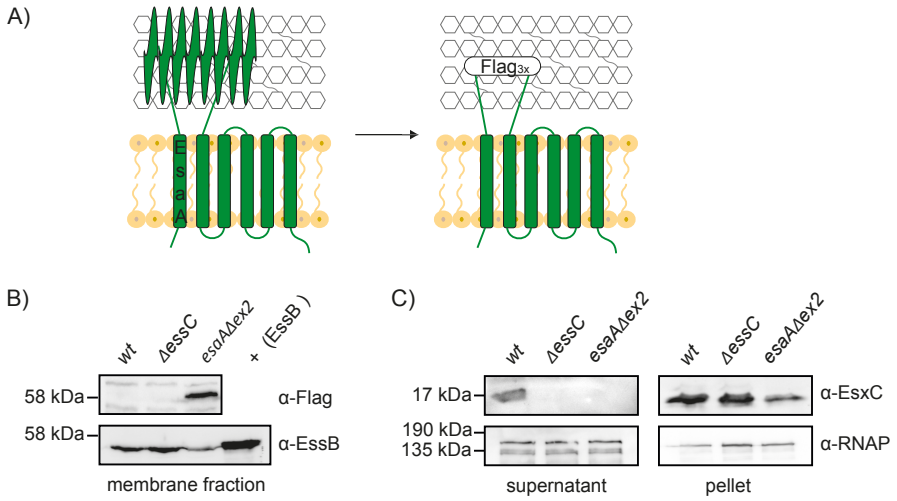

Fig. 32: *EsaAΔex2* mutant and its impact on EsxC secretion.
A) Schematic representation of *esaAΔex2* mutant comprising a $Flag_3$-tag instead of aa 275-689. B) Western blot against $Flag_3$-tag and EssB confirming location of EsaAΔex2 into the membrane and expression of proteins downstream of EsaA, respectively. C) Western blot of cell culture supernatant against EsxC and RNAP in order to detect EsxC secretion and cell lysis (middle). Western blot of the cell pellet against EsxC in order to confirm EsxC expression (right top). Western blot of the cell pellet against RNAP show the loading control for samples of B) and C) (bottom, right). *EsaAΔex2* was expressed and inserted into the membrane. No EsxC secretion was observed. Expression level of downstream proteins was reduced.

II.4.2.2 The extracellular domain is involved in bacterial competition

Bacteria compete against each other, especially when they require similar nutrients [129]. *S. aureus* secretes the nuclease EssD via the T7SSb to compete with related strains [108]. Another Gram-positive bacterium, *Streptococcus intermedius*, uses the T7SSb to secrete effector proteins for bacterial competition as well [92]. However, it is not known how effector proteins of the T7SSb are delivered into the target cells [133].

Hence, it should be reviewed whether the extracellular domain of EsaA is involved in bacterial competition. Therefore, the Lopez lab tested (Centro Nacional de Biotecnologia (CNB), Madrid) if *S. aureus* USA300 *esaA_Δex2* mutant is deprived in

competing with related strains. For the assay, *S. aureus* USA300 was used as attacker strain and *S. aureus* RN8325-4 as the prey. It was shown that *S. aureus* USA300 is superior to *S. aureus* RN8325-4. *S. aureus* RN8325-4 expresses the antitoxin EsaG to inhibit EssD nuclease activity. Therefore, bacterial competition of *S. aureus* USA300 against RN8325-4 is not mediated via EssD. Both bacteria contain the T7SSb. To identify if the killing effect is dependent on Esx substrate secretion, *S. aureus* USA300 *wt and* the mutant *ΔessC* (not secreting Esx substrates) were used as controls*. S. aureus* USA300 *esaA_Δex2* has a significantly reduced killing effect when compared to the controls. *S. aureus* USA300 *wt* and *S. aureus* USA300 *ΔessC* showed no significant difference in killing of the prey (Fig. 33). In consequence, the killing of the prey was not caused by secreted proteins of the T7SSb but mediated by the extracellular domain of EsaA.

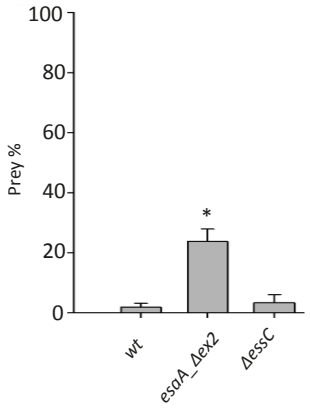

Fig. 33: Bacterial competition assay of *esaA_Δex2*.
S. aureus USA300 was used as attacker strain in bacterial competition with *S. aureus* RN8325-4 (prey). The graph shows survived prey cells after 16 h of growth. (*) Results show a statistical significance for *esaA_Δex2* (student-t-test, p-value of 0.01). The assay was performed by Diana Damián-Aparicio of the Lopez lab (CNB, Madrid).

III. Discussion

III.1 EssC and its functions in the T7SSb

III.1.1 EssC of *S. aureus* forms oligomers

The ATPase of the T7SS, also known as coupling protein, belongs to the FtsK/SpoIIIE protein family. ATPases of the FtsK/SpoIIIE family form active hexameric rings [114].

Results of two studies concerning the core machinery of the Esx-5 T7SSa showed that the Esx-5 contains six copies of EccC [70, 80]. Unlike the Esx-5, the cryo-EM structure of the core complex of Esx-3 contained only two copies of EccC. However, this study demonstrated that Esx-3 was purified in a dimeric state and that high MW oligomers of Esx-3 can be found in the mycomembrane. Moreover, three Esx-3 dimers were fitted into the low-resolution map of Esx-5 [80], resulting in six copies of EccC [74]. In this work I found that full-length EssC oligomerizes in the absence of T7SSb core components and substrates. This result is in line with previous results on EssC of the T7SSb from S. *aureus* RN6390 [99] and from *G. thermodenitrificans* [55]. In contrast, results on the homologous EccC of the T7SSa from *T. curvata* showed that oligomerization of EccC depends on the presence of the secreted substrate [76]. Wang et al. also proposed a hexameric model for EccC in *M. tuberculosis*. The packing of the EccC-D3 crystals of Esx-5 from *M. tuberculosis* showed a six-fold screw axis symmetry. In addition, they suggested that a region in EccC-D3, containing a short α-helix, would be responsible for hexameric assembly. This α-helix has a different orientation in the D3 domains of Esx-1, Esx-2, Esx-3 and Esx-5 of *M. tuberculosis* [124]. The α-helix would be located between α6 and β5 and is absent in the *S. aureus* EssC-D3. Nevertheless, in this work I found that EssC-D3 domain was expressed in different oligomeric states. I observed that domains D2 and D3 of EssC as well as EssCΔD3 formed oligomers. In summary, this work supports with several independent studies that the EssC protein of T7SSb forms oligomers and because of its relation to the FtsK/SpoIIIE family, presumably hexamers.

III.1.2 The coupling protein EssC interacts with Esx substrates

The T4SS is widely spread and a well-studied secretion machinery, transporting substrates through several membranes. It is build up by four major components. One of them is an ATPase, which is related to the FtsK/SpoIIIE family. This protein, T4CP,

forms hexamers, hydrolyzes ATP to energize substrate secretion and acquires substrates via its C-terminus. These substrates contain one and/or two secretion signals. After the substrate is recognized by the T4CP, it is passed along to the next component of the T4SS to be transported through the channel in the inner membrane. Translocation through the inner membrane is facilitated by three ATPase of the system, among them T4CP [116].

In line with this, several studies of the T7SSa describe interaction between substrates and the ATPase and therefore EccC was designated as coupling protein [76, 82, 124]. However, interaction studies of the small Esx substrates and EssC in the T7SSb have been lacking. This study provides structural insights of the EssC-D3 from *S. aureus* and discovered a hydrophobic surface-exposed patch, which is important for substrate secretion. In EccC-D3 T7SSa this pocket is responsible for the interaction with the C-terminal peptide of EsxB. Three amino acids, I1163, I1179 and L1208 in EccC-D3 from *T. curvata* mediate substrate binding [76]. In EccC-D3 Esx-1 from *M. tuberculosis*, the corresponding amino acids, A425, L442 and V471 were confirmed to be involved in substrate interaction as well [124]. In this study, I carried out an alanine scan of the potential substrate-binding site in EssC-D3 and identified two amino acids, L1358 and S1374, affecting EsxC secretion. These amino acids correspond to I1179 and L1208 of *T. curvata* and L442 and V471 of *M. tuberculosis*. In contrast, the third corresponding amino acid N1342 did not decrease secretion activity. *In vitro* crosslinking experiments were performed to corroborate interaction between substrates and EssC-D3. Although interaction between substrate and EssC-D3 from *S. aureus* was not detectable, the results of the secretion assay along with the striking structural similarity of EssC-D3 from *S. aureus* to two D3 domains of T7SSa, binding to the C-terminal peptide of EsxB, suggest that EssC-D3 also interacts with Esx substrates.

Co-migration and double pull-down assays as well as fluorescence quenching experiments, confirmed the coupling mechanism of EssC with the substrates EsxB and EsxC. Additionally, I observed that EssCΔD3, which lacks the D3 domain, binds substrates. The results of fluorescence quenching experiments indicated that the EssC-D2 domain might be able to bind Esx substrates. Rosenberg et al. reported that domains D1 and D2 of EccC from *T. curvata* comprise hydrophobic patches

similar to the binding pocket in the D3 domain [76]. So far, there is no evidence that the DUF domain could contain a hydrophobic patch as well.

Consequently, I suggest a model where the domains D2 and D1 are able to interact with the substrates. The substrates get into contact with EssC via the most distal ATPase domain D3 and are passed along the other ATPase domains until they reach the membrane pore (Fig. 34).

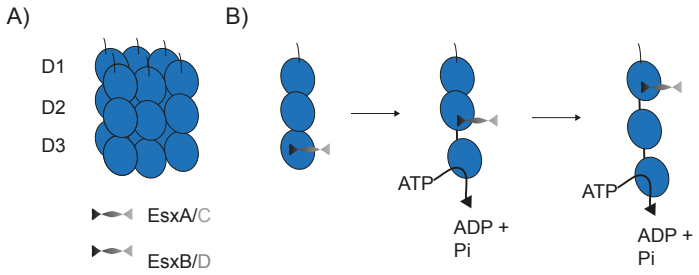

Fig. 34: Model of substrate transport along the ATPase domains of EssC.
A) Hexameric organization of the ATPase. B) The substrate binds to the ATPase EssC-D3. The binding initiates a conformational change and therefore the substrate can be passed along the ATPase domains. The EssC-D3 contributes actively to ATP hydrolysis.

It should be considered, that not all substrates might bind to the same substrate-binding site. Jäger et al. implied that EsxC and EsxA are secreted by a different mechanism. The T7SSb locus can be divided into four different modules. These modules can be conserved or versatile in their gene composition [77]. The second module encompasses EssC. Considering the second module, T7SSb of *S. aureus* strains can be grouped into four variants (EssC1-4). These groups exhibit sequence variability, which increases towards the C-terminus of the EssC. Expression of the groups EssC-2, -3 and -4 in an *essC-1* deletion strain could restore EsxA secretion. Interestingly, secretion of EsxC could not be restored by EssC-2, -3 and -4. Consequently, EsxC and EsxA are secreted via different mechanisms in *S. aureus* strains belonging to the groups of EssC-2,-3 and -4 [77, 126].

III.1.3 ATPase activity of EssC-D3

Genome sequencing identified homologues of the FtsK/SpoIIIE protein in mycobacteria and Gram-positive bacteria, showing two or more FtsK/SpoIIIE-like domains. This evidence led to the conclusion that EssC of *S. aureus* contains C-terminal ATPase domains [51]. Later on, Zoltner et al. demonstrated that *G. thermodenitrificans* contains three ATPase domains based on bioinformatical

predictions and determined the structure of EssC-D2 and D3. This topology was adopted for EssC of *S. aureus* and deletion of the most distal ATPase domain D3 diminished substrate secretion [55]. Recently it was shown, that the DUF domain of EccC from the mycobacterial Esx-3 has ATPase activity [74]. Sequence comparisons suggest that the DUF of the T7SSb could also have ATPase activity (Fig. S 2).

The crystal structure of SaEssC-D3 did not show bound ATP. However, structural comparison to the D3 domain of *T. curvata*, which binds ATP [76], revealed, that in *Sa*EssC-D3 an α-helix extends into the nucleotide-binding pocket and prevents ATP binding. Another study concerning the D3 domain of *G. thermodenitrificans* also demonstrated that an extension of an α-helix, that contains a Walker A motif, interferes with ATP binding. Zoltner et al. proposed that conformational changes of this α-helix would provide the space to accommodate ATP and consequently restore nucleotide binding of *Gt*EssC-D3 [55]. The extended α-helix of *Sa*EssC-D3 does not include a Walker A motif but comprises an arginine at position 1302, which may functionally replace the lysine of the Walker A motif and mediates ATP binding. In agreement with this, experiments presented in this work showed that SaEssC-D3 as well binds ATP with low affinity but does not exhibit ATPase activity in presence or absence of secreted substrates.

I found that mutations in the Walker B motif in the SaEssC-D3 have diametric effects on substrate secretion- either boosting or abolishing secretion. Although not detectable *in vitro*, ATPase activity of SaEssC-D3 plays a critical role in the mechanism of the T7SSb *in vivo*.

In the coupling protein EccC from *T. curvata* ATPase domains are connected via a linker and ATPase domains D1 and D2 contain a linker-pocket, which includes a conserved arginine interacting with the linker and leading to a conformational change. Mutating the arginine in the pocket of D1 stimulated ATPase activity in presence of substrate EsxB. Moreover, mutation of a catalytic residue in D1 inhibited ATP activity indicating that ATP hydrolysis was mediated by D1 alone. Mutation of the corresponding amino acids in D2 and D3 did not result in increased ATP hydrolysis. Further mutational studies showed that D2 and D3 regulate the ATPase activity of D1 instead of actively contributing to ATP turnover [76]. Indeed, it should be considered that EssC-D3 of *S. aureus* has a regulating effect as well and mutation

in the Walker B motif of EssC-D3 downregulates the ATPase activity of the D2 and/or D1 domain.

Besides the Walker A and Walker B motif, the arginine finger plays an important role for ATP hydrolysis [120]. Moreover, arginine residues of neighboring subunits could complete the catalytic site of the domain. The D1 domain in *T. curvata* contains a conserved arginine finger, which is required for ATP hydrolysis. The sequence alignment of EccC and EssC (Fig. S 2) detects several conserved arginine residues in all ATPase domains, which might be required to build a complete catalytic site for ATP hydrolysis.

In summary, the interplay between the ATPase domains could explain why purified EssC-D3 is not active by itself and how mutations in the Walker B motif affect the secretion activity.

III.1.4 Summary

In this work I showed that EssC-D3 ATPase activity is mandatory for substrate secretion. I identified two amino acids, L1358 and S1374, which are critical for secretion. Structural comparisons with substrate recognition domains from T7SSa suggest, that these amino acids are responsible for binding a specific signal peptide at the C-terminus. Thus, this work corroborates that T7SSa and T7SSb use similar substrate recognition mechanisms.

Furthermore, this study provides experimental evidence that domain D2 and/or D1 serve as additional substrate binding sites on the coupling protein. In the secretion model of Zoltner et al. [55], the ATPase domains D1-D3 assemble to a tube-like structure in the cytosol, whereas domain D3 forms the outermost ring layer and domain D1 the layer closest to the membrane. I therefore propose that the small Esx substrates interact with the D3 layer first and are then transferred along the ATPase domains towards the membrane pore. It could be speculated that this mechanism works similar to the "rotary inchworm" mechanism of the FtsK protein (Fig. 10, I.7.1). The ATPase domains D1, D2 and D3 undergo conformational changes and push the substrates towards the central pore, while they are transferred from subunit to subunit of the hexamer.

Different studies report flexibility of the ATPase domains [74, 76, 80]. This flexibility along with conformational changes triggered by substrate and ATP binding and ATP hydrolysis might create the mechanical motion required for this translocation process.

III.2 The extracellular domain of EsaA and its function

Among the T7SSb core components EsaA is the only protein, which contains several transmembrane helices. It therefore was suggested to build the pore of the T7SSb [93]. Although this hypothesis has not been proven. So far, interaction of EsaA with other T7SSb core components is limited to EssB [100].

This study focuses on the extracellular segment of EsaA. I showed that the extracellular segment forms a single domain and consists to 70 % of α-helices. X-ray data are limited to 4 Å and structure elucidation by molecular replacement failed due to the lack of homologous structures. Heavy metal atom screens were then performed, in order to obtain phases. Structure resolution is still in progress.

III.2.1.1 The extracellular domain of EsaA is required for substrate secretion

The *S. aureus esaAΔex2* mutant was unable to secrete EsxC substrate. Consequently, the extracellular domain is required for substrate secretion. Bobrovsky et al. proposed, that the hydrolase EssH, which cleaves wall peptides, helps EssB and EsaA to span through the cell wall and therefore mediates substrate secretion [94]. Shaving experiments confirmed that EsaA is detectable on the extracellular surface [96]. This supports the hypothesis, that EsaA extends through the cell wall and thereby enables substrate translocation (Fig. 35).

III.2.1.2 The extracellular domain of EsaA is involved in bacterial competition

It is common knowledge that bacteria, which colonize the same niche, compete against each other [129]. Indeed, it was shown that the T7SSb is involved in bacterial competition. *Streptococcus intermedius* and *S. aureus* use the T7SSb to export effector proteins to compete with other strains [91, 108]. *S. aureus* secretes the nuclease EssD, which is inactivated by EsaG in the producing bacteria [108]. On this account, I raised the question whether the T7SSb has other mechanisms to contribute to bacterial competition. The *S. aureus esaAΔex2* showed a reduced killing effect when compared to *S. aureus wt* and *S. aureus ΔessC*. Thus, the increased survival rate of *S. aureus* RN8325-4 does not depend on the secretion of T7SSb effector proteins but on the presence of the extracellular domain. The extracellular domain thus plays a role in bacterial competition, which does not rely on substrate secretion of the T7SSb.

Recently it was demonstrated, that the T1SS secretes toxic proteins, which mediate the killing of the neighboring bacteria by cell-to-cell contact. These toxins, CdzC and CdzD, associate with surface exposed proteins of the producer cell and form fibril-like aggregates up to 250 nm. These aggregates contact a competitor in close proximity and disrupt the inner membrane [138]. In addition, other secretion systems like the T4SS and T6SS use long filaments to contact neighboring cells as well to deliver effector proteins [133].

Negative stain pictures of the extracellular domain from EsaA showed fibril-like structures larger than 100 nm. Deletion of the extracellular domain, which is surface exposed, reduced the killing effect. Consequently, I propose that the extracellular domain associates with toxins in order to reach out to a competitor and/or mediates direct cell-to-cell contact with neighboring cells for bacterial competition (Fig. 35).

III.2.1.3 Homologues of EsaA indicate the function as a phage receptor

The T7SSb of *B. subtilis* encodes a protein, called YueB, exhibiting a similar topology as EsaA. Structure predictions propose six transmembrane domains and an extracellular domain, which includes 70 % of the whole protein. By 90 % sequence coverage EsaA and YueB only share 17 % sequence similarity (Clustal Omega). Secondary structure prediction of YueB, using the online tools PsiPred [145] and Quick 2D [147], calculated that the protein mainly consists of α-helices, which is in agreement with the CD spectroscopy data of the extracellular domain from EsaA. Expression of recombinant full-length EsaA always resulted in two bands. This phenomenon could be observed for YueB as well and is substantiated by cell wall protease processing the extracellular domain of YueB [90]. YueB is a phage receptor and an orthologous of the phage infection protein (Pip), found in *Lactococcus lactic* [151]. YueB is involved in the irreversible adsorption of SPP1 phages. YueB orthologous share identical topologies but only little overall sequence similarity, as detected for EsaA and YueB. The N-terminal region of Pip proteins encloses conserved residues, which are suggested to play a role in phage binding [90]. Sequence alignment revealed that EsaA also shares conserved amino acids with the Pip and YueB and therefore could be involved in phage adsorption (Fig. S 5, Fig. 35).

III.3 Conclusion

This study provides first mechanistic insights into the substrate interaction of the motor ATPase EssC from the pathogen *S. aureus* USA300. It could be indicated that the most distal ATPase domain D3 of EssC mediates substrate binding through a shallow, hydrophobic groove on the surface. In addition, I showed that substrate binding is not restricted to the D3 domain, but can be mediated by EssC-D2 and/or D1. My results demonstrate that the D3 domain is important for ATPase activity. Whether the D3 domain contributes actively to ATP hydrolysis for substrate translocation or has a regulating effect on the other ATPase domains has to be elucidated. However, mutation of the Walker B motif in EssD-D3 had a diametric effect on substrate translocation- boosting or abolishing substrate secretion.

The second project focused on the extracellular part of EsaA. I found that this segment folds into a α-helical domain, which is essential for protein secretion. Bobrovsky et al. proposed that the extracellular domain of EsaA could facilitate the substrates secretion through the cell wall [94]. This hypothesis is in line with the results of the secretion assay of this study. Moreover, in collaboration with the Lopez lab (CNB, Madrid), we revealed an additional function of the extracellular domain in bacterial competition, which is independent of the T7SSb activity.

Taken together, I propose a model of the T7SSb, which has a similar architecture and function compared to the T7SSa (Fig. 35). All membrane components are required for an active T7SSb and therefore build the membrane embedded secretion apparatus. Studies on the mycobacterial T7SSa Esx-3 and Esx-5 suggest that the interior of the secretion pore is formed by the ATPase of the system. Based on known homologous structures of motor ATPases from the Ftsk/SpoIIIB family, Zoltner et al suggested that the EssC hexamer builds a tube-like structure and forms a central channel, which would be sufficiently wide to translocate Esx substrates [55]. Consequently, EssC forms the central channel and is surrounded by the other membrane proteins, which build a scaffold to stabilize the complex and mediate opening/closing of the channel. Substrates interact with the most distal ATPase domain and are passed along the ATPase domains to the membrane pore. Conformational changes of the ATPase domains triggers opening/closing of the central channel. ATP hydrolysis provides the energy for this mechanical motion. On the extracellular site, EsaA facilitates substrate secretion through the 20-40 nm thick

cell wall. This mechanism could be mediated by EssB. EssB interacts with EsaA [100] and has a cytoplasmic and extracellular domain. Therefore EssB could notices conformational changes in the cytoplasm of the ATPase domains and reports to the extracellular domain of EsaA to support substrate secretion through the cell wall.

In addition, the extracellular domain of EsaA T7SSb is involved in bacterial competition, which does not depend on secretion of T7SSb substrates. A possible function would be direct or indirect (mediated by another protein) interaction with a neighboring competitor. I observed fibril-like structure, which indicates that EsaA might be responsible for cell-to-cell contact.

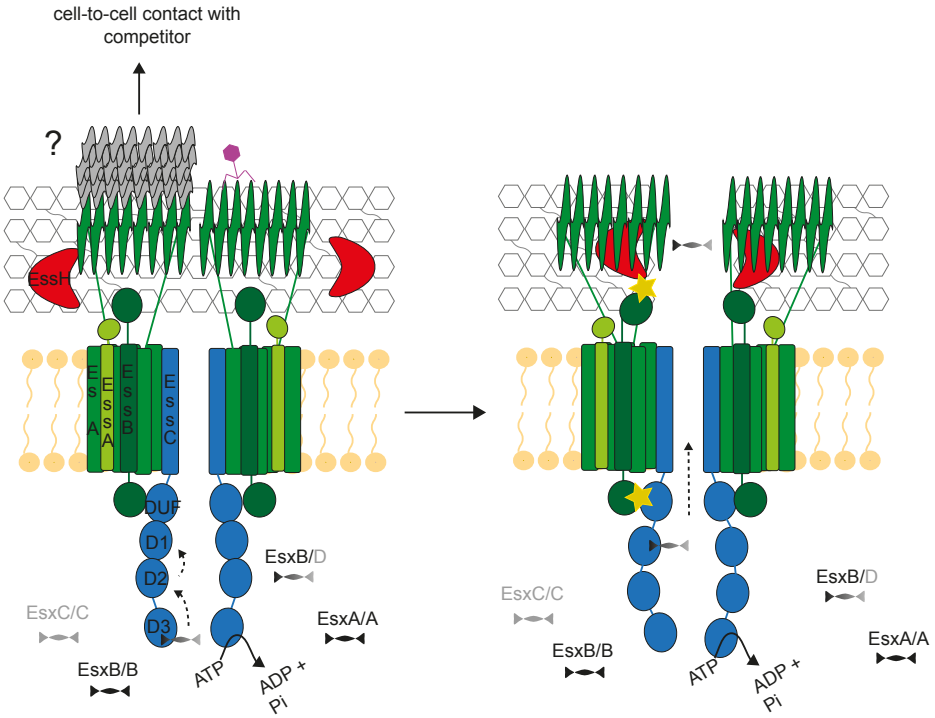

Fig. 35: Model of the architecture and possible mechanism of T7SSb from *S. aureus*.
EssC (blue) builds the central channel, which is surrounded by the scaffold proteins (EsaA, EssA, EssB (green)). Substrate binding and ATP hydrolysis triggers conformational change in the ATPase domains. The conformational change is noticed by EssB. Subsequently, EsaA, EssB and EssH facilitate substrate (grey, back) secretion through the cell wall. Stars indicate interaction of EssB. The extracellular domain of EsaA could be a possible phage receptor (Phage in purple). EsaA interacts with another protein (grey), building fibril-like structures and thereby supports bacterial competition by establishing cell-to-cell contact with a competitor.

III.3.1 Importance

The T7SSb is important for long-term pathogenicity of the *S. aureus*. Burts et al. showed that deletion of the small substrates EsxA and EsxB as well as the coupling protein EssC reduced the ability of *S. aureus* Newman to establish kidney or liver abscesses in infected mice four days post infection [43]. Hence, the T7SSb is a potential target to control and possibly clear *S. aureus* infections.

Moreover a drug therapy, targeting the T7SSb, addresses a different mechanism of *S. aureus* infections when compared to common treatments with antibiotics. A drug targeting the T7SSb could therefore be used as adjuvant to the common anti-microbial treatment.

Both investigated proteins are indispensable for substrate secretion. Consequently drugs targeting these proteins would inhibit substrate export and prevent abscess formation in several organs over a long time period. This work identified a surface-exposed substrate-binding site in EssC, which is required for toxin secretion. EsaA is a promising target, too. The domain is necessary for substrate translocation and exposed to the surface. Therefore the domain is accessible for potential drugs, which do not have to diffuse through the membrane of the bacteria.

IV. Material and Methods

IV.1 Material

IV.1.1 Common material and chemicals

Consumables and common chemicals were purchased from Merck (Darmstadt), Sigma-Aldrich (Steinheim), AppliChem (Darmstadt) and Roth (Karlsruhe). Kit systems and material for molecular techniques were purchased by New England Biolabs (NEB, Frankfurt am Main) and Macherey-Nagel (Düren).

IV.1.2 Special chemicals and consumables

Table 4: List of all special consumables used in this study

Compound	Supplier
Ambicin L (recombinant Lysostaphin)	Ambiproducts
Ampicillin	Roth
BATCH system Kit	Euromedex
Centrifugal concentrators (10, 100 kDa)	Millipore
Chemiluminescence substrate kit 12	Pierce
Crystalgen plates (24 well)	Jena Bioscience
Crystallization Screens	Hampton Research
Bis-Tris gel (4-16 %)	Thermo Fisher Scientific
BN-PAGE (3-12 % gels, buffers)	Thermo Fisher Scientific
5-Brom-4-chlor-3-indoxyl-β-D-galactopyranosid (X-gal)	Roth
n-Dodecyl β-D-maltoside (DDM)	Anatrace
Disuccinimidyl suberate (DSS)	Thermo Fisher Scientific
Dithiothreitol (DTT)	Roth
Chloramphenicol	Roth
Erythromycin	Roth
Glass beads, 0.25-0.5 mm	Roth
5 ml HiTrap-His column	GE Healthcare
1 ml HiTrap-Strep column	GE Healthcare
In-Fusion HD cloning Kit	Takara Bio Inc.
Circular siliconized cover slides	Jena Bioscience

Kanamycin	Roth
4x LDS sample buffer	Thermo Fisher Scientific
Lysogeny broth (LB) medium	Roth
Lysozyme	Roth
Monolith NT.115 Capillaries	Nanotemper
M9 minimal medium	Sigma Aldrich
Papain	Thermo Fisher Scientific
Protease inhibitor cocktail	Roth
Protein Labeling Kit-Red-NHS 2nd generation (MO-L011)	Nanotemper
Para-formaldehyde	Thermo Fisher Scientific
Phusion® High-Fidelity PCR Master Mix with GC Buffer	Invitrogen
Proteinase K	Merck
Rotiphorese® NF- acrylamide/bis (37.5:1, 40 %)	Roth
Roti®-PVDF membrane	Bio-Rad
Seleno-L-methionine	Sigma Aldrich
Sephacryl S-200 HR	GE Healthcare
Sephacryl S-300 HR	GE Healthcare
Superdex75 10/300 GL	GE Healthcare
Superdex 200 10/300 GL	GE Healthcare
Superose6 Increase 10/300 GL	GE Healthcare
Tryptic soy broth (TSB)	Becton Dickinson
Trypsin	Thermo Fisher Scientific
Uranyl acetate	SERVA
96-well sitting-drop crystallization plates Crystalquick™	Greiner Bio-One
384-well Microplate µCLEAR®	Greiner Bio-One
Φ11 phage lysate	AG Lopez, CNB, Madrid

Table 5: List of restriction enzymes used in this work

Restriction enzyme	Supplier
AfeI	New England Biolabs
BamHI-HF	New England Biolabs
DpnI	New England Biolabs
EcoRI-HF	New England Biolabs
HindIII-HF	New England Biolabs
XbaI-HF	New England Biolabs

Table 6: List of crystal screens used in this work

Name	**Supplier**
Crystal Screen, Crystal Screen 2	Hampton Research
Index Screen HT	Hampton Research
JCSG+	Molecular Dimensions
Nextal PEG Suite	Qiagen
Optimix^{TM}3	Fluidigm
Optimix^{TM} PEG	Fluidigm
PEGs Suite,	Qiagen
Wizard 1+2, Wizard 3+4	Emeral BioSystems

IV.1.3 Laboratory equipment and softwares

Table 7: List of all equipment necessary to conduct experiments

Equipment	**Supplier**
Äkta pure	GE healthcare
Avanti J-20 XPI Centrifuge	Beckman & Coulter
10 Cell Density Meter Ultrospec 10	Ge Amersham
Cell homogenizer Fastprep24	MP Biomedicals
CLARIOstar®	BMG LABTECH
Cooling centrifuge 5427 R	Eppendorf
Cryo-loop	Hampton Research
CrystalCapTM, sample holder magnetic	Hampton Research

CryoVial	Hampton Research
Crystal storage pucks	Jena Bioscience
Dawn 8+ MALS detector	Wyatt Technology
EmulsiFlex-C3 homogenizer	ATA Scientific
Electrophoresis system Mini-Protean Tetra Cell	Bio-Rad
Electrophoresis system XCell SureLock	Bio-Rad
Falcon 3EC Direct Electron Detector	Thermo Fisher Scientific
Gel iX imager	Intas Science Imaging
Horizontal electrophoresis systems Perfect Blue Mini S, M	Peqlab
Analytic Honey Bee 963	Digilab
ImageQuant LAS4000 biomolecular imager	GE Healthcare
J-810 spectropolarimeter	Jasco
Lissy	Zinsser Analytik
Monolith NT.115	Nanotemper
Multifuge X3R	Thermo Fisher Scientific
Nanodrop 2000	Peqlab
Polyallomer tubes (1 ml)	Beckman & Coulter
Polycarbonat bottle (70 ml)	Beckman & Coulter
Polypropylen bottle (1 L)	Beckman & Coulter
PowerPac HC High current power supply	Bio-Rad
Optilab T-rEX refractive-index detector	Wyatt Technology
Tecnai™ G2 Spirit Twin,	FEI
Thermocycler T3	Biometra
Fixed angle rotors type 45Ti, 70Ti, MLA-130, J-LITE JLA-8.1000	Beckman & Coulter
Ultracentrifuge MAX-XP	Beckman & Coulter
Ultracentrifuge OptimaTM L-100 XP	Beckman & Coulter
Wetblotter Mini Trans-Blot Cell	Bio-Rad

Table 8: List of all software used for data analysis

Software	Source/Reference
ASTRA 6	Wyatt Technology
AxioVision	ZEISS
CCP4	[152]
COOT	[153]
ImageJ/Fiji	OpenSource
MARS	BMG LABTECH
MO.Affinity Analysis	Nanotemper
MO.Control	Nanotemper
Office 365 (2011)	Microsoft
Phenix 1.11.1-2575	OpenSource
Unicorn 6	GE healthcare
PyMOL	DeLano Scientific LLC
SerialEM	[154]
SHELX	[155]
Spectra Manager	Jasco
XDS	[156]

IV.1.4 Buffer formulations

IV.1.4.1 Protein purification buffers

Buffer A	300 mM NaCl, 50 mM Tris, pH 8.0, 3 mM DTT
Buffer A_m	300 mM NaCl, 50 mM Tris, pH 8.0, 3 mM DTT, 0.05 % DDM
Buffer A_{SeMet}	300 mM NaCl, 50 mM Tris, pH 8.0, 5 mM DTT
Buffer B_{Strep}	300 mM NaCl, 50 mM Tris, pH 8.0, 3 mM DTT, 2.5 mM D-desthiobitin (DTB)
Buffer $B_{m\text{-}Strep}$	300 mM NaCl, 50 mM Tris, pH 8.0, 3 mM DTT, 0.05 % DDM, 2.5 mM DTB

Buffer B_{His}	300 mM NaCl, 50 mM Tris, pH 8.0, 3 mM DTT, 250 mM imidazole, pH 8.0
Buffer $B_{SeMet-His}$	300 mM NaCl, 50 mM Tris, pH 8.0, 5 mM DTT, 250 mM imidazole, pH 8.0
Buffer C	150 mM NaCl, 20 mM Tris, pH 8.0, 3 mM DTT
Buffer C_m	150 mM NaCl, 20 mM Tris, pH 8.0, 3 mM DTT, 0.05 % DDM
Buffer C_{SeMet}	150 mM NaCl, 20 mM Tris, pH 8.0, 5 mM DTT

IV.1.4.2 Other buffers

10x ATPase buffer	20 mM HEPES, pH 8.0, 10 mM NaCl, 5 % glycerol, 1 mM $MgCl_2$, 0.5 mM TCEP
5 % Blocking solution	2.5 g milk powder ad up to 50 ml with TBS-T
3x DNA sample buffer	0.1 mM Orange G, 30 % (v/v) glycerol
4x Laemmli-buffer	250 mM Tris-HCl,, 40 % (v/v) glycerol 4 % SDS, 0.02 % (w/v) bromophenol blue 10 % (v/v) β-mercaptoethanol, pH 6.8
Lysis buffer	20 mM Tris, 10 mM EDTA, pH 7.5
1x PBS	37 mM NaCl, 1.8 mM KH_2PO_4, 2.7 mM KCl, 10 mM Na_2HPO_4,1.8 mM KH_2PO_4, pH 8.0 or pH 7.4

Running buffer	25 mM Tris, 192 mM glycine , 0.1 % (w/v) SDS pH 8.3
Separation gel	2.5 ml 1.5 M Tris-HCl pH 8.8, 100 µl 10 % (w/v) SDS, 50 µl 10 % (w/v) APS 15 µl TEMED 5 % 10 % 12 % 15 % 9.5 4.8 4.2 3.6 ml ddH_2O 2 2.5 3.1 3.8 ml acrylamide/bis (37.5:1, 40 %)
Stacking gel (6.7 %)	2.5 ml ddH_2O, 1.5 ml 0.5 M Tris-HCl, pH 6.8 0.6 ml acrylamide/bis (37.5:1, 40 %) 50 µl 10 % (w/v) SDS, 20 µl 10 % (w/v) APS 20 µl TEMED
Stripping buffer	1.5 g glycine, 10 µl 10 % (w/v) SDS, 1 ml Tween20, adjust to pH 2.2, ad up to 100 ml with ddH_2O
50x TAE	2 M Tris,1 M acetic acid, 0.05 M EDTA, pH 8.0
1x TAE	20 ml 50x TAE-Buffer ad up to 1 L with ddH_2O
10x TBS	200 mM Tris, 1.5 M NaCl, pH 7.4
1x TBS-Tween 20 (TBS-T)	100 ml 10x TBS, 500 µl Tween20 ad up to 1 L with ddH_2O
10x Trace elements	5 g EDTA, 0.05 g $ZnCl_2$, 0.01 g $CuCl_2$, 0.01 g $CoCl_2$, 0.01 g H_3BO_3, 1.6 g $MnCl_2$, pH 7.0 ad up to 1 L with ddH_2O

10x Transfer buffer	860 mM glycine, 250 mM Tris-HCl
1x Transfer buffer	100 ml 10x transfer buffer, 200 ml methanol 700 ml ddH_2O

IV.2 Methods

IV.2.1 Molecular biology techniques

IV.2.1.1 Cloning

IV.2.1.1.1 Cloning procedure

Cloning was performed using the Phusion polymerase (Invitrogen) and In-Fusion cloning Kit (Takara Bio Inc.). For vector linearization restriction enzymes (RE, NEB) or primers were used. All primers are listed in VII.4.

PCR reaction was performed as follows:

Master Mix

5x buffer	10 µl
100 µM Primer FW	2.5 µl
100 µM Primer RV	2.5 µl
10 mM dNTPs	1 µl
Phusion Polymerase	0.5 µl
DNA	40-60 ng
ddH_2O	ad up to 50 µl

Program

1) Initial denaturation	20-30 s at 98°C
2) Denaturation	10 s at 98°C
3) Annealing	10 s at T_m Primer
4) Extension	1000 bp/ 30 s at 72 °C
5) Final extension	5-10 min at 72 °C

*30 cycles of step 2-4

Vectors, which were linearized via PCR, were subsequently restricted with DpnI. Restriction reaction for all enzymes were performed as follows:

Master Mix		Program	
10x buffer	6 µl	Restriction	1 h at 37 °C
PCR reaction	50 µl	Reaction Stop	ad 10 µl of DNA
RE	1 µl (per RE)		sample buffer
ddH_2O	ad up to 60 µl		

After PCR or vector restriction, the sample was analyzed via agarose gel electrophoresis. The fragment was excised and purified using a PCR Clean-up Kit (Macherey-Nagel). Afterwards In-Fusion reaction was conducted with the purified DNA-fragments and the linearized vector as follows:

Reaction Mix	
Fragment(s)	30 ng
Linearized vector	30-60 ng
In-Fusion Polymerase	1 µl
ddH_2O	ad up to 10 µl

The reaction mix was incubated for 15 min at 50 °C and subsequently 2.5 µl solution were used for transformation into *E. coli* (IV.2.1.2.1).

IV.2.1.1.2 Cloning strategy of constructs

Table 9 lists all templates, fragment size, vectors and primers used for cloning. *EssC*-IBA3C-TwinStrep II was generated by cloning full-length *essC* into the IBA103 vector containing a C-terminal TwinStrep II-tag using primers X1/X2 to linearize the vector and X3/X4 to amplify *essC*. The *essC*-TwinStrep II was transferred into the IBA3C vector, using the primers X5/X6 and RE *HindIII* and *XbaI*. A TEV cleavage site was introduced into *essC*-TwinStrep II-IBA3C using the primers X7/X8 and the RE *AfeI* and *XbaI*. *EssCΔd3* was cloned into the IBA3C TwinStrep II-tag by using the primers X11/X12 for gene amplification and X9/X10 for vector linearization.

EssC-d3 was cloned into the pET16b vector using the X13/X14 for vector linearization and X15/X16 for gene amplification. *EssC-d2d3, esaA_ex2 to esaA_ex7* and *esxB* were cloned into the pET16b vector as described for *essC-d3* with the

primers X13-X32. *EsxB*-pET20b and *esxC*-pET20b were provided by the Lopez lab (CNB, Madrid). Stop-codon for *esxB*-Stop-pET20b and *esxC*-Stop-pET20b was introduced, using site directed mutagenesis with primers X33/X34 and X35/X36, respectively. Full-length EsaA and EsaA_ex1 were cloned into the IBA3C. The vector was linearized with X37/X38 and the genes were amplified using the primer X39/X40 and X41/X42. *EssC* and *essCΔd3* were cloned into the pLac vector using X43/X44 for vector linearization and X45/X46 and X47/X48 for gene amplification. The single point mutations were inserted into *essC* by splitting the gene into two fragments, whereby the overlapping primers contained the point mutation. For example, the mutation C1235A was inserted by generating the full-length *essC* with X49/X50 and X51/X52, whereby the primers are overlapping and harbor the point mutation. Both fragments were inserted into pLac vector, which was linearized using X43/X44. All point mutations were generated as described for C1235A using the primers X43 to X92. The pMAD vector was used for the markerless gene deletion of *essC*. The vector, harboring 400 bp upstream and downstream of the essC, was provided by the Lopez lab (CNB, Madrid). The markerless deletion of the extracellular domain of *esaA* was performed by inserting *esaA*, missing the aa 275-689, into the pMAD vector. The vector was restricted using *EcoRI* and *BamHI*. Two fragments, containing the N-terminal part (bp 1-825) and C-terminal part (bp 2067-3027), were generated by using the primers X93/X94 and X95/X96 and introduced into the pMAD vector. The primers included a $Flag_{3x}$-tag, that was inserted instead of the extracellular domain.

Genes *esxB* and *esxC* were cloned into the vector pKNT25, containing the fusion protein for the bacterial two-hybrid assay. The vector was restricted using *EcoRI* and *HindIII*. The genes were amplified using X97/X98 for *esxB* and X99/X100 for *esxC*. *EsaA*, *essB* and *essC,* inserted into the pUT18 and pUT18C vector, comprising the fusion protein at the N-terminus or C-terminus were supplied by the Ohlsen lab, Institute for Molecular Infection Biology (IMIB), Würzburg.

IV.2.1.1.3 Cloning into S. aureus USA300

The markerless gene deletion for *essC* was introduced into the genome of *S. aureus* USA300 in order to generate the *S. aureus ΔessC*. The markerless domain deletion for *esaA* was introduced into the genome of *S. aureus* USA300 to generate the *S. aureus esaAΔex2*. All other constructs, inserted into the pLac vector (*essC, essCΔd3*

and *essC-point mutations)* were only introduced into *S. aureus ΔessC* but not integrated into the genome. The pMAD and pLac vectors are temperature sensitive in *S. aureus* and only replicate at/less than 30 °C. After transformation into *S. aureus* RN4420 (IV.2.1.2.2), blue colonies were grown in TSB medium containing 2 µg/ml erythromycin at 30 °C for 6 h and used for phage production. For that purpose 300 µl cell suspension was incubated with 5 mM $CaCl_2$ at 57 °C for 90 s. Afterwards, 100 µl of φ11 phage lysate, supplied by the Lopez lab (CNB, Madrid), in dilutions $1x10^{-3}$, $1x10^{-4}$, $1x10^{-5}$ was mixed with the cells and rested for 15-60 min at room temperature. Afterwards, cell suspension was added to 3 ml TSB-soft agar supplemented with 20 mM $MgSO_4$ and spread on LB plates. Phage hollows were harvested after 16-18 h at 30 °C by scrapping off the soft agar layer with 3 ml TSB, centrifuged for 10 min at 4000 x g and filtered two times through 0.2 µm filters. 100 µl phage lysate, containing the plasmid, were incubated with 300 µl *S. aureus* USA300, which were grown for 6 h at 37 °C. The *S. aureus* USA300 cells suspension was heat shocked for 90 s at 57 °C and supplemented with 5 mM $CaCl_2$ before incubation with phage lysate. The cell suspension was incubated for 15-60 min at room temperature and spread on 100 mM X-gal, 150 µg/ml erythromycin and 20 mM sodium citrate. The plates were incubated for 2-3 d at 30 °C. Blue colonies were used for the 1st and 2nd recombination as described in [157].

For the 1st recombination *S. aureus* USA300 cells, containing the plasmid, were grown for 6 h at 42 °C in TSB and spread on TSB plates, supplemented with 150 mM erythromycin and 100 mM X-Gal. Thereby the vector is inserted into the genome. For the 2st recombination a blue colony was incubated in TSB for 5-6 h at 30 °C and shifted to 42 °C for another 3 h. The cell suspension ($1x10^{-3}$, $1x10^{-4}$, $1x10^{-5}$) was spread on TSB plates, containing X-Gal. Thereby the vector backbone was excised and only the fragment was left in the genome.

Table 9: Cloning strategies for pET, IBA and pLac vectors

Gene	Source	Boundaries gene [nt]	Vector	Vector linearization	Primers for gene
essC	codon optimized (codopt) for *E. coli*	1-4440	IBA103	X1/X2	X3/X4
essC	essC-IBA103	1-4440	IBA3C-Twin-Strep II	*HindIII/XbaI*	X5/X6
essC	essC-Twin-StrepII-IBA3C	1-4440	IBA3C-Twin-Strep II	*AfeI/XbaI*	X7/X8
essCΔd3	codopt for *E. coli*	1-3744	IBA3C	X9/X10	X11/X12
essC-d3	codopt for *E. coli*	3744-4440	pET16b	X13/X14	X15/X16
essC-d2d3	codopt for *E. coli*	2931-4440	pET16b	X13/X14	X17/X18
esaA_ex2	codopt for *E. coli*	825-2067	pET16b	X13/X14	X19/X20
esaA_ex3	codopt for *E. coli*	612-2067	pET16b	X13/X14	X21/X22
esaA_ex4	codopt for *E. coli*	741-2067	pET16b	X13/X14	X23/X24
esaA_ex5	codopt for *E. coli*	825-2007	pET16b	X13/X14	X25/X26
esaA_ex6	codopt for *E. coli*	825-1806	pET16b	X13/X14	X27/X28
esaA_ex7	codopt for *E. coli*	939-1935	pET16b	X13/X14	X29/X30
esxB	*S. aureus* USA300_FPR3757	1-312	pET16b	X13/X14	X31/X32

esxB-Stop	*esxB*-pET20b	1-312	pET20b	X33/X34	-
esxC-Stop	*esxC*-pET20b	1-390	pET20b	X35/X36	-
esaA	codopt for *E. coli*	1-3027	IBA3C	X37/X38	X39/X40
esaA_ex1	codopt for *E. coli*	141-2412	IBA3C	X37/X38	X41/X42
essC	*S. aureus* USA300_FPR3757	1-4440	pLac	X43/X44	X45/X46
essCΔd3	*S. aureus* USA300_FPR3757	1-3744	pLac	X43/X44	X47/X48
essC-C1325A	*S. aureus* USA300_FPR3757	1-4440	pLac	X43/X44	X49/X50 and X51/X52
essC-N1342A	*S. aureus* USA300_FPR3757	1-4440	pLac	X43/X44	X53/X54 and X55/X56
essC-L1358A	*S. aureus* USA300_FPR3757	1-4440	pLac	X43/X44	X57/X58 and X59/X60
essC-Q1363A	*S. aureus* USA300_FPR3757	1-4440	pLac	X43/X44	X61/X62 and X63/X64
essC-F1370A	*S. aureus* USA300_FPR3757	1-4440	pLac	X43/X44	X65/X66 and X67/X68
essC-S1374A	*S. aureus* USA300_FPR3757	1-4440	pLac	X43/X44	X69/X70 and X71/X72
essC-Y1376A	*S. aureus*	1-4440	pLac	X43/X44	X73/X74 and

	USA300_FPR3757				X75/X76
essC-Y1376F	*S. aureus* USA300_FPR3757	1-4440	pLac	X43/X44	X77/X78 and X79/X80
essC-N1379A	*S. aureus* USA300_FPR3757	1-4440	pLac	X43/X44	X81/X82 and X83/X84
essC-D1380A	*S. aureus* USA300_FPR3757	1-4440	pLac	X43/X44	X85/X86 and X87/X88
essC-L1358/S1374	*essC-L1358A* pLac	1-4440	pLac	X43/X44	X89/X90 and X91/X92
esaA_Δex2	*S. aureus* USA300_FPR3757	1-825/2067-3027	pMAD	*EcoRI/BamHI*	X93/94 and X95/96
esxB	*S. aureus* USA300_FPR3757	1-312	pKNT25	*EcoRI/BamHI*	X97/X98
esxC	*S. aureus* USA300_FPR3757	1-390	pKNT25	*EcoRI/BamHI*	X99/X100

IV.2.1.2 Transformation

IV.2.1.2.1 *Transformation into E. coli*

BL21 star (Thermo Fisher Scientific) and Stellar cells (Takara Bio Inc.) were chemically competent. Cells were stored at -80 °C and put on ice before usage. 2.5 µl of In-Fusion reaction or 1 µg of DNA were added to the cells and incubated for 20 min on ice. After the heat shock at 42 °C for 45 s, cells were chilled on ice for 3 min and supplemented with 500 µl SOC-medium (supplied with competent cells). Cells recovered for 1 h at 37 °C. In-Fusion reactions were not shaken.

IV.2.1.2.2 Transformation into S. aureus RN4220

S. aureus RN4220 were electro-competent cells (supplied by the Lopez lab (CNB, Madrid)). 1 µg plasmid DNA was used for transformation. Cells were incubated with DNA for 15 min on ice and transferred into pre-chilled 0.1 cm electroporation cuvette. After pulsing, cells were immediately supplemented with 500 µl TSB, recovered for 2 h at 30 °C and spread on TSB plates containing 2 µg/ml erythromycin and 100 mM X-Gal. Plates were incubated for 2 d at 30 °C.

IV.2.2 Protein expression and purification

IV.2.2.1 Membrane proteins EsaA, EssC and EssCΔD3

LB medium, supplemented with 25 µg/ml chloramphenicol, was inoculated with an overnight culture of BL21 star cells comprising *esaA*-IBA3C, *essC*-TEV-TwinStrep II-IBA3C or *essCΔD3*-TEV-TwinStrep II-BA3C vector, in a 1/100 ratio. Bacteria were grown at 37 °C, while shaking by 200 rpm until OD_{600}=0.5 and cooled down to 18 °C. Overexpression was induced with 0.2 µg/ml anhydrotetracycline (AHT) and bacteria grew for 20 h at 18 °C, shaking by 180 rpm. All following steps were performed at 4 °C. Bacteria were centrifuged at 4 000 x g for 15 min. The cell pellets were dried, resuspended in buffer A and broken by three passages using an EmulsiFlex-C3 homogenizer (ATA Scientific). To separate unbroken cells from the cell extract, the sample was centrifuged at 6 000 x g for 10 min. Cell lysate and cell membrane were separated by another centrifugation step at 100 000 x g for 70 min. The membrane pellet was resuspended in 50 ml buffer A and incubated with 0.5 % DDM for 1 h, while stirring. After another centrifugation step at 100 000 x g for 70 min, solubilized membrane proteins were present in the supernatant. The supernatant was applied to

a 1 ml HiTrap-Strep column (GE Healthcare), which was equilibrated in buffer A_m. After sample application the column was washed with 30 CV buffer A_m and protein was eluted with 100 % buffer $B_{m\text{-}Strep}$. The peak fraction was collected and concentrated to 500 µl using a 100 kDa concentrator (Millipore). The sample was subsequently purified by SEC, using a superose6 Increase column (GE Healthcare) and buffer C_m. Peak fractions were analyzed by SDS-PAGE and BN-PAGE (Thermo Fisher Scientific).

For expression of EssC and EssCΔD3 LB medium and all buffers were supplemented with 10 mM $MgCl_2$. Chromatography programs are described in Table 10.

Table 10: Chromatography programs

Program	1 ml HiTrap-Strep	5 ml HiTrap-His	SEC
Equilibration	1 ml/min, 10-15 CV with buffer A	5 ml/min,10-15 CV with buffer A	2 CV buffer C
Sample application	max 0.5 ml/min	max 2.5 ml/min	max. speed as suggested by the supplier
Wash step 1	0.5 - 1 ml/min, 10 CV with buffer A	2.5- 5 ml/min, 20 CV with buffer A	-
Wash step 2	-	2.5- 5 ml/min, 20 CV with 20 % buffer B	-
Elution	0.5 ml/min, 10 CV with 100 % buffer B	2.5 ml/min, 10 CV with 100 % buffer B	1.2 CV with buffer C

IV.2.2.2 Cytosolic proteins

LB medium supplemented with antibiotics was inoculated 1/100 with an overnight culture of BL21 star cells, containing the vector with the gene of interest. Bacteria were grown at 37 °C, shaking at 200 rpm, until OD600=0.5, cooled down to 26 °C and induced with IPTG or AHT, depending on the plasmid (Table 11). Bacteria grew at 26 °C and were centrifuged at 4 000 x g for 15 min at 4 °C. All following steps were performed at 4 °C. Cell pellets were dried, resuspended in buffer A and cells were broken by three passages using an EmulsiFlex-C3 homogenizer (ATA Scientific). Cell debris were separated from cytosolic fraction by a centrifugation step with 40

000 x g for 70 min. The supernatant was purified using AC. The AC column (GE Healthcare) was equilibrated with 10 CV of buffer A. The sample was applied to the column, washed with buffer A until the baseline was reached and eluted with buffer B. AC protocols can be found in Table 10. The peak fraction was collected and samples containing a TEV cleavage site were treated with the protease (IV.2.2.4). Samples without a TEV cleavage site were concentrated using a 10 kDa concentrator and purified by SEC with buffer C. Peak fractions were analyzed by SDS-PAGE. Detailed information about antibiotics, inducer, expression time, TEV-cleavage, AC and SEC columns are provided in Table 11.

IV.2.2.3 EsaA_ex2 expression for Selenomethionine crystallography

A pre-culture using LB medium supplemented with 100 µg/ml ampicillin including five freshly transformed colonies of *esaA_ex2*-pET16b, was grown for 6-8 h at 37 °C at 180 rpm. The pre-culture was used to set up an overnight culture at 37 °C at 180 rpm in M9 minimal medium (1/100 dilution). The M9 minimal medium was enriched with 20 % glucose, 1 mM $MgSO_4$, 0.3 mM $CaCl_2$, 10x trace elements and 1 % thiamin and biotine and supplemented with 100 µg/ml ampicillin.

10 L M9 minimal medium was inoculated with the overnight culture (1/100 dilution) and grown until the OD_{600}=0.5 at 37 °C, 200 rpm. The culture was supplemented with 0.5 g of leucine, isoleucine, valine and selenomethionine and 1 g of lysine, threonine and phenylalanine per 10 L and incubated for 15 min at 26 °C. Afterwards, the culture was induced with 1 mM Isopropyl-β-D-thiogalactopyranosid (IPTG) and grown for 20 h at 26 °C at 180 rpm. The culture was harvested and purified as described for cytosolic proteins (IV.2.2.2). All buffers contained 5 mM DTT (buffer A_{SeMet}, $B_{SeMet\text{-}His}$, C_{SeMet}).

IV.2.2.4 TEV cleavage and dialysis

After AC, the peak fraction was collected and protein concentration was measured. 1:10 (w/w) ratio, TEV protease to protein, was used for cleavage overnight, dialyzing in the corresponding buffer A, supplemented with 0.5 mM EDTA. Subsequently the sample was dialyzed again for 2-4 h in buffer A, resulting in a total dilution of 1:10 000. Afterwards the sample was separated from TEV protease, which contains a His_{6x}-tag by AC. The flow through was collected and used for further purification via SEC as described in IV.2.2.2.

Table 11: Detailed information for expression of cytosolic proteins

Protein	Vector	LB supplement	Induction	Expression time	TEV cleavage	Sample application	Buffers	AC column	SEC column
EssC-D3	pET16b	100 µg/ml ampicillin 10 mM $MgCl_2$	1 mM IPTG	3 h	yes	2.5 ml/min supplemented with 20 mM imidazole	Buffer A, B_{His}, C supplemented with 10 mM $MgCl_2$	1 x 5 ml HiTrap-His	Superdex 75 pg
EssC-D2D3	pET16b	100 µg/ml ampicillin 10 mM $MgCl_2$	1 mM IPTG	2 h	yes	2.5 ml/min supplemented with 20 mM imidazole	Buffer A, B_{His}, C supplemented with 10 mM $MgCl_2$	1 x 5 ml HiTrap-His	Sephacryl-S200 HR
EsxB	pET16b	100 µg/ml ampicillin	1 mM IPTG	16 h	yes	2.5 ml/min supplemented with 20 mM imidazole	Buffer A, B_{His}, C supplemented with 10 mM $MgCl_2$	1 x 5 ml HiTrap-His	Superdex 75 pg
EsxC	pET20b	100 µg/ml ampicillin	1 mM IPTG	16 h	no	2.5 ml/min supplemented with 20 mM imidazole	Buffer A, B_{His}, C supplemented with 10 mM $MgCl_2$	1 x 5 ml HiTrap-His	Superdex 75 pg
EsaA_ex1	IBA3C	25 µg/ml chloramphenicol	0.2 µg/ml AHT	20 h	no	0.5 ml/min	Buffer A, B_{Strep}, C	2 x 1 ml HiTrap-Strep	Sephacryl-S300 HR
EsaA_ex2	pET16b	100 µg/ml ampicillin	1 mM IPTG	7 h	yes	2.5 ml/min supplemented with 20 mM imidazole	Buffer A, B_{His}, C	1 x 5 ml HiTrap-His	Sephacryl-S200 HR
EsaA_ex3-7	pET16b	100 µg/ml ampicillin	1 mM IPTG	7-16 h	yes	2.5 ml/min supplemented with 20 mM imidazole	Buffer A, B_{His}, C	1 x 5 ml HiTrap-His	Sephacryl-S200 HR

IV.2.3 X-ray crystallography

IV.2.3.1 Crystallization of proteins

For crystallization the protein solution was concentrated to 5, 10 and 15 mg/ml, using concentrators (Millipore). Different crystal screens were used (Table 6). 30 µl mother liquor was applied to the well in sitting drop plates and 0.3 µl protein was mixed 1:1 with mother liquor. Afterwards plates were incubated at 18 °C. Pipetting was performed by the Honey Bee 963 robot (Digilab). When crystals appeared hanging drop experiments were performed, screening different pH, PEG's and PEG concentrations. 600 µl mother liquor was used and 1.5 µl protein was mixed 1:1 with mother liquor. Crystals were grown at 18 °C, 12 °C or 4 °C. For harvesting, the crystals were transferred into mother liquor, supplemented with 25-30 % glycerol, PEG400 or MPD as cryo-protectant and flash frozen with liquid nitrogen.

IV.2.3.2 Data analysis and structure determination for EssC-D3 and EsaA_ex2

IV.2.3.2.1 EssC-D3

Native data collection was done at the beamline 14.1 at the Helmholtz Zentrum (Berlin, Germany) at 100 K and indexed, integrated and scaled to 1.7 Å resolution using the XDS software package. The phase problem was solved by single-wavelength anomalous dispersion of sulfur atoms (S-SAD). Data was collected at beamline id23eh1 of the European Synchrotron Radiation Facility in Grenoble (ESRF), indexed, integrated, and scaled to a 1.7 Å resolution, using the XDS software package. The phase problem was solved with SHELX. The initial model for EssC-D3 was built by AUTOBUILD. Refinement was done by alternating rounds of model building with COOT and PHENIX. The refinement protocol included initial rigid body refinement, cartesian and individual B factor refinement.

IV.2.3.2.2 EsaA_ex2

Data collection was performed on at the ESRF, beamline ID30-A3. The collected data were processed using the XDS software package. POINTLESS from the CCP4 package was used for space-group determination. The Matthews coefficient and the solvent content were calculated using MATTHEWS_COEF. Structure could not be solved due to a lack of homologues.

IV.2.4 Electron microscopy- negative stain

Electron microscopy of negative stained samples is a method to image particles and screen the quality of the sample. The sample is fixed on a grid using heavy atom salt solutions like uranyl acetate or ammonium molybdate and dried afterwards. Heavy atoms interact with the electron and the distribution of heavy atoms is visualized [158].

IV.2.4.1 Sample preparation and analysis

A carbon-coated copper mesh grid was glow discharged before usage. 3 µl sample (10-20 nM) was applied to the grid for 30 seconds. The sample was carefully taken off with filter paper. Subsequently, the grid was wetted with 3x 3 µl drops of 3 % (w/v) uranyl acetate, incubated for 30 s with the last drop and blotted with filter paper. Afterwards the grid was washed with 3x 3 µl ddH_2O drops and blotted with filter paper. The grid was dried for 5 min on air. All steps were performed at room temperature.

The grid was analyzed using EM (Tecnai™ G2 Spirit Twin, FEI) at high tension of 120 kV and a magnification of 4200-fold. EM images were recorded with a Falcon 3EC direct detector. The software SerialEM was used for automated data acquisition.

IV.2.5 Biochemical assay

IV.2.5.1 Limited proteolysis

Protein, 150 µg recombinant EsaA_ex1, was incubated for 1 h with 1.5 µg trypsin or papain at room temperature and samples were taken every 15 min. The reaction was stopped with 3x protease inhibitor cocktail (Roche). Samples were separated via 12 % SDS-PAGE. The prominent band at 48 kDa was excised and analyzed by mass spectrometry (MS). The MS experiment and data analysis was performed by the Schlosser lab, Rudolf-Virchow Center (RVZ), Würzburg.

IV.2.5.2 Size-exclusion chromatography-multi-angle light scattering (SEC-MALS)

SEC, using a sephacryl200 12/300 GL column, was coupled to a Dawn 8+ MALS detector and an Optilab T-rEX refractive-index detector (Wyatt Technology) to carry out SEC-MALS experiments. The column was equilibrated for 2 CV with buffer A and 4 mg/ml EsaA_ex2 was used for sample application. SEC was performed with 0.5

ml/min at room temperature. Data was analyzed using the ASTRA6 software (Wyatt Technology).

IV.2.5.3 Circular dichroism (CD) and thermal unfolding experiments

The Jasco J-810 spectropolarimeter was used to perform CD spectroscopy and thermal unfolding experiments. Spectra of EsaA_ex2 was recorded from 195 to 260 nm at 50 nm/min with a response time of 2 s and band width of 1 nm at 4 °C. Analysis showed a strong signal for an α-helical structure. Therefore, thermal unfolding experiments were conducted at 224 nm from 4 °C to 70 °C, at a bandwidth of 2 nm and 16 s response time. Temperature was increased by 1 K/min. 5 µM of EsaA_ex2 was used in 50 mM 1x PBS pH 8.0.

IV.2.5.4 Co-migration assays

IV.2.5.4.1 Double pull-down assay

The construct of the ATPase *essC*-IBA3-TwinStrep II was transformed into BL21 star cells together with the substrate *esxB*-Stop-pET20 and *esxC*-Stop-pET20. One successful transformed colony was used for a pre-culture. 6 L LB medium, supplemented with 100 µg/ml ampicillin and 25 µg/ml chloramphenicol, were inoculated, starting at OD_{600}=0.05. Samples were expressed and processed as described for *essC*-IBA3-TEV-TwinStrep II until the AC step (IV.2.2.1). First, the sample was applied to the HiTrap-Strep column. The peak fraction was collected and subsequently applied to the HiTrap-His column. Samples were used for SDS-PAGE and western blot analysis. Western blots were performed using α-His-HRP and α-Strep-HRP.

IV.2.5.4.2 Pull-down assay with SEC

The constructs of the ATPase *essC*-IBA3-TEV-TwinStrep II and *essCΔD3*-TEV-IBA3-TwinStrep II were transformed into BL21 star cells together with the substrates *esxB*-Stop-pET16b and *esxC*-Stop-pET16b, as described in chapter IV.2.1.2.1. One successful transformed colony was used for a pre-culture. 6 L LB medium, supplemented with 100 µg/ml ampicillin and 25 µg/ml chloramphenicol, were inoculated, starting at OD_{600}=0.05. Expression and purification were done as described for EssC in chapter IV.2.2.1. 500 µg sample were applied to the SEC. After SEC, 10 µl of peak fractions were used for BN-PAGE and subsequently analyzed via

western blot. The western blot was performed with antibody against the substrate (EsxB and EsxC). Afterwards, the blot was stripped and the membrane analyzed, using the α-Strep-HRP antibody to detect the EssC.

IV.2.5.5 Fluorescence quenching experiment

Affinity measurements were performed using the Monolith NT.115 from Nanotemper. Protein samples, recombinant EssC, EssC-ΔD3, and EssC-D2D3 of high MW oligomer and EssC-D3 monomer, were labeled using the protein labeling kit RED-NHS 2nd generation (Nanotemper). Labeling procedure was conducted according to the manufacturers protocol. Concentration of labeled protein was determined and assay was performed as suggested by the MO.Control software (Nanotemper).
ATPase, ATP and substrate were equilibrated in 150 mM NaCl, 20 mM Tris, pH 8.0, 10 mM $MgCl_2$, 1 mM DTT and 0.05 % DDM. Substrate was titrated to the ATPase as follows:

- 0.5 nM EssC: 0.65 mM to 19.8 nM EsxB
- 20 nM EssCΔD3: 0.5 mM to 16.8 nM EsxB
- 10 nM EssC-D2D3: 1 mM to 33.6 nM EsxB
- 1 nM EssC-D3: 0.1 mM to 3.1 pM EsxB
- 6 nM EssC: 100 mM to 3.1 nM ATP
- 6 nM Essc-D3: 100 mM to 3.1 nM ATP

The reactions were incubated for 20 minutes before measurements. The assay was performed at room temperature using Monolith NT.115 Capillaries (Nanotemper).
The fluorescence intensity was used for data analysis using the MO.Affinity Analysis software (Nanotemper).

IV.2.5.6 Crosslinking experiments

IV.2.5.6.1 Crosslinking in vivo

In vivo crosslinking was performed using the crosslinker PFA. For this purpose *S. aureus* USA300 pre-cultures were grown in TSB medium overnight at 30 °C and washed with 1x PBS, pH 7.4. The pellets were resuspended in 1 ml TSB and cultures of 30 ml TSB were set up, starting at OD_{600}=0.05. Cultures were grown for 6 h at 28 °C, reaching OD_{600}=2. Cells were centrifuged at 2770 x g at room temperature, resuspended in 1x PBS, pH 7.4. and incubated for 30 min at room temperature with

0.6 % PFA. The reaction was stopped with 100 mM Tris, pH 8.0. The membrane fraction was isolated as described in chapter IV.2.6.1. The pellets were solved in 100 µl 200 mM NaCl and 50 mM Tris, pH 7.4 and 1x SDS samples buffer was added. The samples were boiled for 20 min at 50 °C, followed by 5 min at 100 °C. Proteins were separated on a 5 % SDS-PAGE and subsequently analyzed via western blot.

IV.2.5.6.2 Crosslinking in vitro

In vitro crosslinking was performed with the crosslinker DSS. To this effect, proteins had to be transferred to 20 mM HEPES pH 7.4, 150 mM NaCl, 10 mM $MgCl_2$ and 3 mM DTT. Recombinant protein, EssC-D3 monomer was mixed with either EsxB or EsxC. 0.5 µM EssC-D3 was mixed with 5 µM Substrate and 50x excess of DSS. Samples were incubated for 2 h on ice. The reactions were stopped by adding 1x LDS sample buffer and boiled for 10 min at 70 °C. Proteins were separated using a 4-12 % Bis-Tis gel.

IV.2.5.7 ATPase activity assay

ATPase activity was measured by determining the turnover rates of NADH, which is coupled to ATP hydrolysis. NADH decreases proportional to ATP, which is linked to a regeneration system involving the phosphoenolpyruvate (PEP), pyruvat kinase (PK) and lactate dehydrogenase (LDH). NADH absorbance at 340 nm was monitored for 20 min using the CLARIOstar and the MARS software. For ATPase assay EssC-D3 monomer was used and conducted at room temperature. ATP was supplied automatically after 100 s to start the reaction. All experiments were performed in triplicates and the reaction was set up as follows:

Compound	**Concentration**
EssC-D3	1 µM
EsxC-peptide (substrate)	50 µM
LDH	2.7 U
PK	1.8 U
PEP	2 mM
10x ATPase buffer	1x buffer
ATP	2.5 mM
ddH_20	ad up to 50 µl

As positive controle the ATPase p97 provided by Petra Hänzelmann, Schindelin lab, RVZ, Würzburg, was used. Reaction was conducted as described in [159].

IV.2.5.8 Gel electrophoresis

IV.2.5.8.1 SDS-PAGE

SDS gel electrophoresis was performed, using equipment from Bio-Rad. Recipes for stacking and separation gel are provided in IV.1.4. Protein solution was supplemented with 1x SDS samples buffer, boiled at 99 °C for 10 min and rested for 3 min on ice. Protein samples, including the marker ROTI®Mark Standard (Roth) or Color Prestained Protein Standard, Broad Range (NEB), were load on the gel and separated for 1 h by constant 180 V. The gel was incubated in Coomassie-blue stain for 1-3 h and afterwards rinsed in water.

IV.2.5.8.2 Blue native-PAGE

BN gel electrophoresis was performed, using equipment, buffers and 3-12 % gels from Life Technologies. Light and dark blue buffer was prepared following the manufacturers protocol (Thermo Fisher Scientific). 10 µl of sample were mixed with 3.5 µl of native page buffer and 1/4 of detergent concentration, present in the protein sample. Final volume was 15 µl. 10 µl were load on the gel and run at 150 V, using the 1x dark blue buffer as cathode buffer. After 30 min, the cathode buffer was exchanged for 1x light blue buffer and run at 150 V for another 30 min. Afterwards voltage was set to 250 V and gel electrophoresis was performed for 45-60 min. BN-PAGE was carried out at 4 °C. The gel was stained with Coomassie-blue for 1-3 h.

IV.2.5.8.3 Agarose gel electrophoresis

1 % agarose gels were used to detect PCR and RE reactions. Agarose gels were supplemented with SYBR^{TM} Safe DNA Gel Stain 1 % (Thermo Fisher Scientific). In order to determine the size of DNA fragments 5 µl of 1 kb DNA ladder (NEB) was loaded and gels were run at 100 V for 30 min. Gels were exposed using Gel iX20 imaging system of Intas Science Imaging.

IV.2.5.9 Western blot analysis

IV.2.5.9.1 Protein transfer

Western blots were performed, using the wet blot system from Bio-Rad. Proteins were transferred onto a PVDF membrane (GE Healthcare). The membrane was activated before blotting by incubation for 1 min in 100 % methanol, followed by water and 1x transfer buffer. Whatman paper and sponges were equilibrated in 1x transfer buffer and the stack was assembled in the transfer cassette. The chamber was completely filled with 1x transfer buffer, including an ice pack. Proteins were transferred for 1 h by 100 V, while stirring.

IV.2.5.9.2 BN-PAGE membrane treatment

After protein transfer, the PVDF membrane was incubated for 15 min in 8 % acetic acid to fix the proteins. The membrane was rinsed in water and air-dried. Afterwards the membrane was re-activated with 100 % methanol for 30 s and shortly washed in TSB-T before adding blocking solution. Further steps were carried out as described in IV.2.5.9.3.

IV.2.5.9.3 Blocking, antibody incubation and development of the western blot membrane

After protein transfer the membrane was incubated in blocking solution for 1 h at room temperature. Before incubation in primary antibody, three washing steps for 5 min per step were performed in TSB-T. Incubation with primary antibody was carried out overnight at 4 °C. Afterwards membrane was washed three times for 5 minutes with TBS-T again and the secondary antibody was applied for 2 h at room temperature. Incubation of membrane with combined primary/secondary antibody was done for 2 h at room temperature. Subsequently the membrane was washed again in TSB-T (3x for 5 min) and developed with the enhanced chemiluminescence substrate kit 12 (Pierce) and the ImageQuant LAS4000 biomolecular imager. Images were processed using ImageJ. Antibody, dilution and solution and dilutions are listed in Table 12.

IV.2.5.9.4 Membrane stripping

All steps were done at room temperature. The membrane was incubated twice for 10 minutes in 50 ml stripping buffer. Afterwards the membrane was washed twice for 10 min in 1x PBS, pH 7.4, followed by two wash steps for 5 min with TBS-T. Membrane

was developed and if no signal was detected, membrane was treated as in IV.2.5.9.3.

Table 12: Antibodies used in this work

Antibody	Dilution	Solution	Supplier
α-His-HRP	1:5000	1 % milk-TSB-T	Sigma-Aldrich
α-StrepII-HRP	1:10000	1 % milk-TSB-T	IBA
α-EssB-rabbit	1:5000	5 % milk-TSB-T	Geibel lab
α-EssC-rabbit	1:1000	5 % milk-TSB-T	Palmer lab
α-EsxB-rabbit	1:380	5 % milk-TSB-T	Geibel lab
α-EsxC-rabbit	1:1000	5 % milk-TSB-T	Geibel lab
α-Flag-mouse	1:1000	1 % milk-TSB-T	Sigma-Aldrich
anti-mouse IgM-HRP	1:20000	TSB-T	Thermo Fisher Scientific
anti-rabbit IgG-HRP	1:5000	TSB-T	Life Technologies
α-RNAP-mouse	1:10000	1 % milk-TSB-T	Sigma-Aldrich

IV.2.6 Microbiology techniques

IV.2.6.1 Secretion assay

S. aureus USA300_FPR3757 pre-cultures were grown in TSB medium overnight at 30 °C and washed with 1x PBS before usage. TSB medium was supplemented with 150 µg/ml erythromycin for cultures containing the pLac vector. The pellet was resuspended in 1 ml TSB and main cultures of 30 ml TSB were set up starting at OD_{600}=0.05. Cultures were grown until OD_{600}=1, while shaking at 28 °C at 180 rpm. Afterwards cultures were centrifuged at 2770 x g for 10 min at room temperature, the supernatant was passed through a 0.2 µm filter and the cell pellet was frozen at -20 °C. All further steps were conducted at 4 °C. The supernatant was precipitated using 5 % trichloroacetic acid overnight. The samples were centrifuged at 6 000 x g for 15 min and carefully washed with 100 % ice-cold acetone. The precipitate was air-dried, resuspended in 100 µl 1x Laemmli buffer, 10 mM Tris, pH 8.0 for 2 h at 65 °C and rested overnight at room temperature. The samples were subsequently analyzed via western blot.

The cell pellets were resuspended in 1 ml lysis buffer supplemented with 50 µg/ml lysostaphin, 1 mM PMSF and 250 mg glass beads. After incubation for 10 min at 37 °C, samples were mechanically lysed, using the FastPrep24 shaker. Cell lysis was performed twice by 40 s with a speed of 6.5 m/s and the samples rested on ice in between. Glass beads were removed by centrifugation for 10 min at 4000 x g at 4 °C and the 800 µl supernatant was transferred in polyallomer tubes and centrifuged for 35 min at 100 000 x g at 4 °C. The pellet was resuspended in buffer A and incubated for 10 min at 50 °C. Supernatant (cytosolic fraction) and pellet were supplemented with 1x LDS sample buffer. Samples were analyzed, using western blot. Detailed information for SDS-PAGE and western blots are listed in Table 13.

Table 13: Detailed information for SDS-PAGE and western blot of samples from secretion assay

Detection	Samples	Sample load	SDS gel	Primary antibody	Protein size
EsxC secretion	supernatant	40 µl	15 %, 1.5 mm	α-EsxC-rabbit	~15 kDa
Precipitation control	supernatant	10 µl	12 %, 1 mm	α-His-HRP	~24 kDa
lysis control	supernatant	10 µl	12 %, 1 mm	α-RNAP-mouse	~150 kDa
EsxC expression	cell lysate	20 µl	15 %, 1 mm	α-EsxC-rabbit	~15 kDa
loading control	cell lysate	10 µl	12 %, 1 mm	α-RNAP-mouse	~150 kDa
EssC expression	membrane fraction	20 µl	3-12 % Bis-Tris, 1 mm	α-EssC-rabbit	~170 kDa
EsaA_Δex2 expression	membrane fraction	20 µl	12 %, 1 mm	α-Flag-mouse	60 kDa

IV.2.6.2 Bacterial two-hybrid

Bacterial two-hybrid assays were performed using the Euromedex system. Two fragments, T18 and T25, of the adenylate cyclase are catalytically active and hydrolyze ATP when in close proximity to each other. ATP hydrolysis can be monitored by expression of β-galactosidase [143]. The plasmids pKT25 and pUT18 were transformed into *E. coli* BTH101. 2.5 ng per plasmid was used for transformation and recovered cell suspension was spread on LB plates, supplemented with 100 µg/ml streptomycin, 100 µg/ml ampicillin and 50 µg/ml kanamycin. Cells were incubated overnight at 30 °C. A colony was incubated for 8 h at 30 °C and spread on LB plates, containing 0.5 mM IPTG, 50 mM X-gal, 100 µg/ml streptomycin, 100 µg/ml ampicillin and 50 µg/ml kanamycin. Blue colonies were used for bacterial two-hybrid assay. 10 colonies per sample were incubated in 1 ml LB medium, supplemented with 100 µg/ml streptomycin, 100 µg/ml ampicillin and 50 µg/ml kanamycin and incubated over night at 30 °C, while shaking at 160 rpm. Next day, spot cultures were transferred onto LB plates, containing 100 µg/ml streptomycin, 100 µg/ml ampicillin, 50 µg/ml kanamycin, 0.5 mM IPTG and 100 mM X-gal. Colonies grew for 2-5 days at 18 °C.

IV.2.6.3 Competition assay

The competition assay was performed, using the *S. aureus* USA300 as attacker strain and *S. aureus* RN8325-4 as prey strain. Attacker and prey strain were grown in 3 ml TSB for 3-4 h at 37 °C, while shaking at 200 rpm. A main culture was set up with 30 ml TSB and starting at OD_{600}=0.1. For the assay 1 ml of attacker and prey strain were centrifuged at 2770 x g for 5 min and pellets were resuspended in 1 ml TSB medium. Attacker and prey strains were mixed 1:1 in 200 µl and grown overnight at 37 °C, while shaking at 200 rpm. Cells were plated in $1x10^{-3}$ and $1x10^{-4}$ dilutions, incubated at 37 °C overnight and cfu/ml was counted the next day. *S. aureus* USA300 colonies turn yellow to orange, whereas RN8325-4 colonies are white and therefore they are distinguishable. Following reactions were conducted:

1) *S. aureus* USA300 vs. prey (RN8325-4)
2) *esaA_Δex2* vs. prey
3) *ΔessC* vs. prey

V. References

1. Alvan, G., C. Edlund, and A. Heddini, *The global need for effective antibiotics-a summary of plenary presentations.* Drug Resist Updat, 2011. **14**(2): p. 70-6.
2. Saga, T.Y., K., *History of antimicrobial agents and resistant.* Jpn. Med. Assoc. J., 2009. **137**: p. 103–108.
3. Organization, W.H., *Antimicrobial resistance: global report on surveillance 2014.* 2014.
4. Gould, I.M., *Treatment of bacteraemia: meticillin-resistant Staphylococcus aureus (MRSA) to vancomycin-resistant S. aureus (VRSA).* Int J Antimicrob Agents, 2013. **42 Suppl**: p. S17-21.
5. Foster, T.J., *Antibiotic resistance in Staphylococcus aureus. Current status and future prospects.* FEMS Microbiol Rev, 2017. **41**(3): p. 430-449.
6. Humphreys, H., *Staphylococcus.* 2012: p. 176-182.
7. Prevention, C.f.D.C.a., *Antibiotic resistance threats in the united states.* 2019.
8. Rossolini, G.M., et al., *Update on the antibiotic resistance crisis.* Curr Opin Pharmacol, 2014. **18**: p. 56-60.
9. Prevention, C.f.D.C.a., *Antibiotic resistance threats in the united states.* 2013.
10. Fluit, A.C., *Livestock-associated Staphylococcus aureus.* Clin Microbiol Infect, 2012. **18**(8): p. 735-44.
11. Mediavilla, J.R., et al., *Global epidemiology of community-associated methicillin resistant Staphylococcus aureus (CA-MRSA).* Curr Opin Microbiol, 2012. **15**(5): p. 588-95.
12. Mendes, R.E., L.M. Deshpande, and R.N. Jones, *Linezolid update: stable in vitro activity following more than a decade of clinical use and summary of associated resistance mechanisms.* Drug Resist Updat, 2014. **17**(1-2): p. 1-12.
13. Rossi, F., et al., *Transferable vancomycin resistance in a community-associated MRSA lineage.* N Engl J Med, 2014. **370**(16): p. 1524-31.
14. T, F., *Chapter 12 Staphylococcus.* Medical Microbiology. 4th edition, 1996. **4th edition**.
15. Marshall, J.H., and Rodwell, E.S., *3rd International Symposium on Carotenoids Other Than Vitamin A, September 4-7. .* International Union of Pure and Applied Chemistry, Cluj, Romania,, 1972: p. pp.56-57.
16. Ogston, A., *Micrococcus Poisoning.* J Anat Physiol., 1882. **16**(4): p. 526-567.
17. Giesbrecht, P., J. Wecke, and B. Reinicke, *On the morphogenesis of the cell wall of staphylococci.* Int Rev Cytol, 1976. **44**: p. 225-318.
18. Kluytmans, J., A. van Belkum, and H. Verbrugh, *Nasal carriage of Staphylococcus aureus: epidemiology, underlying mechanisms, and associated risks.* Clinical Microbiology Reviews, 1997. **10**(3): p. 505-520.
19. von Eiff, C., et al., *Nasal carriage as a source of Staphylococcus aureus bacteremia. Study Group.* N Engl J Med, 2001. **344**(1): p. 11-6.
20. Huang, S.S. and R. Platt, *Risk of methicillin-resistant Staphylococcus aureus infection after previous infection or colonization.* Clin Infect Dis, 2003. **36**(3): p. 281-5.
21. Tong, S.Y., et al., *Staphylococcus aureus infections: epidemiology, pathophysiology, clinical manifestations, and management.* Clin Microbiol Rev, 2015. **28**(3): p. 603-61.
22. Brugger, S.D., L. Bomar, and K.P. Lemon, *Commensal-Pathogen Interactions along the Human Nasal Passages.* PLoS Pathog, 2016. **12**(7): p. e1005633.

23. Jenkins, A., et al., *Differential expression and roles of Staphylococcus aureus virulence determinants during colonization and disease.* mBio, 2015. **6**(1): p. e02272-14.
24. Otto, M., *Staphylococcus aureus toxins.* Curr Opin Microbiol, 2014. **17**: p. 32-7.
25. Wang, R., et al., *Identification of novel cytolytic peptides as key virulence determinants for community-associated MRSA.* Nat Med, 2007. **13**(12): p. 1510-4.
26. Clauditz, A., et al., *Staphyloxanthin plays a role in the fitness of Staphylococcus aureus and its ability to cope with oxidative stress.* Infect Immun, 2006. **74**(8): p. 4950-3.
27. de Haas, C.J., et al., *Chemotaxis inhibitory protein of Staphylococcus aureus, a bacterial antiinflammatory agent.* J Exp Med, 2004. **199**(5): p. 687-95.
28. Berends, E.T., et al., *Nuclease expression by Staphylococcus aureus facilitates escape from neutrophil extracellular traps.* J Innate Immun, 2010. **2**(6): p. 576-86.
29. Gresham, H.D., et al., *Survival of Staphylococcus aureus inside neutrophils contributes to infection.* J Immunol, 2000. **164**(7): p. 3713-22.
30. Higgins, J., et al., *Clumping factor A of Staphylococcus aureus inhibits phagocytosis by human polymorphonuclear leucocytes.* FEMS Microbiol Lett, 2006. **258**(2): p. 290-6.
31. Moreillon P1, E.J., Francioli P, McDevitt D, Foster TJ, François P, Vaudaux P., *Role of Staphylococcus aureus coagulase and clumping factor in pathogenesis of experimental endocarditis.* Infect Immun. , 1995. **63**
(12): p. 4738-43.
32. Rooijakkers, S.H., et al., *Staphylococcal complement inhibitor: structure and active sites.* J Immunol, 2007. **179**(5): p. 2989-98.
33. Thammavongsa, V., et al., *Staphylococcus aureus synthesizes adenosine to escape host immune responses.* J Exp Med, 2009. **206**(11): p. 2417-27.
34. McCormick, J.K., J.M. Yarwood, and P.M. Schlievert, *Toxic shock syndrome and bacterial superantigens: an update.* Annu Rev Microbiol, 2001. **55**: p. 77-104.
35. Falugi, F., et al., *Role of protein A in the evasion of host adaptive immune responses by Staphylococcus aureus.* mBio, 2013. **4**(5): p. e00575-13.
36. Cheng, A.G., et al., *A play in four acts: Staphylococcus aureus abscess formation.* Trends Microbiol, 2011. **19**(5): p. 225-32.
37. Kobayashi, S.D., N. Malachowa, and F.R. DeLeo, *Pathogenesis of Staphylococcus aureus abscesses.* Am J Pathol, 2015. **185**(6): p. 1518-27.
38. Cheng, A.G., et al., *Genetic requirements for Staphylococcus aureus abscess formation and persistence in host tissues.* FASEB J, 2009. **23**(10): p. 3393-404.
39. Hammel, M., et al., *The Staphylococcus aureus extracellular adherence protein (Eap) adopts an elongated but structured conformation in solution.* Protein Sci, 2007. **16**(12): p. 2605-17.
40. Scriba, T.J., et al., *The Staphyloccous aureus Eap protein activates expression of proinflammatory cytokines.* Infect Immun, 2008. **76**(5): p. 2164-8.
41. Stanley, S.A., et al., *Acute infection and macrophage subversion by Mycobacterium tuberculosis require a specialized secretion system.* Proc Natl Acad Sci U S A, 2003. **100**(22): p. 13001-6.

42. Pym, A.S., et al., *Recombinant BCG exporting ESAT-6 confers enhanced protection against tuberculosis.* Nat Med, 2003. **9**(5): p. 533-9.
43. Burts, M.L., et al., *EsxA and EsxB are secreted by an ESAT-6-like system that is required for the pathogenesis of Staphylococcus aureus infections.* Proc Natl Acad Sci U S A, 2005. **102**(4): p. 1169-74.
44. Green, E.R. and J. Mecsas, *Bacterial Secretion Systems: An Overview.* Microbiol Spectr, 2016. **4**(1).
45. Puhar, A. and P.J. Sansonetti, *Type III secretion system.* Curr Biol, 2014. **24**(17): p. R784-91.
46. Costa, T.R., et al., *Secretion systems in Gram-negative bacteria: structural and mechanistic insights.* Nat Rev Microbiol, 2015. **13**(6): p. 343-59.
47. Sørensen, A.L., et al., *Purification and characterization of a low-molecular-mass T-cell antigen secreted by Mycobacterium tuberculosis.* Infection and immunity, 1995. **63**(5): p. 1710-1717.
48. Houben, D., et al., *ESX-1-mediated translocation to the cytosol controls virulence of mycobacteria.* Cell Microbiol, 2012. **14**(8): p. 1287-98.
49. Abdallah, A.M., et al., *Type VII secretion--mycobacteria show the way.* Nat Rev Microbiol, 2007. **5**(11): p. 883-91.
50. Bitter, W., et al., *Systematic genetic nomenclature for type VII secretion systems.* PLoS Pathog, 2009. **5**(10): p. e1000507.
51. Pallen, M.J., *The ESAT-6/WXG100 superfamily – and a new Gram-positive secretion system?* Trends in Microbiology, 2002. **10**(5): p. 209-212.
52. Huppert, L.A., et al., *The ESX system in Bacillus subtilis mediates protein secretion.* PLoS One, 2014. **9**(5): p. e96267.
53. Garufi, G., E. Butler, and D. Missiakas, *ESAT-6-like protein secretion in Bacillus anthracis.* J Bacteriol, 2008. **190**(21): p. 7004-11.
54. Akpe San Roman, S., et al., *A heterodimer of EsxA and EsxB is involved in sporulation and is secreted by a type VII secretion system in Streptomyces coelicolor.* Microbiology, 2010. **156**(Pt 6): p. 1719-1729.
55. Zoltner, M., et al., *EssC: domain structures inform on the elusive translocation channel in the Type VII secretion system.* Biochem J, 2016.
56. Groschel, M.I., et al., *ESX secretion systems: mycobacterial evolution to counter host immunity.* Nat Rev Microbiol, 2016. **14**(11): p. 677-691.
57. Tinaztepe, E., et al., *Role of Metal-Dependent Regulation of ESX-3 Secretion in Intracellular Survival of Mycobacterium tuberculosis.* Infect Immun, 2016. **84**(8): p. 2255-2263.
58. Serafini, A., et al., *The ESX-3 secretion system is necessary for iron and zinc homeostasis in Mycobacterium tuberculosis.* PLoS One, 2013. **8**(10): p. e78351.
59. Tufariello, J.M., et al., *Separable roles for Mycobacterium tuberculosis ESX-3 effectors in iron acquisition and virulence.* Proc Natl Acad Sci U S A, 2016. **113**(3): p. E348-57.
60. Portal-Celhay, C., et al., *Mycobacterium tuberculosis EsxH inhibits ESCRT-dependent CD4(+) T-cell activation.* Nat Microbiol, 2016. **2**: p. 16232.
61. Gey Van Pittius, N.C., et al., *The ESAT-6 gene cluster of Mycobacterium tuberculosis and other high G+C Gram-positive bacteria.* Genome Biol, 2001. **2**(10): p. RESEARCH0044.
62. Elliott, S.R. and A.D. Tischler, *Phosphate responsive regulation provides insights for ESX-5 function in Mycobacterium tuberculosis.* Curr Genet, 2016.

63. Ates, L.S., et al., *Essential Role of the ESX-5 Secretion System in Outer Membrane Permeability of Pathogenic Mycobacteria.* PLoS Genet, 2015. **11**(5): p. e1005190.
64. Sampson, S.L., *Mycobacterial PE/PPE proteins at the host-pathogen interface.* Clin Dev Immunol, 2011. **2011**: p. 497203.
65. Newton-Foot, M., et al., *The plasmid-mediated evolution of the mycobacterial ESX (Type VII) secretion systems.* BMC Evol Biol, 2016. **16**(1): p. 62.
66. Houben, E.N., K.V. Korotkov, and W. Bitter, *Take five - Type VII secretion systems of Mycobacteria.* Biochim Biophys Acta, 2014. **1843**(8): p. 1707-16.
67. Laencina, L., et al., *Identification of genes required for Mycobacterium abscessus growth in vivo with a prominent role of the ESX-4 locus.* Proc Natl Acad Sci U S A, 2018. **115**(5): p. E1002-E1011.
68. Brodin, P., et al., *Dissection of ESAT-6 system 1 of Mycobacterium tuberculosis and impact on immunogenicity and virulence.* Infect Immun, 2006. **74**(1): p. 88-98.
69. Ohol, Y.M., et al., *Mycobacterium tuberculosis MycP1 protease plays a dual role in regulation of ESX-1 secretion and virulence.* Cell Host Microbe, 2010. **7**(3): p. 210-20.
70. Houben, E.N., et al., *Composition of the type VII secretion system membrane complex.* Mol Microbiol, 2012. **86**(2): p. 472-84.
71. Wagner, J.M., et al., *Structures of EccB1 and EccD1 from the core complex of the mycobacterial ESX-1 type VII secretion system.* BMC Struct Biol, 2016. **16**(1): p. 5.
72. Zhang, X.L., et al., *Core component EccB1 of the Mycobacterium tuberculosis type VII secretion system is a periplasmic ATPase.* Faseb j, 2015. **29**(12): p. 4804-14.
73. Kurniawati, S., et al., *Cloning and Protein Expression of eccB5 Gene in ESX-5 System from Mycobacterium tuberculosis.* Biores Open Access, 2020. **9**(1): p. 86-93.
74. Famelis, N., et al., *Architecture of the mycobacterial type VII secretion system.* Nature, 2019. **576**(7786): p. 321-325.
75. Poweleit, N., et al., *The structure of the endogenous ESX-3 secretion system.* Elife, 2019. **8**.
76. Rosenberg, O.S., et al., *Substrates Control Multimerization and Activation of the Multi-Domain ATPase Motor of Type VII Secretion.* Cell, 2015. **161**(3): p. 501-12.
77. Warne, B., et al., *The Ess/Type VII secretion system of Staphylococcus aureus shows unexpected genetic diversity.* BMC Genomics, 2016. **17**(1): p. 222.
78. Dave, J.A., et al., *Mycosin-1, a subtilisin-like serine protease of Mycobacterium tuberculosis, is cell wall-associated and expressed during infection of macrophages.* BMC Microbiol, 2002. **2**: p. 30.
79. van Winden, V.J., et al., *Mycosins Are Required for the Stabilization of the ESX-1 and ESX-5 Type VII Secretion Membrane Complexes.* mBio, 2016. **7**(5).
80. Beckham, K.S., et al., *Structure of the mycobacterial ESX-5 type VII secretion system membrane complex by single-particle analysis.* Nat Microbiol, 2017. **2**: p. 17047.
81. Daleke, M.H., et al., *General secretion signal for the mycobacterial type VII secretion pathway.* Proc Natl Acad Sci U S A, 2012. **109**(28): p. 11342-7.

82. Champion, P.A., et al., *C-terminal signal sequence promotes virulence factor secretion in Mycobacterium tuberculosis.* Science, 2006. **313**(5793): p. 1632-6.
83. Korotkova, N., et al., *Structure of EspB, a secreted substrate of the ESX-1 secretion system of Mycobacterium tuberculosis.* J Struct Biol, 2015. **191**(2): p. 236-44.
84. Strong, M., et al., *Toward the structural genomics of complexes: crystal structure of a PE/PPE protein complex from Mycobacterium tuberculosis.* Proc Natl Acad Sci U S A, 2006. **103**(21): p. 8060-5.
85. Ates, L.S., E.N. Houben, and W. Bitter, *Type VII Secretion: A Highly Versatile Secretion System.* Microbiol Spectr, 2016. **4**(1).
86. Chen, Y.H., et al., *Characterization of EssB, a protein required for secretion of ESAT-6 like proteins in Staphylococcus aureus.* BMC Microbiol, 2012. **12**: p. 219.
87. Baptista, C., H.C. Barreto, and C. Sao-Jose, *High levels of DegU-P activate an Esat-6-like secretion system in Bacillus subtilis.* PLoS One, 2013. **8**(7): p. e67840.
88. Ramsdell, T.L., et al., *Linked domain architectures allow for specialization of function in the FtsK/SpoIIIE ATPases of ESX secretion systems.* J Mol Biol, 2015. **427**(5): p. 1119-32.
89. van den Ent, F. and J. Lowe, *Crystal structure of the ubiquitin-like protein YukD from Bacillus subtilis.* FEBS Lett, 2005. **579**(17): p. 3837-41.
90. Sao-Jose, C., C. Baptista, and M.A. Santos, *Bacillus subtilis operon encoding a membrane receptor for bacteriophage SPP1.* J Bacteriol, 2004. **186**(24): p. 8337-46.
91. Whitney, J.C., et al., *A broadly distributed toxin family mediates contact-dependent antagonism between gram-positive bacteria.* Elife, 2017. **6**.
92. Klein, T.A., et al., *Molecular Basis for Immunity Protein Recognition of a Type VII Secretion System Exported Antibacterial Toxin.* J Mol Biol, 2018. **430**(21): p. 4344-4358.
93. Kneuper, H., et al., *Heterogeneity in ess transcriptional organization and variable contribution of the Ess/Type VII protein secretion system to virulence across closely related Staphylocccus aureus strains.* Mol Microbiol, 2014. **93**(5): p. 928-43.
94. Bobrovskyy, M., et al., *EssH peptidoglycan hydrolase enables Staphylococcus aureus type VII secretion across the bacterial cell wall envelope.* J Bacteriol, 2018.
95. Zoltner, M., et al., *The architecture of EssB, an integral membrane component of the type VII secretion system.* Structure, 2013. **21**(4): p. 595-603.
96. Dreisbach, A., et al., *Profiling the surfacome of Staphylococcus aureus.* Proteomics, 2010. **10**(17): p. 3082-96.
97. Casabona, M.G., et al., *Functional analysis of the EsaB component of the Staphylococcus aureus Type VII secretion system.* Microbiology, 2017. **163**(12): p. 1851-1863.
98. Burts, M.L., A.C. DeDent, and D.M. Missiakas, *EsaC substrate for the ESAT-6 secretion pathway and its role in persistent infections of Staphylococcus aureus.* Mol Microbiol, 2008. **69**(3): p. 736-46.
99. Jager, F., et al., *Membrane interactions and self-association of components of the Ess/Type VII secretion system of Staphylococcus aureus.* FEBS Lett, 2016. **590**(3): p. 349-57.

100. Ahmed, M.M., et al., *The transmembrane domain of the Staphylococcus aureus ESAT-6 component EssB mediates interaction with the integral membrane protein EsaA, facilitating partially regulated secretion in a heterologous host.* Arch Microbiol, 2018. **200**(7): p. 1075-1086.
101. Mielich-Suss, B., et al., *Flotillin scaffold activity contributes to type VII secretion system assembly in Staphylococcus aureus.* PLoS Pathog, 2017. **13**(11): p. e1006728.
102. Anderson, M., et al., *Secretion of atypical protein substrates by the ESAT-6 secretion system of Staphylococcus aureus.* Mol Microbiol, 2013. **90**(4): p. 734-43.
103. Sundaramoorthy, R., P.K. Fyfe, and W.N. Hunter, *Structure of Staphylococcus aureus EsxA suggests a contribution to virulence by action as a transport chaperone and/or adaptor protein.* J Mol Biol, 2008. **383**(3): p. 603-14.
104. Korea, C.G., et al., *Staphylococcal Esx proteins modulate apoptosis and release of intracellular Staphylococcus aureus during infection in epithelial cells.* Infect Immun, 2014. **82**(10): p. 4144-53.
105. Cruciani, M., et al., *Staphylococcus aureus Esx Factors Control Human Dendritic Cell Functions Conditioning Th1/Th17 Response.* Front Cell Infect Microbiol, 2017. **7**: p. 330.
106. Poulsen, C., et al., *WXG100 protein superfamily consists of three subfamilies and exhibits an alpha-helical C-terminal conserved residue pattern.* PLoS One, 2014. **9**(2): p. e89313.
107. Anderson, M., et al., *EsaD, a secretion factor for the Ess pathway in Staphylococcus aureus.* J Bacteriol, 2011. **193**(7): p. 1583-9.
108. Cao, Z., et al., *The type VII secretion system of Staphylococcus aureus secretes a nuclease toxin that targets competitor bacteria.* Nature Microbiology, 2016. **2**: p. 16183.
109. Iyer, L.M., et al., *Comparative genomics of the FtsK-HerA superfamily of pumping ATPases: implications for the origins of chromosome segregation, cell division and viral capsid packaging.* Nucleic Acids Res, 2004. **32**(17): p. 5260-79.
110. Barre, F.X., *FtsK and SpoIIIE: the tale of the conserved tails.* Mol Microbiol, 2007. **66**(5): p. 1051-5.
111. Bath, J., et al., *Role of Bacillus subtilis SpoIIIE in DNA transport across the mother cell-prespore division septum.* Science, 2000. **290**(5493): p. 995-7.
112. Cattoni, D.I., et al., *Structure and DNA-binding properties of the Bacillus subtilis SpoIIIE DNA translocase revealed by single-molecule and electron microscopies.* Nucleic Acids Res, 2014. **42**(4): p. 2624-36.
113. Patel, S.S. and K.M. Picha, *Structure and function of hexameric helicases.* Annu Rev Biochem, 2000. **69**: p. 651-97.
114. Massey, T.H., et al., *Double-stranded DNA translocation: structure and mechanism of hexameric FtsK.* Mol Cell, 2006. **23**(4): p. 457-69.
115. Alvarez-Martinez, C.E. and P.J. Christie, *Biological diversity of prokaryotic type IV secretion systems.* Microbiol Mol Biol Rev, 2009. **73**(4): p. 775-808.
116. Christie, P.J., N. Whitaker, and C. Gonzalez-Rivera, *Mechanism and structure of the bacterial type IV secretion systems.* Biochim Biophys Acta, 2014. **1843**(8): p. 1578-91.
117. Atmakuri, K., E. Cascales, and P.J. Christie, *Energetic components VirD4, VirB11 and VirB4 mediate early DNA transfer reactions required for bacterial type IV secretion.* Mol Microbiol, 2004. **54**(5): p. 1199-211.

118. Hormaeche, I., et al., *Purification and properties of TrwB, a hexameric, ATP-binding integral membrane protein essential for R388 plasmid conjugation.* J Biol Chem, 2002. **277**(48): p. 46456-62.
119. delToro, D., et al., *Walker-A Motif Acts to Coordinate ATP Hydrolysis with Motor Output in Viral DNA Packaging.* J Mol Biol, 2016. **428**(13): p. 2709-29.
120. Guo, P., et al., *Controlling the Revolving and Rotating Motion Direction of Asymmetric Hexameric Nanomotor by Arginine Finger and Channel Chirality.* ACS Nano, 2019. **13**(6): p. 6207-6223.
121. Wendler, P., et al., *Structure and function of the AAA+ nucleotide binding pocket.* Biochim Biophys Acta, 2012. **1823**(1): p. 2-14.
122. Schwartz, C., et al., *Revolution rather than rotation of AAA+ hexameric phi29 nanomotor for viral dsDNA packaging without coiling.* Virology, 2013. **443**(1): p. 28-39.
123. Gomis-Ruth, F.X., et al., *The bacterial conjugation protein TrwB resembles ring helicases and F1-ATPase.* Nature, 2001. **409**(6820): p. 637-41.
124. Wang, S., et al., *Structural insights into substrate recognition by the type VII secretion system.* Protein Cell, 2020. **11**(2): p. 124-137.
125. Tanaka, Y., et al., *Crystal structure analysis reveals a novel forkhead-associated domain of ESAT-6 secretion system C protein in Staphylococcus aureus.* Proteins, 2007. **69**(3): p. 659-64.
126. Jager, F., H. Kneuper, and T. Palmer, *EssC is a specificity determinant for Staphylococcus aureus type VII secretion.* Microbiology, 2018. **164**(5): p. 816-820.
127. Human Microbiome Project, C., *Structure, function and diversity of the healthy human microbiome.* Nature, 2012. **486**(7402): p. 207-14.
128. Krismer, B., et al., *The commensal lifestyle of Staphylococcus aureus and its interactions with the nasal microbiota.* Nat Rev Microbiol, 2017. **15**(11): p. 675-687.
129. Jamet, A., A. Charbit, and X. Nassif, *Antibacterial Toxins: Gram-Positive Bacteria Strike Back!* Trends Microbiol, 2018. **26**(2): p. 89-91.
130. Gonzalez, D.J., et al., *Microbial competition between Bacillus subtilis and Staphylococcus aureus monitored by imaging mass spectrometry.* Microbiology, 2011. **157**(Pt 9): p. 2485-2492.
131. Hibbing, M.E., et al., *Bacterial competition: surviving and thriving in the microbial jungle.* Nat Rev Microbiol, 2010. **8**(1): p. 15-25.
132. Zhang, D., et al., *Polymorphic toxin systems: Comprehensive characterization of trafficking modes, processing, mechanisms of action, immunity and ecology using comparative genomics.* Biol Direct, 2012. **7**: p. 18.
133. Klein, T.A., S. Ahmad, and J.C. Whitney, *Contact-Dependent Interbacterial Antagonism Mediated by Protein Secretion Machines.* Trends Microbiol, 2020. **28**(5): p. 387-400.
134. Zoued, A., et al., *Architecture and assembly of the Type VI secretion system.* Biochim Biophys Acta, 2014. **1843**(8): p. 1664-73.
135. Cascales, E. and C. Cambillau, *Structural biology of type VI secretion systems.* Philos Trans R Soc Lond B Biol Sci, 2012. **367**(1592): p. 1102-11.
136. Fronzes, R., P.J. Christie, and G. Waksman, *The structural biology of type IV secretion systems.* Nat Rev Microbiol, 2009. **7**(10): p. 703-14.
137. Kanonenberg, K., C.K. Schwarz, and L. Schmitt, *Type I secretion systems - a story of appendices.* Res Microbiol, 2013. **164**(6): p. 596-604.

138. Garcia-Bayona, L., M.S. Guo, and M.T. Laub, *Contact-dependent killing by Caulobacter crescentus via cell surface-associated, glycine zipper proteins.* Elife, 2017. **6**.
139. Garcia-Bayona, L., K. Gozzi, and M.T. Laub, *Mechanisms of Resistance to the Contact-Dependent Bacteriocin CdzC/D in Caulobacter crescentus.* J Bacteriol, 2019. **201**(8).
140. Healthcare, G.
141. Diederichs, K. and P.A. Karplus, *Improved R-factors for diffraction data analysis in macromolecular crystallography.* Nat Struct Biol, 1997. **4**(4): p. 269-75.
142. Brunger, A.T., *Free R value: a novel statistical quantity for assessing the accuracy of crystal structures.* Nature, 1992. **355**(6359): p. 472-5.
143. Karimova, G., et al., *A bacterial two-hybrid system based on a reconstituted signal transduction pathway.* Proc Natl Acad Sci U S A, 1998. **95**(10): p. 5752-6.
144. Hoffman, E.A., et al., *Formaldehyde crosslinking: a tool for the study of chromatin complexes.* J Biol Chem, 2015. **290**(44): p. 26404-11.
145. Buchan, D.W.A. and D.T. Jones, *The PSIPRED Protein Analysis Workbench: 20 years on.* Nucleic Acids Res, 2019. **47**(W1): p. W402-W407.
146. Piovesan, D., et al., *MobiDB 3.0: more annotations for intrinsic disorder, conformational diversity and interactions in proteins.* Nucleic Acids Res, 2018. **46**(D1): p. D471-D476.
147. Zimmermann, L., et al., *A Completely Reimplemented MPI Bioinformatics Toolkit with a New HHpred Server at its Core.* J Mol Biol, 2018. **430**(15): p. 2237-2243.
148. Perez-Iratxeta, C. and M.A. Andrade-Navarro, *K2D2: estimation of protein secondary structure from circular dichroism spectra.* BMC Struct Biol, 2008. **8**: p. 25.
149. Herzik, M.A., Jr., M. Wu, and G.C. Lander, *High-resolution structure determination of sub-100 kDa complexes using conventional cryo-EM.* Nat Commun, 2019. **10**(1): p. 1032.
150. Liu, Y., D.T. Huynh, and T.O. Yeates, *A 3.8 A resolution cryo-EM structure of a small protein bound to an imaging scaffold.* Nat Commun, 2019. **10**(1): p. 1864.
151. Mooney, D.T., M. Jann, and B.L. Geller, *Subcellular location of phage infection protein (Pip) in Lactococcus lactis.* Can J Microbiol, 2006. **52**(7): p. 664-72.
152. Winn, M.D., et al., *Overview of the CCP4 suite and current developments.* Acta Crystallogr D Biol Crystallogr, 2011. **67**(Pt 4): p. 235-42.
153. Emsley, P. and K. Cowtan, *Coot: model-building tools for molecular graphics.* Acta Crystallogr D Biol Crystallogr, 2004. **60**(Pt 12 Pt 1): p. 2126-32.
154. Mastronarde, D.N., *Automated electron microscope tomography using robust prediction of specimen movements.* J Struct Biol, 2005. **152**(1): p. 36-51.
155. Sheldrick, G.M., *A short history of SHELX.* Acta Crystallogr A, 2008. **64**(Pt 1): p. 112-22.
156. Kabsch, W., *Xds.* Acta Crystallogr D Biol Crystallogr, 2010. **66**(Pt 2): p. 125-32.
157. Yepes, A., et al., *Reconstruction of mreB expression in Staphylococcus aureus via a collection of new integrative plasmids.* Appl Environ Microbiol, 2014. **80**(13): p. 3868-78.

158. Böttcher, B., *Transmission Electron Microscopy: Preparation of Specimens.* 2012.
159. Hanzelmann, P. and H. Schindelin, *Structural Basis of ATP Hydrolysis and Intersubunit Signaling in the AAA+ ATPase p97.* Structure, 2016. **24**(1): p. 127-139.

VI. Abbreviations

aa	Amino acids
AC	Affinity chromatogrpahy
AHT	Anhydrotetracycline
ATP/ADP/AMP	Adenosine tri/di/mono-phosphate
BN-PAGE	Blue-Native gel electrophoresis
CC	Clonal complex
CD	Circular dichroism
CHIP	Chemotaxis inhibiting protein
CFP-10	Culture filtrate protein-10kDa
ClfA	Clumping factor A
CNB	Centro Nacional de Biotecnologí
codopt	codon optimized for *E. coli*
DDM	n-Dodecyl β-maltoside
DSS	Disuccinimidyl suberate
DTT	Dithiothreitol
eDNA	extracellular esoxyribonucleic acid
ESAT-6	Early secreted antigenic target-6
FHA	Forkhead-associated
Gt	*Geobacillus thermodenitrificans*
HAI	Health care-associated infection
IMIB	Institute for Molecular Infection Biology
IPTG	Isopropyl-β-D-thiogalactopyranosid
LB	Lysogeny broth
LDH	Lactate-dehydrogenase
MALS	Multi-angle light scattering
MS	Mass spectrometry
MRSA	Methicillin-resistant *Staphylococcus aureus*
Mt	*Mycobacterium tuberculosis*
Ms	*Mycobacterium smegmatis*
MW	Molecular weight
NADH/NAD^+	Nicotinamidadenindinukleotid

NEB	New England Biolabs
PFA	Para-formaldehyde
PEP	Phosphophenolpyruvate
Pip	Phage infection protein
PK	Pyruvat kinase
PMSF	Phenylmethylsulfonyl fluoride
PSM	Phenol-soluble modulin
RNAP	RNA polymerase subunit β
RE	Restriction enzyme
Sa	*Staphylococcus aureus*
RVZ	Rudolf Virchow Center
SAC	Staphylococcal abscess community
SCIN	staphylococcal complement inhibitor
SDS-PAGE	sodium dodecyl sulfate polyacrylamide gel electrophoresis
SEC	Size-exclusion chromatography
S-SAD	Single-wavelength anomalous dispersion of sulfur atoms
SpA	Staphylococcal protein A
Tc	*Thermomonospora curvata*
TSB-T	TSB-Tween20
TSST-1	Toxic shock syndrome toxin-1
T1SS	Type I secretion system
T4SS	Type IV secretion system
T6SS	Type VI secretion system
T7SS	Type VII secretion system
T7SSa	Type VIIa secretion system
T7SSb	Type VIIb secretion system
wt	*Wild type*
X-gal	5-bromo-4-chloro-3-indolyl-β-D-galactopyranoside
% (v/v)	% (volume/volume)
% (w/v)	% (weight/volume)

VII. Appendix I

VII.1 List of figures

VII.2 List of supplemental figures

VII.3 List of tables

VII.4 List of primers

Primer	Sequence 5'-3'
X1	GGGAGCGCTTGGAGCCA
X2	TGTATATCTCCTTCTTAAAGTTAAAC
X3	AGAAGGAGATATACAATGCACAAACTGATTATTAAATA
X4	GCTCCAAGCGCTCCCTTTGAACCAACGGATTTTC
X5	TCGACAAAAATCTAGATTTGTTTAACTTTAAGAAGGAG
X6	TTCACAGGTCAAGCTTTTATTTCTCGAACTGCGGG
X7	TCGACAAAAATCTAGATTTGTTTAACTTTAAGAAGGAG
X8	CTGCGGGTGGCTCCAAGCGGATTGGAAGTACAGGTTTTCAGCGCTCC CTTTGAACC
X9	AGCGCTGAAAACCTGTAC
X10	TGTATATCTCCTTCTTAAAGTTAAAC
X11	AGAAGGAGATATACAATGCACAAACTGATTATTAAAT
X12	ACAGGTTTTCAGCGCTCGGAATATCATTCGGCG
X13	GCTGAGCAATAACTAGCATAAC
X14	TGTATATCTCCTTCTTAAAGTTAAAC
X15	TACTTCCAATCCGGAATGCCGATGATGCCGGAC
X16	TAGTTATTGCTCAGCTTATTTGAACCAACGGATTTTC
X17	TACTTCCAATCCGGAATGTCAGATGACGCCA
X18	TAGTTATTGCTCAGCTTATTTGAACCAACGGATTTTC
X19	TAGTTATTGCTCAGCTTATTTCGGTTCTTGCGGTT
X20	TACTTCCAATCCGGAATGTCACAAAAAGACTCGGT
X21	TACTTCCAATCCGGAATGGACTTTCCGGAACTGT
X22	TAGTTATTGCTCAGCTTATTTCGGTTCTTGCGGTT
X23	TACTTCCAATCCGGAATGGATTACAATGTTAGCACC
X24	TAGTTATTGCTCAGCTTATTTCGGTTCTTGCGGTT
X25	TACTTCCAATCCGGAATGTCACAAAAAGACTCGGT
X26	TAGTTATTGCTCAGCTTATTTGGAGATGTCTTCTTTG
X27	TACTTCCAATCCGGAATGTCACAAAAAGACTCGGT
X28	GATTGACAGTATGGAAGAAAATTAGTTATTGCTCAGC
X29	TACTTCCAATCCGGAATGCAAACGGTTAAAGAAAAC
X30	GCTGAGCAATAACTATTAATTTTCTTCCATACTGTCAATC

X31	GAAAACCTGTACTTCCAATCCGGAATGGGTGGATATAAAGGTATTA
X32	TAGTTATTGCTCAGCTCATGGGTTCACCCTATC
X33	GTGAACCCATGACTCGAGCACCACCACC
X34	GTGCTCGAGTCATGGGTTCACCCTATC
X35	GCAATGAATTAACTCGAGCACCACCACCAC
X36	GGTGGTGCTCGAGTTAATTCATTGCTTTATTAAAAT
X37	AGCGCTTGGAGCCACC
X38	TTTTTGCCCTCGTTATCTAGATTTTTGTCGA
X39	TAACGAGGGCAAAAAATGAAAAAGAAAAATTGGATTTAC
X40	GTGGCTCCAAGCGCTAATCAGGCGTTCCTTTTTGA
X41	TAACGAGGGCAAAAAATGAACAAAATCCATATCGCA
X42	GTGGCTCCAAGCGCTTCCACCAACCGGGTTCGACATAAAG
X43	TATAGGACTGAGGCAAACTAGT
X44	AACTAGAAACCTCCTGAATATTTTA
X45	CAGGAGGTTTCTAGTTATGCATAAATTGATTATAAAAT
X46	GTTTGCCTCAGTCCTATACTATTTAAACCATCTAATCTTTTG
X47	CAGGAGGTTTCTAGTTATGCATAAATTGATTATAAAAT
X48	GTTTGCCTCAGTCCTATAT TAAGGAATATCATTTGGTG
X49	CAGGAGGTTTCTAGTTATGCATAAATTGATTATAAAAT
X50	CTTGAGTCTGCGATTGCAATCGCATAT
X51	GAAAAATATGCGATTGCAATCGCAGACT
X52	GTTTGCCTCAGTCCTATACTATTTAAACCATCTAATCTTTTG
X53	CAGGAGGTTTCTAGTTATGCATAAATTGATTATAAAAT
X54	TCTTCGGCAAATGCAGCCACTTGA
X55	TCAAGTGGCTGCATTTGCCGAAGA
X56	GTTTGCCTCAGTCCTATACTATTTAAACCATCTAATCTTTTG
X57	CAGGAGGTTTCTAGTT ATGCATAAATTGATTATAAAAT
X58	CTTCAATCATTGCTTGATGAATCGC
X59	GCGATTCATCAAGCAATGATTGAAG
X60	GTTTGCCTCAGTCCTATACTATTTAAACCATCTAATCTTTTG
X61	CAGGAGGTTTCTAGTTATGCATAAATTGATTATAAAAT
X62	CCATTTCTCTTGCCTTTAAGTCTTC
X63	GAAGACTTAAAGGCAAGAGAAATGG

X64 GTTTGCCTCAGTCCTATACTATTTAAACCATCTAATCTTTTG

X65 CAGGAGGTTTCTAGTTATGCATAAATTGATTATAAAAT

X66 AATCTTTTTCTGCTGGGCCGTC

X67 GACGGCCCAGCAGAAAAAGATT

X68 GTTTGCCTCAGTCCTATACTATTTAAACCATCTAATCTTTTG

X69 CAGGAGGTTTCTAGTTATGCATAAATTGATTATAAAAT

X70 GATAATATAAAGTGCATCTTTTTC

X71 GAAAAAGATGCACTTTATATTATC

X72 GTTTGCCTCAGTCCTATACTATTTAAACCATCTAATCTTTTG

X73 CAGGAGGTTTCTAGTTATGCATAAATTGATTATAAAAT

X74 ATTGATAATTGCAAGTGAATCTTTTTC

X75 GAAAAAGATTCACTTGCAATTATCAAT

X76 GTTTGCCTCAGTCCTATACTATTTAAACCATCTAATCTTTTG

X77 CAGGAGGTTTCTAGTTATGCATAAATTGATTATAAAAT

X78 ATTGATAATGAAAAGTGAATCTTTTTC

X79 GAAAAAGATTCACTTTTCATTATCAAT

X80 GTTTGCCTCAGTCCTATACTATTTAAACCATCTAATCTTTTG

X81 CAGGAGGTTTCTAGTT ATGCATAAATTGATTATAAAAT

X82 CAATAAATGTTTTAAAATCTGCGATAATATAA

X83 TTATATTATCGCAGATTTTAAAACATTTATTG

X84 GTTTGCCTCAGTCCTATACTATTTAAACCATCTAATCTTTTG

X85 CAGGAGGTTTCTAGTT ATGCATAAATTGATTATAAAAT

X86 CAATAAATGTTTTAAATGCATTGATAATA

X87 TATTATCAATGCATTTAAAACATTTATTG

X88 GTTTGCCTCAGTCCTATACTATTTAAACCATCTAATCTTTTG

X89 CAATAAATGTTTTAAATGCATTGATAATA

X90 CAGGAGGTTTCTAGTT ATGCATAAATTGATTATAAAAT

X91 GATAATATAAAGTGCATCTTTTTC

X92 GAAAAAGATGCACTTTATATTATC

X93 CGGGAGCTCGAATTCATGAAAAAGAAAAATTGG

X94 TCGTCATCGTCTTTGTAGTCCTTGTCGTCATCGTCTTTGTAGTCTTTAT
AATCTTGTAACATTTTATC

X95 CAAAGACGATGACGACAAGGACTACAAAGACGATGACGACAAGATTG

	ATAAAGGCAAAAAT
X96	GGCGATATCGGATCCTTAGATTAATCTCTCTTTC
X97	GATTAGCCAAGCTTGCATGGGTGGATATAAAGG
X98	CATGGTCATTGAATTCGATGGGTTCACCCTATCA
X99	GATTAGCCAAGCTTGCATGAATTTTAATGATATTGAAAC
X100	GATGGTCATTGAATTCGAATTCATTGCTTTATTAAAAT

VII.5 Supplemental figures

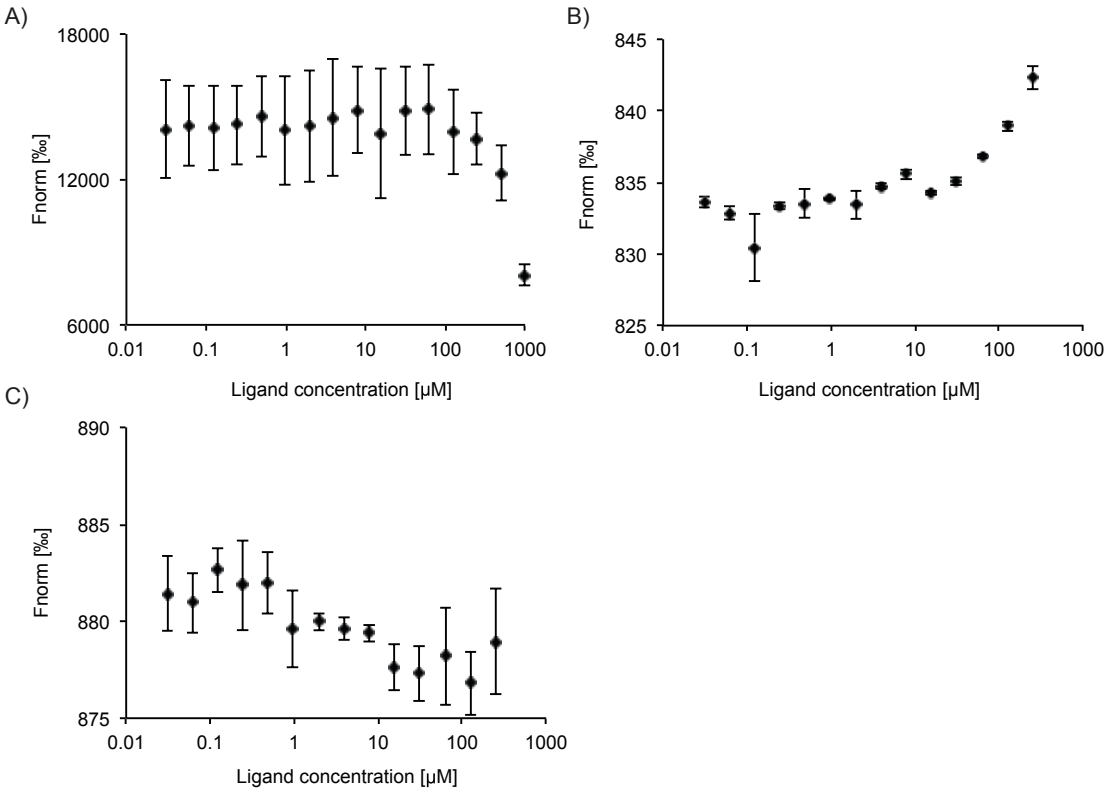

Fig. S 1: Affinity measurements using fluorescence quenching between BSA and different EssC variants.

EssC variants were labeled with fluorophor NT-647 and BSA was titrated to the variant, A) EssC + BSA B) EssC-D2D3+ BSA C) EssC-D3 + BSA. Experiments were carried out as technical duplicates for A). Experiments were carried out as technical triplicates for B) and C). Error bars present the standard deviation. No interaction was detected.

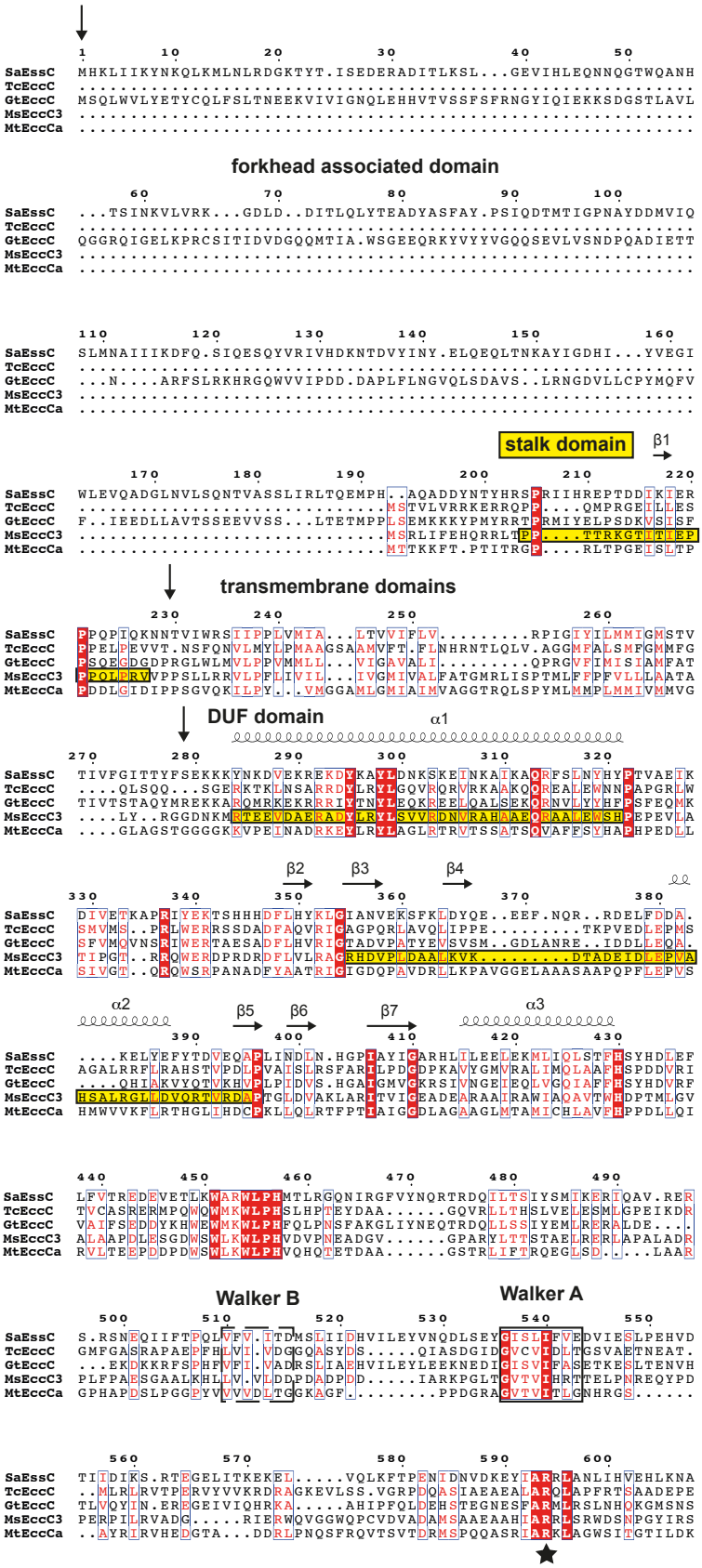
forkhead associated domain
stalk domain
β1
transmembrane domains
DUF domain
α1
β2
β3
β4
α2
β5
β6
β7
α3
Walker B
Walker A
SaEssC
TcEccC
GtEccC
MsEccC3
MtEccCa

,

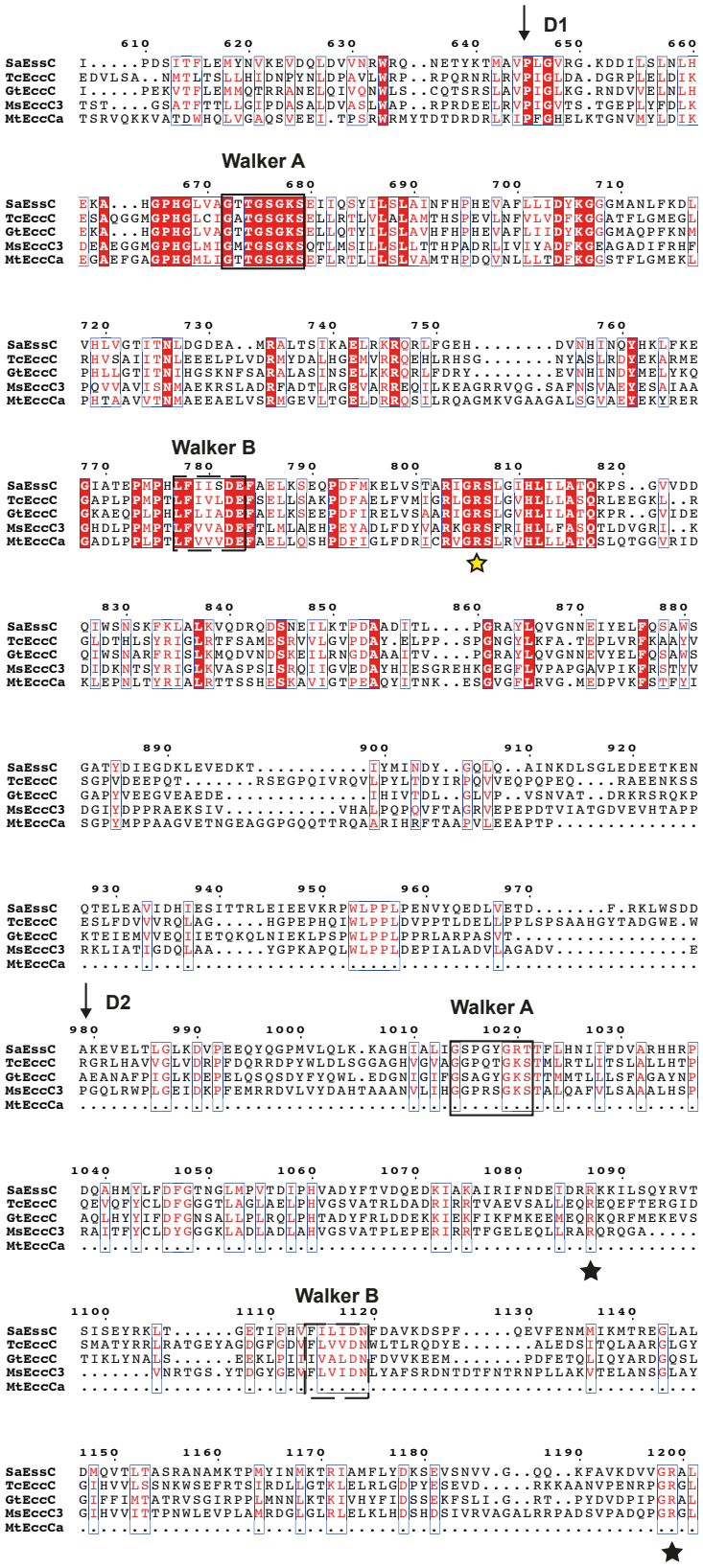
D1
Walker A
Walker B
D2
Walker A
Walker B
SaEssC
TcEccC
GtEccC
MsEccC3
MtEccCa

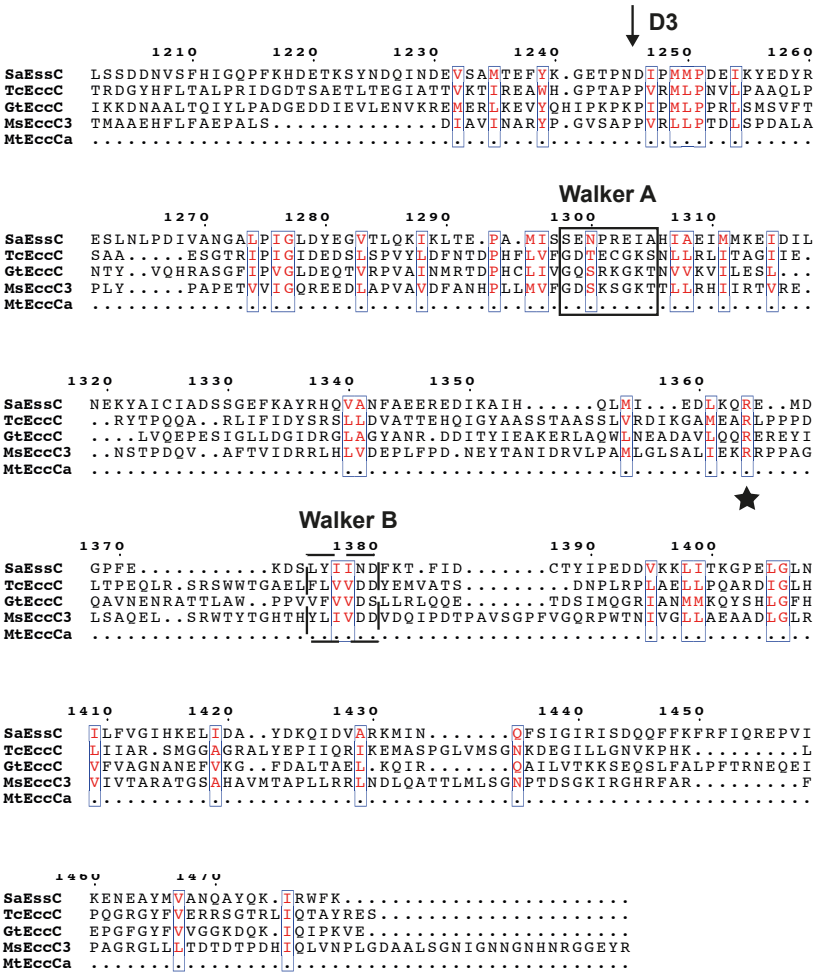

Fig. S 2: Sequence alignment of ATPase of T7SSb from *S. aureus* (*Sa*EssC) and *G. thermodenitrificans* (*Gt*EccC) and ATPase of T7SSa from *T. curvata* (*Tc*EccC), *M. smegmatis* Esx-3 (*Ms*EccC3) and *M. tuberculosis* Esx-1 (*Mt*EccCa).

Stalk domain of *Ms*EccC3 are highlighted in yellow, secondary structure prediction using Quick2D for *Sa*EssC matches elements of the stalk domain from MsEccC3. Walker A motif (GxxxxGKS/T) and Walker B motif (hhhhDE) are highlighted (black boxes) for DUF, D1, D2 and D3 ATPase domain. Star (black) indicate possible arginine fingers. Star (yellow) highlights arginine finger in *T. curvata*. Arginine residue are conserved among T7SSs.

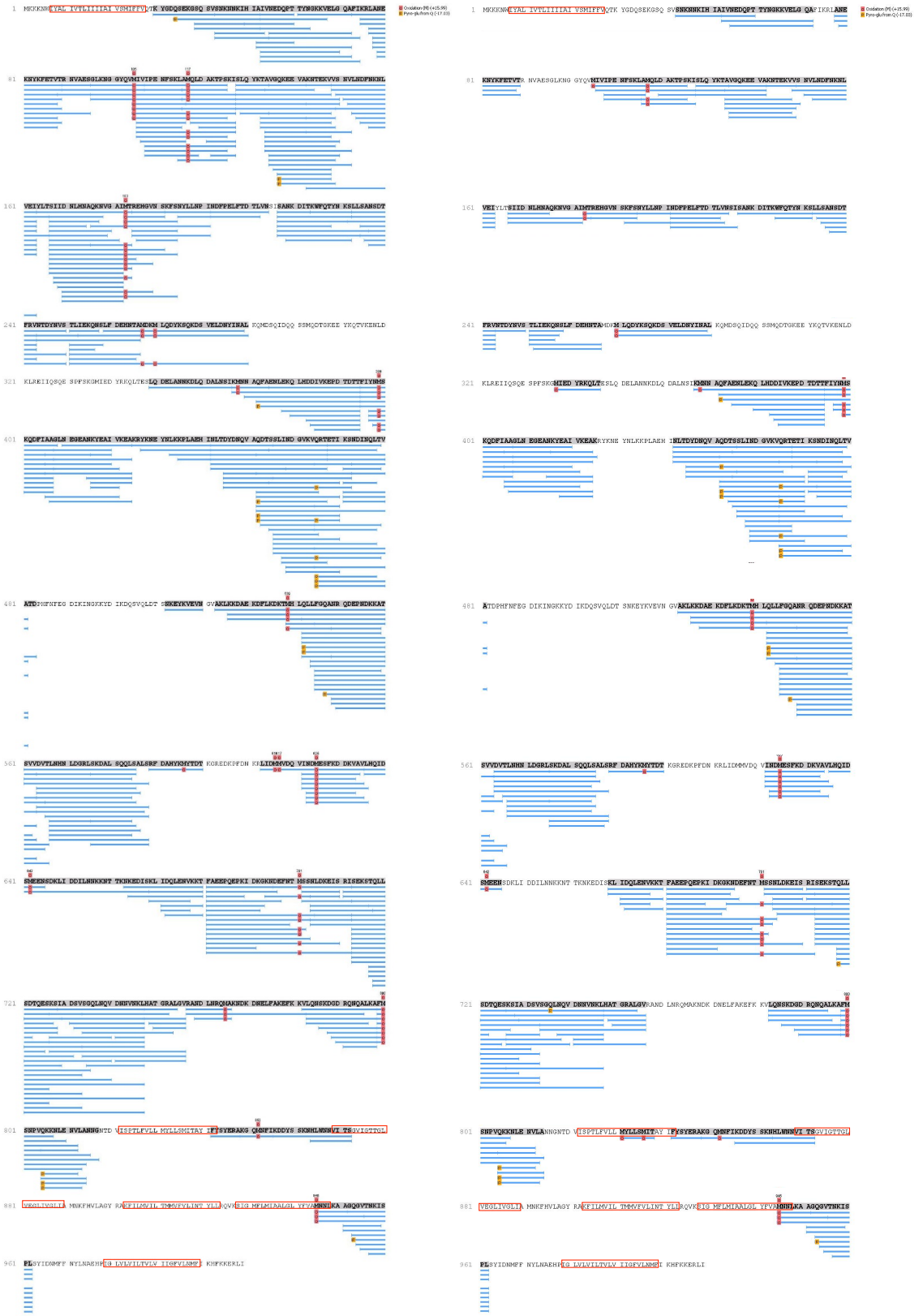

Fig. S 3: Mass spectronomy results of full-length EsaA
Left panel: 100 kDa band in **Fig. 27**A, right panel: 70 kDa band in **Fig. 27**B, blue lines indicate found peptides, red boxes highlight transmembrane domains

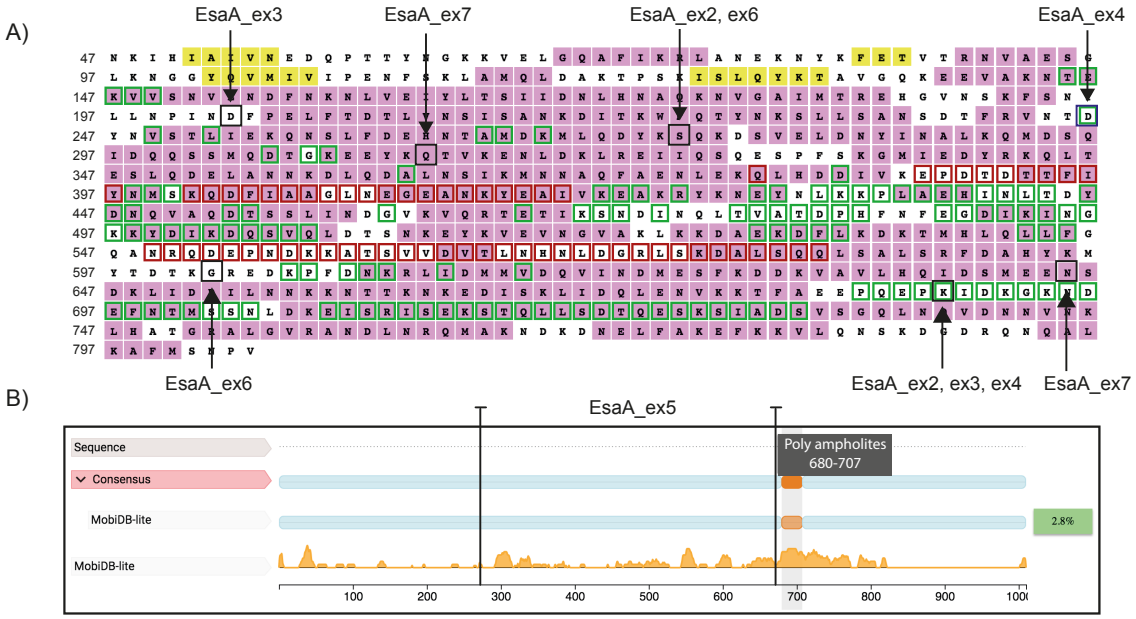

Fig. S 4: Secondary structure prediction of EsaA extracellular domain
A) PSIPRED, pink squares propose a helical structure, yellow squares propose a β-sheet, B) MobiDB, prediction of poly ampholites at 680 aa, boundaries of EsaA_ex-constructs indicated with arrows.

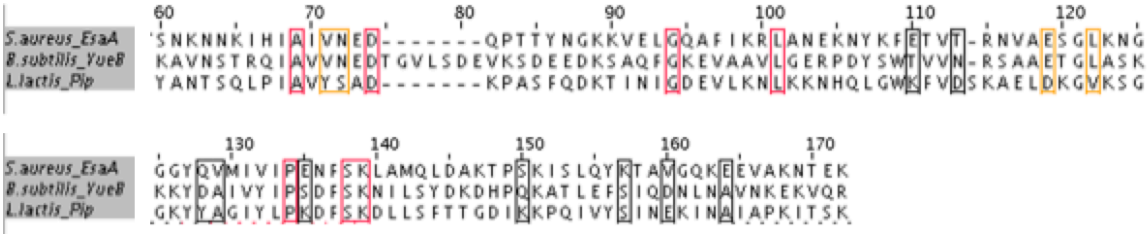

Fig. S 5: Sequence alignment of the N-terminal part of the extracellular domain from EsaA (*S. aureus*) and its homologues YueB (*B. subtilis*) and Pip (*L. lactis*).
Amino acids in boxes are required for phage binding. Red boxes show conserved aa, yellow boxes show conserved aa in YueB and EsaA, black boxes show aa which are not conserved in *S. aureus*

VIII. Appendix B

VIII.1 Affidavit

I hereby confirm that my thesis “Structural and functional elucidation of the Type VII secretion system from *Staphylococcus aureus"* is the result of my own work. I did not receive any help or support from commercial consultants. All sources and/or materials applied are listed and specified in the thesis.
Furthermore, I confirm that this thesis has not yet been submitted as part of another examination process neither in identical nor in similar form.

Hiermit erkläre ich an Eides statt, die Dissertation „Strukturelle und funktionale Analyse des Typ VII Sekretionssystem aus *Staphylococcus aureus*“ eigenständig, d.h. insbesondere selbstständig und ohne Hilfe eines kommerziellen Promotionsberaters, angefertigt und keine anderen als die von mir angegebenen Quellen und Hilfsmittel verwendet zu haben.
Ich erkläre außerdem, dass die Dissertation weder in gleicher noch in ähnlicher Form bereits in einem anderen Prüfungsverfahren vorgelegen hat.

VIII.2 Publications

Nicole Mietrach, Diana Damián-Aparicio, Benjamin-Mielich-Süß, Daniel Lopez and Sebastian Geibel (2020): "Substrate interaction with EssC of the Type VIIb secretion system", J Bacteriol. 2020 Jan; 202 (7)

Nicole Mietrach, Andreas Schlosser and Sebastian Geibel (2019): "Expression, purification and crystallization of the extracellular domain of the EsaA membrane component of the Type VIIb secretion system", Acta Crystallogr F Struct Biol Commun. 2019 Dec 1; 75(Pt 12): 725–730.

Nikolaos Famelis, Angel Rivera-Calzada, Gianluca Degliesposti, Maria Wingender, **Nicole Mietrach**, J. Mark Skehel, Rafael Fernandez-Leiro, Bettina Böttcher, Andreas Schlosser, Oscar Llorca & Sebastian Geibel (2019): "Architecture of the mycobacterial type VII secretion system", Nature, doi:10.1038/s41586-019-1633-1

Benjamin Mielich-Süss, Rabea M. Wagner, **Nicole Mietrach**, Tobias Hertlein, Gabriella Marincola, Knut Ohlsen, Sebastian Geibel and Daniel Lopez (2017): "Flotillin scaffold activity contributes to type VII secretion system assembly in Staphylococcus aureus",PLOS Pathogens November 22, 2017

VIII.3 Acknowledgements

At this point, I like to thank all the people I met along the way. Colleagues, who contributed to this work as well as friends, who have known me since kindergarten or the ones, I met during my studies and the PhD time.

I would like to thank my supervisor Sebastian Geibel for giving me the opportunity to work on an exciting topic and to perform my PhD thesis in his laboratory. Sebastian always saw the positive facts about experimental outcome and motivated me to pursue with my research.

Moreover, I would like to thank my thesis committee Prof. Thomas Müller and Prof. Gilles Phan for their critical feedback, helpful discussions as well as ideas to proceed with my research projects. I would like to thank the Graduate School of Life Science for the support during this time.

A big thanks goes to my colleague Nick Famelis, who always had an answer to my questions and helped me with experimental settings as well as great discussion about research. I also like to thank Rabea Wagner, Gabriella Marincola, Benjamin Mielich-Süß and my twin sister Charlotte Wermser for an amazing work environment. Sharing a lab and spending time with you made work so much easier and enjoyable. I am very glad that you are not only colleagues anymore but also friends after all these years.

I am very grateful that my family is always by my side, especially the women of my family. Thank you for giving me a "save place" at home, where I always can come back and enjoy time far away from research. Thank your for your support. Furthermore, I like to thank my real sister Carolin Noack for endless discussions about different research topics, life and not-working experiments. Thank you for reminding me that there is more than the laboratory.

A special thanks goes to Victoria Scholz and Michele Beer. Your friendship gave me so much strength and encouraged me to finish what I started. I cannot thank you enough for staying at my side during all these years.

VIII.4 Curriculum Vitae